NONSINK DISSOLUTION KINETICS OF POORLY SOLUBLE SUBSTANCES ASSESSED IN A COLUMN APPARATUS

by

SHARON MARIE LAUGHLIN

A thesis submitted in partial fulfillment of the requirements for the degree of

DOCTOR OF PHILOSOPHY
(Pharmacy)

at the

UNIVERSITY OF WISCONSIN-MADISON

1983

NONSINK DISSOLUTION KINETICS OF POORLY SOLUBLE SUBSTANCES ASSESSED IN A COLUMN APPARATUS

Sharon Marie Laughlin

Under the supervision of Professor J.T. Carstensen

A dissolution column was designed for use in evaluation of the effect of various experimental parameters on dissolution rate of poorly and moderately soluble substances. Experimental parameters included five mesh cuts, six recrytallization batches with different specific surface area, four solvents, five flow rates, two column diameters and five initial column loads. Either an analytical or a preparative pump head on a positive displacement pump delivered solvent to the column at a uniform rate. Dissolution profiles for concentration as a function of time were compared; dissolution rate was a function of particle size, total surface area presented to the solvent, and liquid velocity. When concentration and time were expressed in reduced form and the mass-transfer coefficients were identical, the dissolution profiles for compounds of different solubility were superimposable.

Rank order correlation was seen between reduced concentration at early time and five liquid velocities for different initial loads in two columns.

To determine how surface area of nonspherical particles changed during dissolution, several experiments were interrupted after either 25, 50, or 75% of the material had dissolved; remaining crystals were retained for microscopic examination, surface area measurements by krypton adsorption, and subsequent dissolution tests.

A model was derived which described the change in mass undissolved with respect to time as a function of solvent flow rate, the solubility and the mass-transfer coefficient of solute. Two geometric shapes were chosen for this analysis, the rod and sphere. Excellent agreement was found between calculated and measured concentrations for compounds of poor and moderate solubility. The model was versatile and could describe the relationship between area and mass as a function of time for any particle shape.

J. T. Carstensen

to

my parents

ACKNOWLEDGMENTS

To Professor J.T. Carstensen for sharing his knowledge and experience in dissolution research, and for his guidance during my graduate training.

To Professors K.A. Connors, J.R. Robinson, and G. Zografi for their insight, concern, and moral support, and for the extensive use of their laboratory equipment.

To Mr. Jim Wright for many stimulating and valuable discussions.

To my other colleagues at the University of Wisconsin-Madison for submitting to taste testing of multiple formulations from my "other" laboratory.

To the American Foundation for Pharmaceutical Education and to the United States Pharmacopeial Convention for the generous financial support provided through fellowships, and to Dr. Paul Turi of Sandoz and to Dr. Jane Sheridan of Roche for equipment and funding that supported preliminary studies.

TABLE OF CONTENTS

LIST OF TABLES

LIST OF FIGURES

BACKGROUND

Dissolution kinetics of a drug substance are of interest to the pharmaceutical formulator, since it is widely accepted that a drug must be in solution in the body fluids before it can elicit any pharmacological response. Therefore, it is important to determine the physical and chemical parameters which have an effect on dissolution rate; a suitable method of testing dissolution rate and describing the relationship between these parameters is desirable.

The rate at which solids dissolve was first described by Noyes and Whitney in 1897 (1); they proposed an equation which expresses the dissolution rate of a solid as a function of the difference between the solubility and concentration of the compound, and of a proportionality constant which is related to the mass-transfer coefficient of the system.

Nernst presented an important modification to the Noyes-Whitney equation (2); he suggested that the proportionality constant contained a dependence on the surface area of solid exposed to the dissolution medium. Thus, the modified Noyes-Whitney equation was defined; this has served as the basis for many discussions of dissolution kinetics.

A simplification of the modified Noyes-Whitney equation was derived by Hixson and Crowell to describe dissolution kinetics in a dilute solution (3); they assumed that the concentration of the solute was sufficiently small compared to the solubility that the former could be ignored. It was also necessary to assume that particles dissolved isometrically (i.e. the relationship between the surface area and volume of each particle remained constant independent of the particle size). The dilute conditions described here are often referred to as sink conditions, especially in the pharmaceutical literature; for this discussion, sink condition is defined as a situation in which the concentration is less than 15% of the solubility of the compound.

Dissolution of poorly soluble compounds has been described in the literature from many scientific areas. King et al studied dissolution of zinc and magnesium in acids (4,5,6) and of benzoic acid in dilute alkali (7). Geologists Van Name and co-workers reported dissolution kinetics for various metals in iodine, dissolved halogens, and in several acids (8,9,10,11). Dissolution rate of single crystals of nickel sulfate hexahydrate in ethanol-water mixture has been reported (12,13). Nelson compared dissolution rates of various compounds of pharmaceutical interest, including weak acids such as

benzoic acid, salicylic acid, phenobarbital and sulfathiazole (14); dissolution properties of salicylic acid and griseofulvin powders under sink conditions were reported by Ullah and Cadwallader (15,16). While dissolution studies are usually done in dilute conditions, a compound which has low solubility may dissolve to the extent that the concentration rises above 15% of the solubility, and thus nonsink conditions develop. It would be important to determine what parameters give rise to nonsink conditions, and what effect they have on dissolution.

Dissolution is well recognized as necessary and often the rate-limiting step in the sequence of obtaining a pharmacological response following administration of a drug to a patient. Edwards may have been the first to conclude and report that dissolution of a drug in the gastrointestinal tract is the rate process controlling absorption of that drug into the blood stream (17). Although absorption may not always be dissolution-controlled, the possible relationship between these factors should be questioned in the investigation of any drug. The effect of dissolution on drug availability, which has stimulated a great interest in the subject of dissolution kinetics, has been discussed in numerous

reviews (18,19,20,21).

To study dissolution and how it is influenced by various physical, chemical, and biological parameters, a suitable apparatus and experimental procedure must be developed. The ultimate goal of any dissolution procedure is (generally) to obtain dissolution results (in the laboratory) which would simulate or could be related to the biological response obtained from administration of the drug (in the same form, be it a suspension, powder or tablet) to an animal; this is referred to as *in vivo - in vitro* correlation.

In the Levy and Hayes study of local gastrointestinal irritation and absorption of a drug as a function of dissolution rate, the first well-defined dissolution apparatus was described (22). Commonly known as the Levy beaker method, it consisted of a 400 ml pyrex beaker immersed in a constant temperature bath. Its contents of 250 ml of 0.1 *N* HCl were stirred by a 3-blade, 5 cm diameter polyethylene stirrer, centered and immersed to a known depth in the beaker. Constant stirring at 59 rpm was used and following temperature equilibration of the dissolution medium, the dosage form (an aspirin tablet), was introduced in a known, reproducible fashion. Sampling procedures were also well defined. A direct relationship was observed between the dissolution rates of various size

particles and gastrointestinal irritation experienced by the clinical subjects (23). Thus began the search for an apparatus which could provide meaningful correlation between *in vitro* data and an *in vivo* response for all compounds.

Since 1960, the number and type of such dissolution apparatus has grown extensively. No detailed discussion will be presented here of these apparatus; however, reviews of dissolution methodology have been written by numerous authors (24-29). Classifications are often based on associated hydrodynamics (i.e. forced vs. free convection) and/or concentration conditions (i.e. sink vs. nonsink) which develop within the apparatus during a dissolution experiment. Advantages and disadvantages of each system exist and have been stated in many of these reviews. One clear conclusion is that no ideal dissolution methodology has yet been identified which can provide an adequate *in vitro* - *in vivo* correlation for all compounds.

Three basic criteria for any dissolution apparatus and methodology were proposed by Wagner (21). The method must have sufficient flexibility to adapt to the wide range of experimental parameters which might be used in dissolution experiments. It is important that the data obtained be reproducible and accurate. The method must be sufficiently sensitive to allow detection of small differences among

dissolution kinetics of various samples.

A column or flow-through dissolution method is, historically, the newest of the methods utilized in an attempt to meet these criteria. While the first use of column dissolution occurred in the United States, the method has been more popular in Europe in the past two decades. Myers reported the development of a column apparatus designed by Dr. Frank Wiley of the U.S. Food & Drug Administration (30). The vague description contained few details, but it is known that a cylindrical tube contained glass wool used as a filter to retain the dosage form (a tablet here) within the column; recycling of the dissolution fluid to a reservoir or removal of analytical samples was facilitated by a side-arm on the column. Temperature was controlled by immersion of the column into a water bath at 37°C. No further discussion or experimental results were reported about this appparatus.

In 1969, a European investigator, Langenbucher, extensively described the advantages and an evaluation of a column-type dissolution apparatus (31). The advantages noted for column dissolution were the ease of standardization with laboratory equipment and the lack of dependence of column design on arbitrary or material-related parameters. The process which occurs in column dissolution is basically one of mass transfer from a

fixed bed of solid to a liquid stream, which continually flows through material confined in a vertically oriented column. Such processes have been extensively studied in the field of chemical engineering (32-35).

Langenbucher's dissolution cell consisted of a column of known cross-sectional area (i.e. 2 or 4 cm^2) (31). Stainless steel screens and glass beads at either end of the column confined the granular solid to a known volume. An appropriate solvent was transferred by a metering pump from a reservoir through a heat exchanger, for temperature control, and from bottom to top of the column. This eluted volume could then be collected directly or recirculated through the column. Experimental parameters which were studied included three particle diameters of benzoic acid granules, four liquid velocities (i.e. flow rate per cell cross-sectional area), and four initial mass loads; deionized water at 25°C was the dissolution medium.

Based on experimental results and theoretical considerations, Langenbucher concluded that several advantages support further use of column dissolution to study dissolution kinetics. Liquid velocity and mass-specific cell area (i.e. initial weight of sample per cell cross-sectional are) were identified as the only apparatus-dependent parameters of importance; since they are based on flow rate and cell diameter, they are easily

controlled and defined. The reproducibility of ± 9% standard deviation in dissolution of homogeneous granules was considered acceptable. There was no need to define the total dissolution liquid volume prior to the experiment, or to identify organic solvents or adsorbents for use in maintaining sink conditions. Scale-up could be easily achieved by simply maintaining uniform liquid velocity and mass-specific cell area. Data from column dissolution experiments were well described by the cube root law for dissolution from uniform-sized granules; the effects of particle diameter, liquid velocity and initial mass load on dissolution rate were consistent with literature data. The system could also be easily adapted if a change of solvent medium during an experiment (i.e. from gastric to intestinal fluid) was required.

A modification of the Wiley/Myer's column was developed by Baun and Walker in 1969 (36); this column was used to study dissolution kinetics of a dosage form. Hydrochlorothiazide tablets were confined to a known volume of glass tubing. A continuous-duty oscillating pump, controlled by a variable transformer, pumped the fluid at a set rate from a reservoir, bottom to top through the column and back to the reservoir. The contents of this reservoir were then sampled and assayed to determine the amount dissolved as a function time.

A critical parameter in column dissolution is notably the uniformity and rate of solvent flow through the column. The influence of pulsation on dissolution rate was examined by Lerk and Zuurman (37). Aspirin tablets placed in a column dissolved as 0.1 N HCl at 37°C was pumped through the cell at a rate of 120 ml/min. This flow rate was markedly faster than the rate used by previous investigators, but this may have been necessary to elucidate differences among the plunger, centrifugal, and four peristaltic pumps evaluated. Pulsation of peristaltic pumps, which is common and variable between pumps, led to differences in dissolution results as compared to the centrifugal pump. The authors concluded that the centrifugal pump was best since it showed no pulsation, and therefore the dissolution results should be related to the hydrodynamics of the linear fluid velocity. However, use of a centrifugal pump is not simple since integration with a system of check valves and flow meters is required to maintain constant, low velocity flow rates; flow rate must be constantly monitored and adjusted, because back pressure will develop in the column if insoluble materials clog the filters.

The next extensive study of a column apparatus for dissolution was reported in four parts by Tingstad et al (38-41). Several advantages of a flow method, as noted by

Tingstad and Riegelman are: a) a higher degree of flexibility exists in selection of experimental parameters; b) the process yields data in a differential form, which can be treated directly or integrally; c) the solid is confined to a relatively homogeneous low-volume system; d) a noncirculating system prevents excessive accumulation of solute in the system; and e) solvent flow is provided in a controlled, precise and measurable fashion.

The dissolution apparatus used by Tingstad and Riegelman was a glass column, 1.9 cm in diameter, which contained filters to confine the tablet or powder to a known volume (38). Pumping of solvent from a reservoir was provided by a centrifugal constant-capacity pump, the flow rate being controlled by external valves and measured with a flow meter. The column fluid stream was pumped directly to a flow-through cell on a recording spectrophotometer. Dissolution rate of both prednisone tablets and powder in water containing various concentrations (0.0 - 0.5%) sodium lauryl sulfate was monitored. Effect of sample size and flow rate on the amount dissolved in a given time was also studied.

A modified column and procedure were later used by Tingstad *et al* to evaluate dissolution of isosorbide dinitrate tablets (39); the authors wanted to use a column constructed solely of commercially available components.

Here a variable-speed peristaltic pump delivered solvent at 12-14 ml/min. The decreased volume of the column, compared to the one in the previous study, was selected to reduce homogeneity problems to a minimum within the column. A correlation was found between disintegration time and t_{50} (time for 50% of the drug to dissolve). Despite a small problem with filter clogging, due to the presence of slowly soluble or insoluble particles, the authors concluded that the column was acceptable; dissolution results obtained with the column could be used to distinguish differences among several tablet formulations. The data were consistent with Langenbucher's expression for the relationship between dissolution time, liquid velocity and initial equivalent sperical particle diameter.

Next, Tingstad *et al* examined the effect of the type and intensity of agitation within various dissolution apparatus (both flow-through and stirred tank) on dissolution rate (40). Salicylic acid pellets of constant surface area were used in the evaluation. In general, less variation in dissolution kinetics was found for the flow-through method than for various beaker methods. The authors concluded that laminar flow was more probable in a column at low flow rate than in a beaker at slow stirring speed; thus, column dissolution data should provide a meaningful *in vitro* - *in vivo* correlation.

The final portion of the study of Tingstad *et al* addressed the important consideration of hydrodynamics within the flow-through column (41). Polystyrene beads were placed within a column; their movement was documented by a movie camera as water was pumped through the column at various speeds. The occurrence of back-flow, laminar-flow and/or turbulence were dependent on column diameter, fluid velocity and particle size. The position of the solid (i.e. centered versus off-centered) also affected its manner of presentation to the solvent and its dissolution rate; in the previous study, an off-centered tablet had a slower dissolution rate (40).

Seth used a flow-through cell method to study dissolution behavior of dry powder mixtures, wet-granulated mixtures, and compressed tablets of various hydrochlorothiazide formulations (42). He was unable to quantitate the specific influence of various formulations factors and processing techniques due to variation in disintegration time, bed height and surface area exposed to the dissolution fluid.

The beaker, rotating-basket and column methods for dissolution of *p*-acetaminophenol were compared by Bathe *et al* (43). Reproducibility of dissolution results in the beaker and column were found to be within 15-20%; thus these methods were concluded to be the more simple and

favorable forms. Results from the rotating-basket compared poorly with the other methods and this apparatus was judged to be unsatisfactory.

Groves and co-workers addressed some problems described by previous investigators, such as fluctuation in flow due to the type of pump used (i.e. peristaltic versus centrifugal) and changes in fluid velocity due to column filter blockage (44). They also wanted to construct a column of readily available and easily assembled components. Flow was monitored and adjusted by a light-activated switch integrated with a motor adjustment control on the centrifugal pump; this minimized the major problem of fluctuation. To study the hydrodynamics of this system, dye-containing tablets and dye solutions were introduced. Fluid back-flow at Re < 10, visible disturbances in streamlines downstream of tablets at Re > 100, and no significant "dead-space" for Re 10-70 were observed, where Re is the dimensionless Reynolds number for the system.

Carstensen and Dhupar developed dissolution rate equations for monodisperse crystals dissolved in a column at low fluid velocity (i.e. Re 10-100) (45). They were the first authors to report the occurrence of nonsink conditions during dissolution; the large mass of material in the column and its associated bed height are apparently

responsible for the high concentration of solute in the column effluent. In fact, the initial portions of fluid exiting from the column were very close to the compound's solubility. By measuring the concentration simultaneously at several different column heights, they also established that a concentration gradient exists within the column; this profile was well described by an exponential function.

The versatility of a multichannel continuous-flow system was reported by Cakiryildiz and co-workers (46); formulation and processing differences could be discerned from the dissolution profiles of bulk powder, tablets and capsules. Reproducibility of the flow-through method, similar to the USP (paddle) method, was reported to be 1-10% mean RSD (relative standard deviation).

A column apparatus has also been used to study differences in dissolution kinetics between crystals. When two crystal modifications of a disubstituted-pyrimidine were dissolved in a column, different dissolution rate constants could be distinguished for each (47). This observation was less obvious with use of the spin-filter type dissolution apparatus.

Shah and Nelson described a flow-through dissolution cell used to evaluate a convective diffusion model for drug dissolution (48). Dissolution fluid passed in a laminar layer over a compressed pellet of an alkyl p-amino

benzoate which was coplanar with one flat side of the cell. Despite the fact that this represented an idealized system, the convective diffusion model could quantitatively account for the effects of solubility, diffusivity, rate of shear, and geometry and orientation of the solid surface relative to flow.

Ogata et al compared the dissolution and later the bioavailability of film-coated chloramphenicol tablets using eight dissolution methods and six subjects (49,50). The column was considered suitable for testing intrinsic dissolution rate of nondisintegrating drug matrix, but unacceptable for evaluating drug dissolution from disintegrating dosage forms due to clogging of the filter.

Many important features and advantages of a column or flow-through dissolution apparatus have been described. The apparatus parameters of primary importance are liquid velocity and mass-specific cell area, as defined by Langenbucher. The rate of movement of a solvent past a solid is (one of) the most important parameter(s) affecting dissolution kinetics (51,52) and must be carefully considered in selecting a dissolution method; clearly a major advantage of a column apparatus for dissolution experiments is the easily controlled and well defined hydrodynamics within the column. In some cases,

dissolution results from a column apparatus have been consistent with differences between different crystal properties, differences in formulation components and/or processing factors. A column apparatus can be used to study dissolution kinetics under both sink and nonsink conditions; the bed height of solid in the column and flow rate of solvent through it apparently determine which conditions will initially prevail.

A general guideline in dissolution testing has been the selection of experimental condition which will give rise to sink or dilute conditions throughout (most of) the experiment. In fact, some researchers have employed organic solvents into which the solute can partition (53) or insoluble solids onto which the solute can adsorb (54) in order to maintain sink conditions. It has been suggested that the experiments which might provide the most meaningful data for *in vitro* - *in vivo* correlations are those done in sink conditions (53,55). However, the solubility of a compound would vary in different body fluids along the gastrointestinal tract, depending on pH and electrolyte concentrations; the volume of fluid available also varies and is difficult to assess. Therefore, it is not illogical to assume that a drug may be dissolving under nonsink conditions in some biological fluids (56). Thus it may be useful to observe the kinetics

of nonsink dissolution and to derive a mathematical model to describe the relationship between the parameters which affect it.

STATEMENT OF THE PROBLEM

The purpose of this study is:

1. to develop experimental procedures which allow determination of the effect of particle size, column load, specific surface area, solubility, column diameter, solvent flow rate and pulsation on column dissolution kinetics under nonsink conditions for a poorly soluble substance,

2. to study the effect of particle size and specific surface area on column dissolution kinetics under nonsink conditions of a more soluble compound of pharmaceutical interest,

3. to study how surface area of nonspherical particles changes during column dissolution under nonsink conditions, and

4. to develop and test a mathematical model which describes the effect of solubility, flow rate, and column load on dissolution kinetics of both poorly and more soluble compounds.

EXPERIMENTAL

MATERIALS

Potassium sulfate (analytical reagent grade)[1] and acetaminophen[2] were each recrystallized from ASTM Type II water.

Ethanol, U.S.P. (95% ethanol)[3] was used as received. Type II water was obtained from an ion-exchange system[4] which was fed by single distilled water.

Premixed combinations of krypton and helium gases[5] were used in surface area measurements; pure krypton gas[5] and pure helium gas[5] were used for calibration and degassing, respectively. All gases were labeled as 99.995% minimum purity level, and were used as received.

APPARATUS

A Hanson Dissolution Test Station[6] was used for the recrystallization of potassium sulfate; water bath temperature was controlled by the Hanson Solid State Temperature Control[6] unit and a Lauda/Brinkman Bath and

---

1. Mallinckrodt, Inc.
2. McNeil Consumer Products
3. U.S. Industrial Chemicals Co.
4. PCS Water Purifications, Barnstead Co., Division of Sybron Corp.
5. Matheson, Division of Searle Medical Products USA, Inc.
6. Model QC 72 RLB, Hanson Research Corp.

Circulator[7].

Samples for solubility studies were equilibrated in a constant temperature bath equipped either to rotate samples end-over-end at 32 rpm or to agitate samples more than 30 times per minute.

Cenco-Meinzer Sieve Shaker[8] and appropriate combinations of 20, 30, 40, 60, 80, and 100 mesh ASTM sieves[8] were used to separate crystals into various size fractions.

A polarizing microscope[9] was used to observe potassium sulfate and acetaminophen crystals. Photomicrographs of various crystals were taken with black-and-white film[10] in a 35 mm SLR camera.[11]

Surface area measurements were made using the Quantasorb Sorption System.[12] A 1 mV. output chart recorder,[13] connected to the Quantasorb, provided a permanent record of results.

A powder diffractometer[14] was used to expose K_2SO_4 crystals to X-rays; intensty of diffraction at various

---

7. Model RC20T, Lauda/Brinkman, Subsidiary of Sybron Corp.
8. Central Scientific Co., Division of Cenco Instruments Corp.
9. Model POH-2, Nikon, Inc., Instrument Division
10. Plus-X pan, Eastman Kodak Co.
11. Minolta SRT101, Minolta Camera Co., Ltd.
12. Quantachrome Corp.
13. Model IR-18M, Heathkit, Heath Co.
14. Philips Electronics, Inc.

angles was recorded and unit cell dimensions were calculated.

Desiccators containing saturated salt solutions were used to establish the equilibrium moisture content of potassium sulfate at various relative humidities.

Glass capillary tubes containing acetaminophen were heated in a controlled-temperature oil bath[15] to determine melting point of the compound.

Pycnometers and Ostwald viscometers were employed to measure density and viscosity, respectively, of various potassium sulfate solutions.

A specially constructed glass column[16] was designed for the dissolution studies. All dissolution solvent was maintained inside a reservoir in a constant temperature water bath. A positive displacement pump[17] transported fluid from the reservoir to the dissolution column. The pump was equipped with a pulse dampener[17] and either an analytical[17] or preparative pump head.[17]

Three different techniques were employed for analysis of dissolution samples. Acetaminophen concentrations were determined with a recording UV spectrophotometer.[18] Two

---

15. Model 6406-H Capillary Melting Point Apparatus, A.H. Thomas Co.
16. Mr. N.D. Erway, Glass Blowing
17. Altex Model 110A, Altex Scientific Inc., Subsidiary of Beckman Instruments, Inc.
18. UV-Visible Spectrophotometer, Model 559, Perkin Elmer

methods were used to determine potassium ion concentrations. An ion-exchange column, containing an organic strong acid cation exchanger,[19] converted potassium sulfate to H_2SO_4, which was titrated with NaOH[20] solutions to a colorometric endpoint. Potassium ion activity (not concentration) was more frequently quantitated with an ion-selective electrode,[21] an appropriate reference electrode,[22] and a digital pH/mv meter.[23]

METHODOLOGY

Solubility

Ethanol, U.S.P. and Type II water were mixed on a V/V basis at 25°C; mixtures of 30, 35, 40, 45, 50, and 60% V/V ethanol and water were prepared for solubility and dissolution studies. In the following text, for example, a 40% ethanol solution will refer to ethanol mixed with water on a 40% V/V basis.

Clean glass ampuls were filled with an appropriate solvent and sufficient K_2SO_4 to saturate the solution. Sealed ampuls were placed in a water bath of appropriate

---

19. Rexyn AG50(H), Fisher Scientific Co.
20. Mallinckrodt, Inc.
21. Monovalent Cation Electrode, #476220, Corning Science Products, Corning Glass Works
22. Silver/Silver Chloride Double Junction Reference Electrode, #476067, Corning Science Products
23. Orion, Model 701A, Orion Research Incorp.

temperature and were rotated or shaken until equilibrium was reached.

Ampuls were removed from the bath and broken. The contents was filtered, aliquots were measured by weight and/or by volume, and were added to glass vials. The samples were evaporated to dryness, and the weight of K_2SO_4 remaining was determined.

Literature values for the solubility of acetaminophen in water at 25°C are available (57).

Recrystallization

The purpose of recrystallization in all cases was not to increase the purity of the compound, but to obtain a wide distribution of particle sizes of the same compound (i.e. the same polymorph and crystal habit). Acetaminophen and several small batches of potassium sulfate were recrystallized in the same manner. An amount of solid, which exceeded the solubility of the compound at 25°C, was added to approximately 800 ml of Type II water in a one liter beaker. The contents were stirred on a hot plate. All solid dissolved at about 70°C; heating continued until the solution reached approximately 85°C. The solution was quickly filtered through coarse Whatman #2 filter paper. The temperature of the solution decreased as the contents was stirred, leading to precipitation of the compound;

cooling rate could not be carefully controlled with this procedure. After the contents reached room temperature, the beaker was immersed in an ice bath to continue cooling and increase yield of the crystals.

The crystals were subsequently filtered from the liquors. Potassium sulfate crystals were rinsed with ethanol. Both types of crystals were then air-dried at room temperature to constant weight.

The recrystallization procedure described above produced a wide variation in the crystals; surface area and physical appearance (cluster type) varied from one recrystallization batch to the next. Thus, it was necessary to repeat recrystallization on a sufficiently large scale to yield one large batch of crystals for use in all subsequent experiments.

In order to recrystallize this large batch of K_2SO_4, the following procedure was used. Approximately 600 grams of chemical was added to 3600 ml of Type II water in a 4 liter flask. A magnetic stir bar provided mixing as the flask was heated on a hot plate. All the solid dissolved at approximately 77°C; the solution was heated to a final temperature of 85°C, and was immediately filtered through Whatman #2 coarse filter paper. The solution, which had cooled to 75°C, was evenly divided among four plastic round bottom flasks (or stations) of a Hanson Dissolution Test

Apparatus. Each station was stirred by a USP XX fluorocarbon-coated dissolution paddle and covered with an acrylic plate to minimize evaporation; the paddles were rotated at 200 ± 3 rpm. The dissolution drive control unit provided a digital display of the paddle speed 42 times each minute. The water bath surrounding the dissolution flasks was originally set at 37 ± 0.5°C using the Solid State Temperature Control. The heating/cooling coil from the Lauda/Brinkman Bath and Circulating system was also submerged in the bath, and this unit was set to 37°C.

When the hot K_2SO_4 solution was added to the flasks, stirring commenced immediately, the Hanson temperature control system was turned OFF and the Lauda cooling system was reset to 5°C. The water bath temperature increased 2°C within the first 20 minutes, and subsequently decreased to 15°C over approximately 4 hours; this temperature drop caused potassium sulfate to precipitate. Agitation of the water bath was provided by both the air circulation which is part of the instrument design and by a USP paddle which was installed in one of the six station positions with no flask beneath it.

The contents of the four flasks were then vacuum filtered through a Buchner funnel lined with Whatman #2 coarse filter paper, and the crystals were rinsed with 95%

ethanol. They were air-dried at room temperature to constant weight. Crystals from the four beakers were combined and considered one batch for further experiments.

Sieving

Each recrystallization batch was separated into particle size groups using a nest of U.S. Standard sieves shaken on a Cenco sieve shaker for an appropriate time period. Screen numbers 20, 30, 40, 60, 80, and 100 with sieve openings of 840, 590, 420, 250, 177, and 149 μm, respectively, were used to obtain five mesh cuts which are designated as 20/30, 30/40, 40/60, 60/80, and 80/100.

Microscopy and Photomicrographs

Crystals were visually examined with the use of a polarizing light microscope. A sufficient quantity of crystals was distributed on a glass slide, but no dispersion liquid or coverslip was used. Photographs of representative crystals were taken with a 35 mm SLR camera, whose lens was removed. The camera was placed at the top of the microscope, a 4X or 10X lower microscope objective was selected, polarized light was used as needed to enhance contrast, and an appropriate shutter speed was set. All pictures were taken with black-and-white film.

Microscopic examination of potassium sulfate crystals

provided a means to closely observe surface properties of the crystals. After potassium sulfate crystals were rinsed with ethanol, they were observed with 100X magnification; no change in crystal surfaces due to ethanol rinse could be seen.

Surface Area

A commercially available instrument was used to determine the surface area of many samples. A mixture of an adsorbing gas (krypton) and a nonadsorbing gas (helium) is passed through a cell which holds the sample. The principle of the method is to compare the thermal conductivity of the gas both up and downstream of a sample and to quantitate any difference between these.

When the sample cell is immersed in liquid nitrogen (T = 77°K), krypton gas is removed from the gas stream as it is adsorbed onto the solid surface; then the sample cell is returned to a higher or room temperature, and krypton gas is added to the gas stream when it is desorbed from the solid surface. Thus a dynamic measurement of the change in thermal conductivity of the gas stream as it encounters the sample will provide a measure of the amount of krypton gas which was adsorbed onto and later desorbed from the surface of the solid. A previously balanced Wheatstone bridge provides an electrical response when the thermal

conductivity changes; this response is then integrated internally and a digital count is displayed. Generally, only the desorption values are used for calculation; the BET equation relates this quantity to the surface area of the material. The amount of krypton adsorbed and desorbed must be quantitated by measuring a similar electrical response to the injection of a known volume of pure krypton.

A macro or large sample cell was used in all measurements. This allows the analysis of a large sample size, (i.e. several grams), which is necessary when the specific surface area is small (i.e. <0.1 m^2/gm) (58). Krypton, which has a very low vapor pressure (2.63 torr) at 77°K, demonstrates little problem with thermal diffusion and thus is preferred over nitrogen gas for measurement of low surface areas (58). Experiments showed that sample pretreatment, either with heat and/or degassing with helium, gave no significantly different results for surface areas of K_2SO_4; therefore, no pretreatment was used on subsequent samples. However, several hours of pretreatment with gas, either pure helium or krypton mixed with helium, plus elevated temperature was necessary before the surface area of acetaminophen crystals could be determined.

All samples were analyzed at three different combinations of krypton and helium, where the krypton was

present in an amount to give P/Po = 0.090, 0.183, or 0.265; for surface area measurements, it is typical to start with the mixture of lowest 'P/Po' adsorbate concentration and then preceed to higher ratios. A minimum of two adsorption-desorption cycles and two calibrations were completed at each gas mixture. Pure krypton, injected with a microsyringe, was used for calibrations.

X-ray Powder Diffraction

To confirm that recrystallization of K_2SO_4 from water did not change the crystal form, samples were analyzed with X-ray powder diffraction.

Crystals were ground to a very fine powder in a mortar and pestle. Sufficient powder was used to fill the rectangular cavity in the sample holder and the surface was smoothed. A powder diffractometer, using CuKα as a radiation source, was set to scan the sample from 5^{o} to 50^{o} at 1^{o}/minute. Based on the resulting peaks and information from the X-ray Powder Data File #5-0613 for K_2SO_4, (59) three angles corresponding to multiples of Miller indices were selected for further analysis. After setting appropriate time constant, scale factor and multiplier speed, these three angles were scanned at $1/4^{o}$ per minute. The intensity of diffracted radiation at the corresponding angles was recorded on a strip chart recorder.

Equilibrium Moisture Content

Samples of potassium sulfate were spread in glass petrie dishes and placed inside desiccators; these desiccators contained saturated salt solutions which maintain environments of known relative humidity. A range of 22% to 84% RH at 25°C was studied.

Weight change of the samples was monitored; after a minimum of 7 days, little change had occurred and the samples were assumed to have reached equilibrium.

Similarly, a sample of potassium sulfate was dried at 65°C for one week; weight change was recorded.

Density and Viscosity

Solutions of 1.0, 2.0, 3.0, and 4.0 mg/ml K_2SO_4 in 40% ethanol at 25°C were prepared. Density of each solution and of 40% ethanol was measured using calibrated 25 ml pycnometers. Viscosities of these same solutions were measured using Ostwald viscometers of 150 μm capillary diameter. Type II water was used as reference liquid.

Dissolution in a Column Apparatus

A glass column was constructed for use in all the dissolution experiments. A photograph of the 9 mm column is shown in Figure 1. In general, the column is similar to the one described by Langenbucher (31). Each column

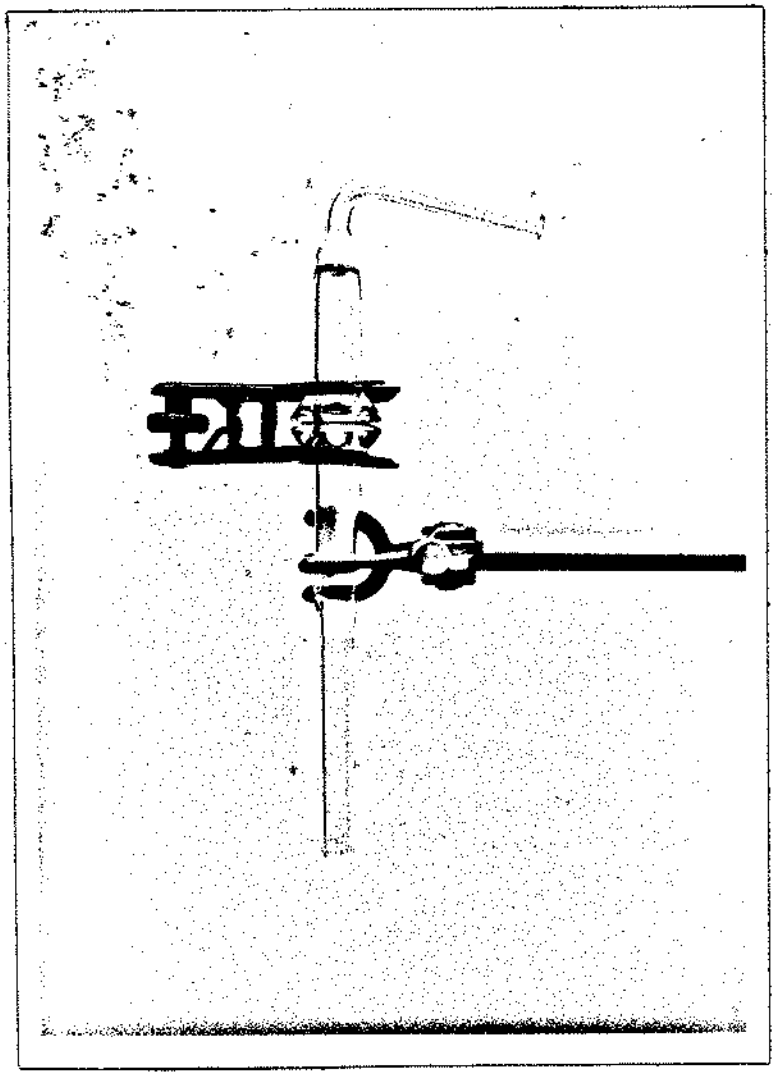

Figure 1. Photograph of 9 mm dissolution column.

consisted of two pieces of glass tube, either 8 mm or 9 mm I.D.; at one end of each piece, an O-ring joint was fused to the glass tube. Fritted glass filters of coarse porosity were fused into each half column at least 4 cm away from the O-ring joint; when the two column parts are joined, these filters define the "length" of the column and confine the solid to a known volume during the dissolution experiment.

Three advantages of this column design are: 1) the total column length can be varied as desired by using column parts of different length; 2) sample introduction is easy since the column is split in half; and 3) this design facilitates easy interruption of a dissolution experiment and removal of undissolved materials from the column.

The top half of the column was tapered above the filter and the tube was bent to an angle greater than 90^{o} to facilitate easy sample collection. An O-ring and clamp were used between the top and bottom portions of the column. The bottom piece was also tapered below the fritted filter. This allowed easy attachment to the fluid pumping system. For the K_2SO_4 dissolution experiments, various ethanol-water mixtures were used as solvent. Water was used for acetaminophen dissolution. Prior to use, these solvents were degassed under vacuum for a short time at room temperature. Then the solvents were maintained in

a constant temperature bath at 25.0 $\pm$ 0.1°C. The solvent was delivered to the dissolution column at a constant rate by a positive displacement pump. For a pumping rate of 0.1 to 9.9 ml/min the analytical pump head was used; a faster pumping rate, 0.3 to 27.7 ml/min in 0.3 ml increments, was provided by a preparative pump head attached to the pump.

On the pump system, the inlet filter assembly consisted of a stainless steel fritted filter attached to teflon tubing; this assembly was placed in the temperature-equilibrated solvent. The other end of the teflon tube was attached to the inlet check valve of the pump.

Stainless steel tubing connected the upper check valve to a pulse dampener; fluid was carried from the dampener by more stainless steel tubing. An empty pre-column (i.e. approximately 6.5 cm long) was attached to this tubing with ferrules and Swagelok fittings.

To begin an experiment, the two clean, dry column parts, an O-ring and clamp, were weighed. A known weight of solid was placed in one portion of the column, the O-ring was centered on the connecting joint and the column was clamped together. This was then weighed again to confirm the initial weight or load of solid in the column. Tygon tubing of appropriate diameter was used to connect the glass dissolution column to the stainless steel

pre-column mentioned above.

Fluid was then transported from the reservoir in the constant temperature bath to the bottom of the column at a pre-set pumping rate. The solvent was pumped from bottom to top of the column to minimize the contribution of free convection to fluid movement; free convection here is due to the density gradient which arises within the column when solute dissolves into the solvent. During all experiments, the pressure reading was barely detectable on the pump gauge; it was always well below 500 psig as indicated on the meter.

Sample collection for all dissolution experiments occurred in the following manner. The column effluent was collected in glass test tubes, which were then covered; samples were collected for one-minute intervals during the first ten minutes. Then every five minutes, the column effluent was collected for either a one or two minute period. Since the column was made of glass, it was possible to watch the movement of the solid within the column as solvent was pumped through it. The time was noted when all the solid had dissolved (i.e. it was no longer visible); samples were generally collected for an additional 30 minutes, and then the experiment ended.

For some experiments, rather than allow all the contents of the column to dissolve, the dissolution was

interrupted. Based on previously generated dissolution profiles, the time for 25, 50, and 75% of the potassium sulfate to dissolve was calculated. The experimental procedure was as follows: at the appropriate time, the pump was stopped and the dissolution column was disconnected from the pre-column. After the O-ring joint was opened, the undissolved contents were rapidly filtered off with coarse porosity filter paper. The column was rinsed with 95% ethanol to obtain quantitative transfer of the K_2SO_4. The undissolved material on the filter paper was also rinsed with ethanol; this solid was dried at room temperature, weighed and retained for further experiments.

Flow rates were frequently monitored by collecting contents of the column during a specified time interval. Although fluctuation was infrequent, it could generally be attributed to insufficient degassing of the solvent or deterioration of the pump seal. Both of these problems were easily remedied.

Preparation of Samples for Analysis

As will be described later, a minimum sample volume of 75 ml was needed if the solution was to be analyzed with the ion-selective electrode; thus, all samples required dilution. It was also determined that the ethanol content of the solution has an effect on the potential recorded.

Therefore, after the volume of each sample was measured to confirm that no significant flow rate fluctuation occurred during the experiment, an aliquot was mixed with a volume of ethanol and diluted to 100 ml with Type II water.

Standard solutions containing known concentrations of potassium ion were prepared by dilution of a 0.5 M K_2SO_4 stock solution; nine solutions with potassium ion concentrations from 10^{-1} to 10^{-5} M were prepared. Standard solutions and samples were prepared to contain the same ethanol concentration.

Potassium sulfate samples analyzed by ion-exchange were first diluted to approximately 50 ml. Acetaminophen samples were diluted with Type II water as needed to have absorbance less than 1.5 at a wavelength of 242.5 nm.

Analytical Techniques

Three different analytical techniques were employed to determine the concentration of solute as a function of time in effluent from the dissolution studies. UV spectroscopy was used for analysis of acetaminophen. Samples were diluted as necessary so that their absorbance at 242.5 nm was less than 1.5; a Beer's law plot was prepared for calculation of concentrations.

The concentrations of K_2SO_4 were determined with either an ion-exchange column or an ion-selective

electrode. Each will be described below, beginning with the latter.

An ion-selective electrode, which is specific for monovalent cations, was used as received. This electrode is approximately eight times more sensitive to potassium ion than to sodium ion, and even less sensitive to lithium and cesium. Its working concentration range is from 10^0 to 10^{-5} moles/liter of monovalent cation. According to the instrument literature, the electrode response is unaffected by pH of the solution as long as it is at least two pH units higher than the pK (where pK is defined as the -log (a_{K^+})). Thus, response of the electrode should follow the Nernst equation for aqueous solution of K_2SO_4 above a potassium ion concentration of 10^{-4}; however, below this concentration some lack of agreement would not be unexpected. When not in use, the electrode was stored in an aqueous solution of 10^{-3} M KCl.

This ion selective electrode must be used in conjunction with a reference electrode. A silver/silver chloride glass double junction reference electrode was selected; this electrode would not exhibit the interference from K^+, Cl^-, or Ag^+ as would be expected with an ordinary single junction reference electrode.

The reference electrode has both an internal and external chamber. Upon receipt from the manufacturer, the

internal chamber contained a Ag/AgCl element surrounded by a solution of 4 M KCl saturated with AgCl. This solution was retained in the internal chamber; when it was necessary to replace this solution, due to evaporation or any other cause, again, a solution of 4 M KCl saturated with AgCl was used.

A 1 M KNO_3 solution was present in the external chamber upon receipt of the electrode from the manufacturer. Since this solution contained the ion which was to be analyzed, it was necessary to replace it with another fully dissociated electrolyte solution to avoid interference. Initially, a 1 M $MgSO_4$ solution was prepared and used in the external chamber. A Nernst-type plot of potential versus logarithm of potassium ion concentration was obtained, but after relatively few determinations, equilibration time became extremely long. The $MgSO_4$ was apparently clogging the external ceramic junction.

After removal of this solution, and cleaning of the electrode with hot Type II water, a 1 M $Mg(NO_3)_2$ solution was prepared and introduced into the outer chamber. Again, this provided a Nernst-type potential vs. logarithm of K^+ concentration response curve, although slightly different than that described above. In general, response times were now acceptable, and junction clogging was minimal. Thus,

the $Mg(NO_3)_2$ solution was used for the remaining experiments. When not in use, the electrode was stored in the 1 M $Mg(NO_3)_2$ solution.

The ion-selective and reference electrodes were plugged into a digital pH/mv meter. Rather than reading a response in pH units, potential in millivolts was read from the digital display.

A minimum of 75 ml of the solution to be analyzed was placed in a small beaker, and the two electrodes were immersed to a depth of not less than 3 cm. The pH meter was turned from Standby to MV. Rather than adding a magnetic stir bar to the solution, the electrodes were agitated in the solution for approximately 40 seconds. Then at one minute intervals, the potential of the solution was noted and recorded, until the potential remained constant for 60 seconds; this was defined as the endpoint of analysis of that sample. The selector dial was changed from MV to Standby, and the electrodes were removed from the solution. They were wiped dry and immersed in the next sample. Note that a typical time required for the signal to stabilize was 3 to 6 minutes, and 8 minutes for K^+ concentration less than 10^{-4} M.

In addition to measuring the potential of the samples, standard solutions of known K^+ concentration were analyzed in the same manner. Thus, each unknown sample was

bracketed by standards. It was important to measure these standards within a relatively short period of measuring the unknown solutions.

For all samples (unknowns and standards) it was necessary to use a Faraday cage which was grounded to the metal case of the pH meter and to a house ground (60,61); Figure 2 shows the Faraday cage used. This helped to minimize aberrant fluctuations in the response of electrode to other than monovalent cation concentrations. In addition, close proximity of a person and movement within 3 feet also caused potential fluctuation. Therefore, following the 40 second agitation, it was necessary to move at least 5 feet away from the electrode in order for the signal to stabilize.

Reproducibility of any measurement made within an hour or two was generally $\pm$ 0.1 mv. However, due to fluctuations in house current, one day to the next, one might see a variation of as much as $\pm$ 2.5 mv. Therefore, it was important to measure and record the potential of all relevant standard solutions each time unknowns were analyzed.

At times, fluctuations in house current led to long equilibration times. There are two methods to overcome this problem. It has been reported (60) that a power-stat transformer will supply constant voltage to the meter, and

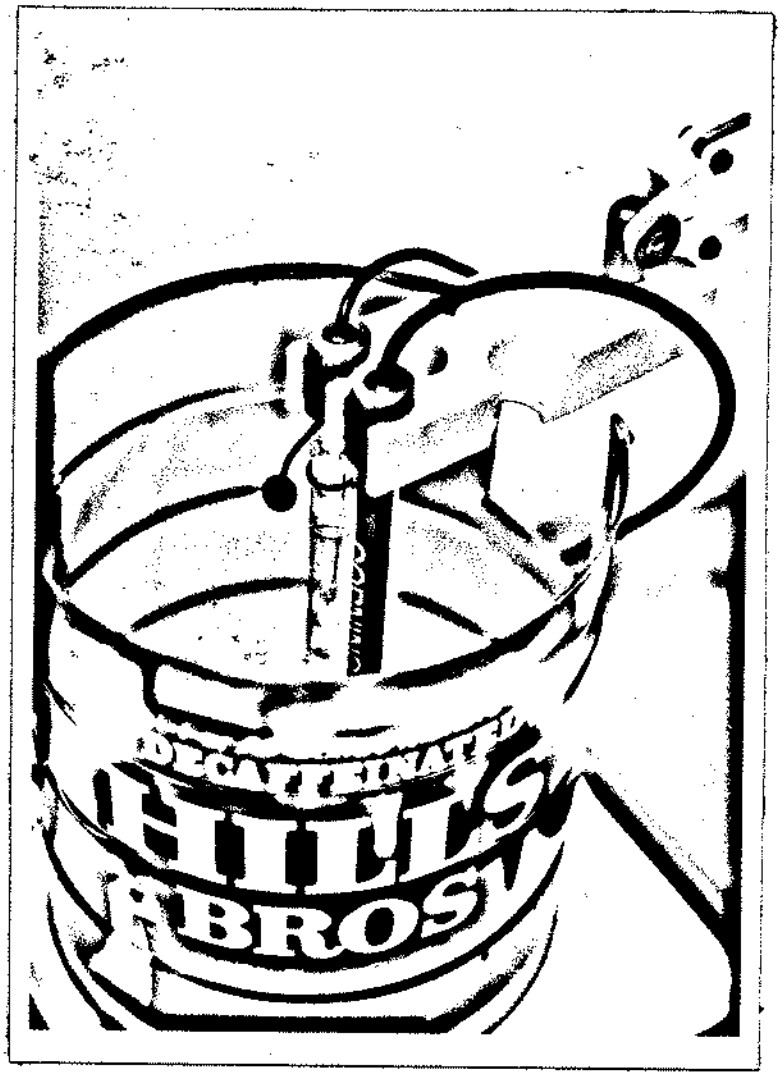

Figure 2. Photograph of Faraday cage and ion-selective and reference electrodes.

thus eliminate this extraneous fluctuation. Another alternative, and the one employed in these studies, was to analyze the samples during a time of day when house current fluctuation was at a minimum (i.e. at night).

In general, response time for ion-selective electrodes is quite long compared to pH electrodes (60,61); theoretically it is predicted to be monotonic and asymptotic and a function of the step-change in sample activities. Therefore, it is best to analyze samples and standards in descending (or ascending) activity levels whenever possible; this procedure should minimize equilibration time.

When equilibration times became extremely long, compared to response times previously noted for solutions of the same activity, it was necessary to change the solutions in the internal and external chambers of the reference electrode. Following removal of these solutions, hot Type II water was used to dissolve any crystals which may have precipitated in either chamber. These liquids were removed, and again 4 M KCl saturated with AgCl for the internal chamber and 1 M $Mg(NO_3)_2$ solution for the external chamber were added. Following any such cleaning of the electrode and change of solutions, an equilibration time of not less than 18 hours was allowed to pass before the electrode was used again.

The alternate method for analysis of K_2SO_4 solutions was the technique of ion exchange (62). Due to long analysis time per sample (i.e. 45-60 minutes), this procedure was used only to validate the ion-selective electrode method described above. An organic strong acid cation exchanger, Rexyn AG50(H), slurried in Type II water, was packed in a 50 ml burette. A 4 $\underline{N}$ H_2SO_4 solution was percolated through the column to generate the acid form of the resin. Based on the weight of resin present, the total exchange capacity was approximately 90 meq. of cation. Assuming about 70% efficiency, this column should be capable of exchanging approximately 5.65 grams K_2SO_4 before regeneration with 4 $\underline{N}$ H_2SO_4 would be required.

Potassium sulfate samples were diluted to a volume of approximately 50 ml. This volume was slowly percolated through the column, followed by about 100-150 ml Type II water; this was sufficient to wash the H^+ out of the column.

Solutions of NaOH were prepared by dilution of a saturated solution. These dilutions were standardized by titration of dried potassium biphthalate, using two drops of phenolphthalein in ethanol (1 g in 100 ml) as an acid-base indicator.

The H_2SO_4 solution from the ion-exchange column was then titrated to a colorometric endpoint with a previously

standardized NaOH solution. Methyl red dissolved in ethanol (0.1 g in 100 ml) was the indicator; a color change from red to yellow was observed over the transition interval of pH 4.2 to 6.2 (63).

RESULTS

Solubility of Potassium Sulfate

The solubility of potassium sulfate in 30, 35, 40, 45, 50, and 60 % V/V ethanol,USP was measured at three different temperatures. The results were determined gravimetrically and are reported in mg/ml in Table 1. Each value is the average of four to six determinations; the standard deviation of each value was less than 1%.

Photomicrographs of Crystals

Variations in crystal shape are best shown by photographs of the crystals. Figure 3 consists of photographs of potassium sulfate crystals from several recrystallization batches. Variation batch-to-batch is noted, as well as heterogeneity within each batch. Any single mesh cut contained a combination of crystal clusters and a small percentage of individual crystals. Magnification factors are listed for each photograph.

Several dissolution experiments were conducted in which, rather than dissolving the entire contents of the column, the dissolution experiment was interrupted when approximately 25, 50, or 75% of the initial load of material had dissolved. Representative photomicrographs of remaining crystals are shown in Figure 4.

TABLE 1. SOLUBILITY OF POTASSIUM SULFATE IN ETHANOL-WATER MIXTURES.

% Ethanol (V/V)	Solubility (mg/ml)*		
	19.9 °C	25.0° C	40.0 °C
30	9.57	10.78	15.00
35	6.33	7.42	11.52
40	4.34	4.70	5.85
45	2.85	3.08	3.82
50	1.85	1.99	2.42
60	0.74	0.78	0.91

* Each value is the mean of 4-6 measurements.

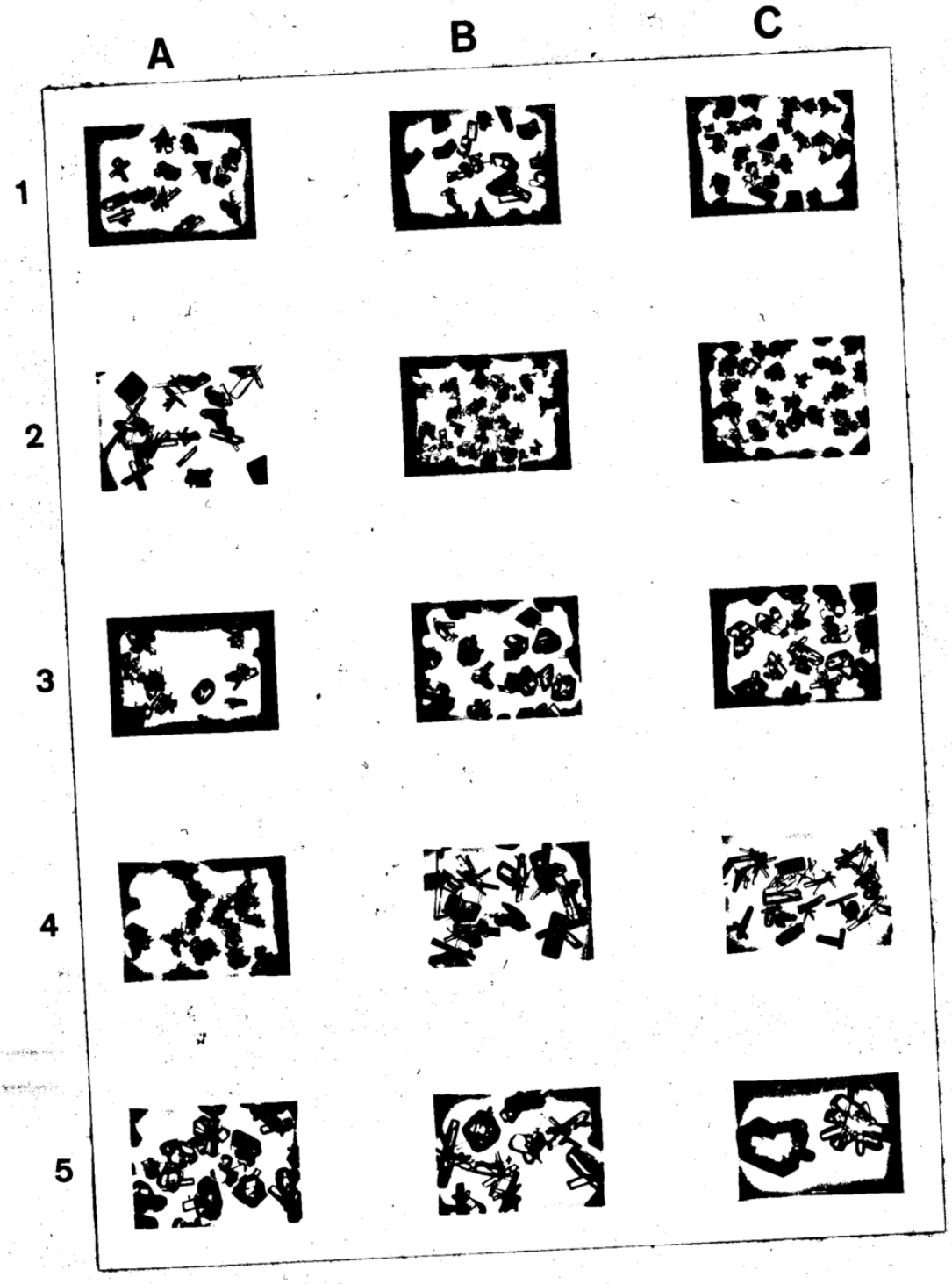
A
B
C
1
2
3
4
5

Surface Area of Recrystallized Solids

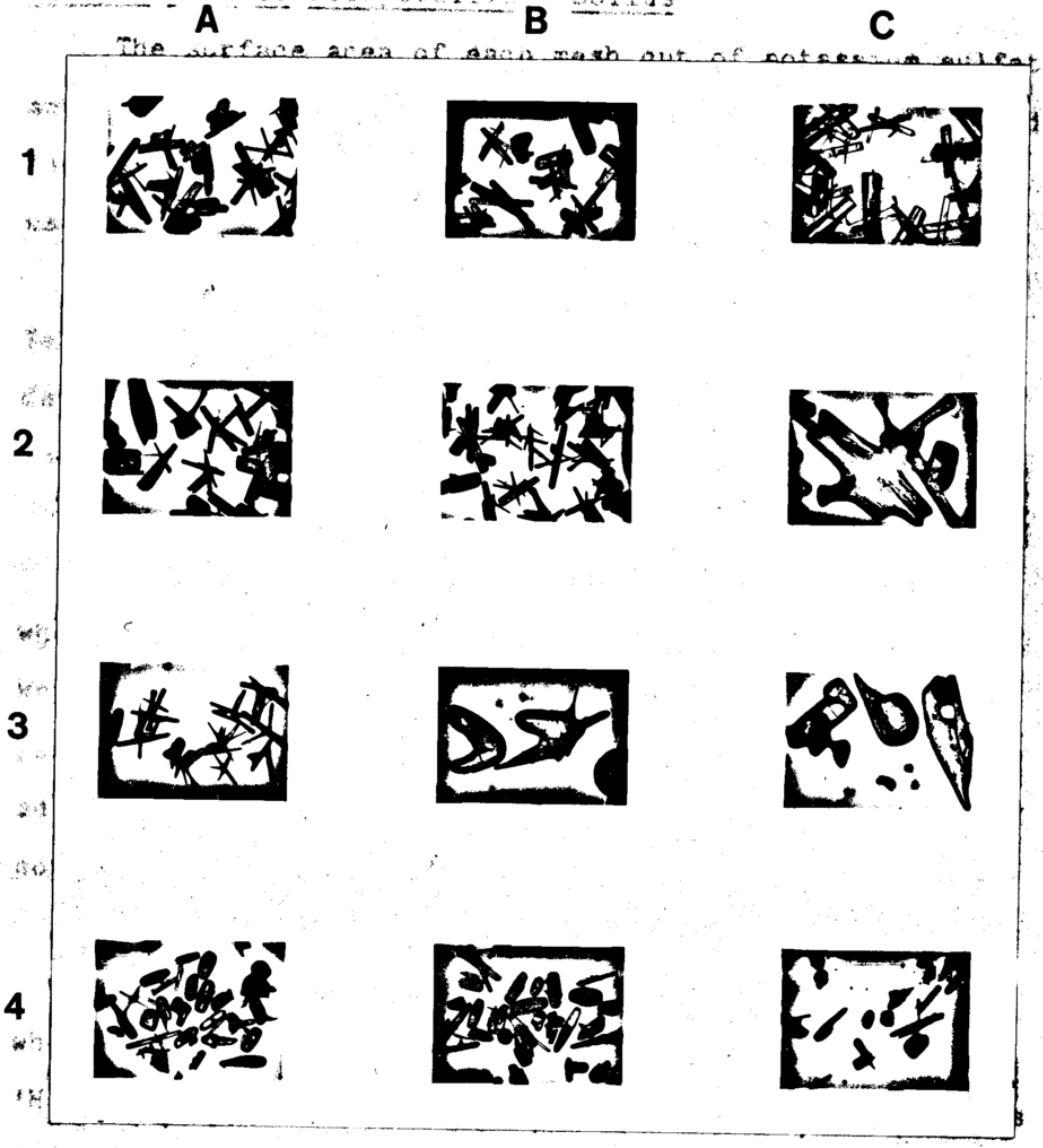

The surface area of each mesh cut of potassium sulfate

the gas constant, and 'T' is absolute temperature.

When (P/Po)/(W(1-P/Po)) is plotted versus (P/Po), Eq. (1) predicts a straight line with slope equal to (D-1)/WmD and intercept equal to 1/WmD; typically, linearity is seen

Surface Area of Recrystallized Solids

The surface area of each mesh cut of potassium sulfate and acetaminophen used in dissolution studies was measured. As described in the previous chapter, gas adsorption was used to quantitate surface area.

To calculate surface area, the Brunauer, Emmett, and Teller (BET) equation (64) was applied to gas adsorption data obtained from use of the Quantasorb Sorption System. The BET equation is:

$$\frac{(P/Po)}{Wm[1 - P/Po]} = \frac{1}{WmD} + \frac{D - 1}{WmD}\frac{P}{Po} \qquad (1)$$

where 'P/Po' is the relative pressure of the adsorbate krypton, 'W' is the weight of krypton sorbed at a particular relative pressure, 'Wm' is the weight of adsorbate corresponding to a complete monolayer, and the constant 'D' is defined by the following expression:

$$D = B \exp\left[(H_1 - H_L)/R\,T\right] \qquad (2)$$

where 'B' is a constant, 'H_1' is the heat of adsorption, 'H_L' is the heat of liquefaction of bulk adsorbate, 'R' is the gas constant, and 'T' is absolute temperature.

When (P/Po)/(W(1-P/Po)) is plotted versus (P/Po), Eq. (1) predicts a straight line with slope equal to (D-1)/WmD and intercept equal to 1/WmD; typically, linearity is seen

in the range $0.05 < P/Po < 0.35$ (58). Algebraic manipulation of the slope and intercept lead to expressions for 'Wm' and 'D'; Wm = 1/(slope + intercept) and D = 1 + (slope/intercept). Then the specific surface area 'As' of the sample is given by:

$$As = \frac{WmNQ}{M_{Kr}WS} \qquad (3)$$

where 'Wm' is defined above, 'N' is Avogadro's number, 'Q' is the cross-sectional area of an adsorbate molecule, 'MKr' is the molecular weight of krypton, and 'Ws' is the sample weight. A cross-sectional area of 19.5×10^{-20} m^2/krypton molecule was assumed in this study (58).

A value for 'W', the weight of krypton sorbed at a particular relative pressure, was calculated from averaged desorption and calibration values as follows:

$$W = \frac{X}{Xc} Vc\left[\frac{PaM_{Kr}}{RT}\right] \qquad (4)$$

where 'X' is the averaged integrated area of desorption peaks at a given relative pressure, 'Vc' and 'Xc' are the volume and averaged integrated area, respectively, of the calibration, and 'Pa' is atmospheric pressure measured in the laboratory at the time of analysis.

Several samples were analyzed multiple times to determine the precision of the method under these experimental conditions. Surface areas of potassium

sulfate and acetaminophen were calculated as described above and all values are reported in Table 2.

X-ray Diffraction of Potassium Sulfate Crystals

Potassium sulfate crystals, ground to a fine powder, were analyzed by X-ray diffraction; the technique, which is based on measurement of the radiation diffracted by planes of the crystal lattice, was used to identify the crystalline phase obtained from recrystallization.

Bragg's law describes the relationship between the radiation and diffraction by various atomic planes in the crystal:

$$m\lambda = 2 d \sin \theta \qquad (5)$$

where 'm' is the order of diffraction, 'λ' is the wavelength of radiation, 'd' is the crystal lattice spacing, and θ is the angle of diffraction (65).

The ASTM X-ray Powder Data File #5-0613 (59) provides information needed to interpret X-ray diffraction results for K_2SO_4. Values for three interplanar spacings (d), the Miller indices to which they correspond (hkl), and the relative intensities (I/I_1) are listed in Table 3. The $CuK\alpha 1$ radiation target had a wavelength of 1.5405 $\mathring{A}$; values for 2θ have been calculated according to Bragg's law and are also listed in Table 3.

The K_2SO_4 sample was slowly scanned from 15-20^{o}, from

TABLE 2. SURFACE AREA OF VARIOUS MESH CUTS OF POTASSIUM SULFATE AND ACETAMINOPHEN

SURFACE AREA OF K_2SO_4 (m^2/g)

RECRYST. BATCH	MESH CUT 20/30	30/40	40/60	60/80	80/100
A			0.025 0.027	0.030	
B		0.012 0.014	0.013	0.017	
C		0.008	0.015	0.017	
D			0.025	0.026	
E			0.039	0.038	
F			0.025	0.028	0.031
G	0.009 0.010	0.011 0.012 0.016	0.020 0.021	0.026 0.027 0.029	0.026 0.028

SURFACE AREA OF ACETAMINOPHEN (m^2/g)

RECRYST. BATCH	MESH CUT 40/60
H	0.058
J	0.060

TABLE 3. PREDICTED AND OBSERVED ANGLES AND UNIT CELL DIMENSIONS FOR X-RAY POWDER DIFFRACTION OF K_2SO_4

d(Å)*	I/I_1*	hkl*	2θ#
2.886	53	200	30.99
5.036	8	020	17.6
3.743	18	002	23.8

	2θ		
Calculated#	30.99	17.6	23.8
Experimental	30.92	17.60	23.75

	Unit Cell Dimensions (Å)		
	a	b	c
Reported*	5.772	10.072	7.486
Experimental	5.996	10.190	7.650

* Ref. 59.
\# Calculated from Bragg's law

22-26°, and from 29-33° at 1/4 degree per minute to precisely identify the angles at which maximum diffraction occurred; these angles were read from the chart recording. Again, Bragg's law was used to convert these experimental values for 2θ to corresponding unit cell dimensions; reported (59) and experimental values for these lattice spacings are also listed in Table 3.

Equilibrium Moisture Content of Potassium Sulfate

Samples of K_2SO_4 exposed to a wide range of relative humidities showed very little weight change. The final weight of each sample reported as a percentage of its initial weight is reported in Table 4 as a function of relative humidity.

A sample of K_2SO_4 dried at 65°C for 7 days reached an equilibrium weight 99.98% of its original weight.

Density and Viscosity of Potassium Sulfate Solutions

In any dissolution experiment the concentration of the solute varied from approximately its solubility to zero concentration. Table 5 lists the density and viscosity of 30, 35, 40, 45, and 50% ethanol and of 1.0, 2.0, 3.0, and 4.0 mg/ml of K_2SO_4 in 40% ethanol at 25°C.

TABLE 4. EQUILIBRIUM MOISTURE CONTENT OF POTASSIUM SULFATE at 25°C

Saturated Salt	%RH*	% Original Weight
$KC_2H_3O_2$	22	99.92
$MgCl_2$	33	99.96
K_2CO_3	43	99.93
NaBr	58	99.96
$NaNO_3$	64	99.95
NaCl	75	100.00
KCl	84	100.02

* Ref. (66).

TABLE 5. DENSITY AND VISCOSITY OF ETHANOL-WATER MIXTURES AND OF K_2SO_4 IN 40% ETHANOL at 25°C

%Ethanol (V/V)	K_2SO_4 (mg/ml)	Density (gm/ml)	Viscosity (cp)
30.0	0.0	0.959	2.010
35.0	0.0	0.952	2.157
45.0	0.0	0.935	NA
50.0	0.0	0.925	2.429
40.0	0.0	0.944	2.246
40.0	1.0	0.945	2.294
40.0	2.0	0.946	2.281
40.0	3.0	0.947	2.279
40.0	4.0	0.947	2.278

Calibration and Use of Ion-Selective Electrode

Unlike standard pH measurements, which require use of only two standards to bracket a wide range of activity (or concentration), measurements of activities of other ions with an ion-selective electrode must be accompanied by multiple calibrations over the concentration range studied. Over a range of five orders of magnitude of potassium ion, for example, the relationship between potential (in millivolts) versus logarithm of potassium ion concentration is nonlinear.

The equilibrium potential values corresponding to a wide range of potassium ion concentration are listed in Table 6. Ionic strength of the solution had no significant effect on the potential values here; this is shown by the use of a 1-1 electrolyte, KCl, as well as a 2-1 electrolyte, K_2SO_4, to establish the range of potassium ion concentrations. These values were measured with the ion-selective and reference electrodes, as described in the previous chapter. For these experiments the outer chamber of the reference electrode contained a 1 M $MgSO_4$ solution.

Due to rapid clogging of the ceramic tip of the reference electrode, the 1 M $MgSO_4$ solution was removed and a 1 M $Mg(NO_3)_2$ solution was used instead. Due to the difference in ionic strength of this solution compared to

TABLE 6. POTENTIAL (mv) AS A FUNCTION OF POTASSIUM ION CONCENTRATION

$[K^+]$	$\log [K^+]$	K_2SO_4 Potential (mv)	KCl Potential (mv)
1×10^{0}	0.0	+ 90.7	---
4×10^{-1}	-0.398	+ 76.5	---
1×10^{-1}	-1.0	+ 51.0	---
4×10^{-2}	-1.398	+ 32.2	---
1×10^{-2}	-2.0	- 0.4	- 0.4
4×10^{-3}	-2.398	- 23.0	---
1×10^{-3}	-3.0	- 59.5	- 59.4
4×10^{-4}	-3.398	- 84.8	---
1×10^{-4}	-4.0	-122.4	-120.8
4×10^{-5}	-4.398	-149.3	---
1×10^{-5}	-5.0	-174.9	-174.0

Note: Solutions contained no ethanol.
Reference electrode external chamber contained 1 M $MgSO_4$

the $MgSO_4$ solution, the range of potentials resulting from the same range of potassium ion concentration was different.

Typical potentials measured for solutions of K_2SO_4 from 10^{-2} to 10^{-5} M are listed in Table 7. These values, as well as those from Table 6, are shown in Figure 5, where potential in millivolts is plotted versus logarithm of potassium ion concentration.

Potential is also dependent on the dielectric constant of the solvent. Values of potential as a function of ethanol concentration at a constant potassium ion concentration are listed in Table 8 and plotted in Figure 6.

Dissolution Experiments

Eight experimental parameters were varied in the dissolution studies to be reported. They were the solute, recrystallization batch, mesh cut, column load, solvent, flow rate, column diameter, and type of pump head. These parameters are more extensively described in Table 9. This table serves as a glossary for Table 10, which is a complete list of all the dissolution runs conducted and the specific experimental parameters in each. Tables 11 through 27 contain the concentrations of solute measured as a function of time for all experiments listed in Table 10.

TABLE 7. POTENTIAL (mv) AS A FUNCTION OF POTASSIUM ION CONCENTRATION

$[K^+]$	LOG $[K^+]$	K_2SO_4 Potential (mv)
1×10^{-2}	-2.0	- 39.2
4×10^{-3}	-2.398	- 69.6
1×10^{-3}	-3.0	-116.4
4×10^{-4}	-3.398	-147.3
1×10^{-4}	-4.0	-192.7
4×10^{-5}	-4.398	-217.2
1×10^{-5}	-5.0	-251.0

Note: Solutions contained 6.5 % ethanol.
Reference electrode external chamber contained 1 M $Mg(NO_3)_2$

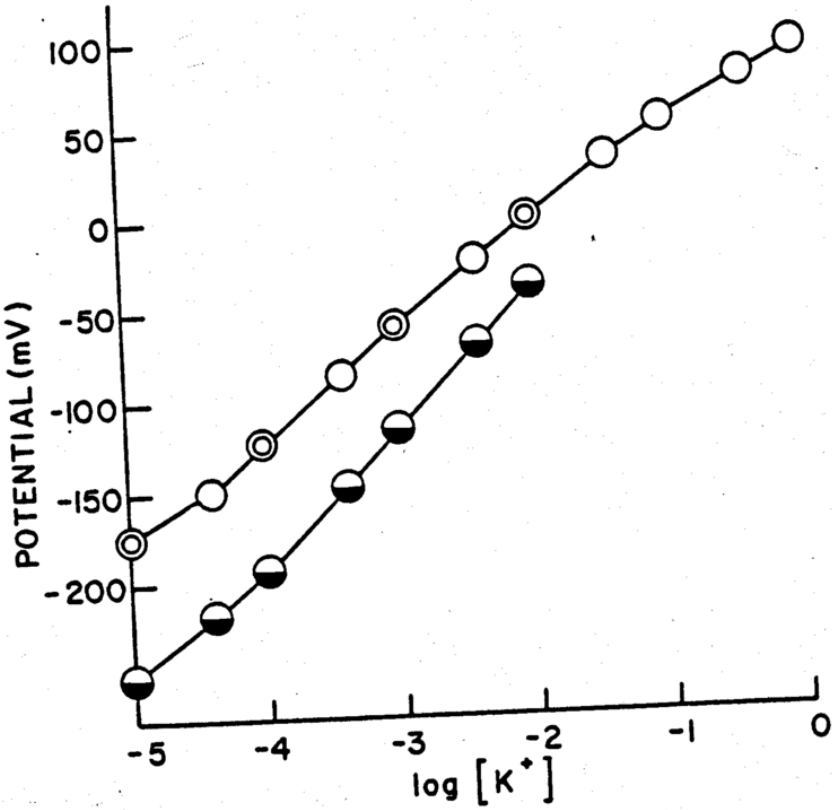
100
50
0
-50
-100
-150
-200
POTENTIAL (mV)
-5
-4
-3
-2
-1
0
log [K+]

TABLE 8. POTENTIAL (mv) AS A FUNCTION OF ETHANOL CONCENTRATION

% Ethanol	Potential (mv)
0	- 36.6
10	- 51.5
20	- 66.2
30	- 81.0

Note: Potassium ion concentration, present as K_2SO_4, was 5×10^{-2} M

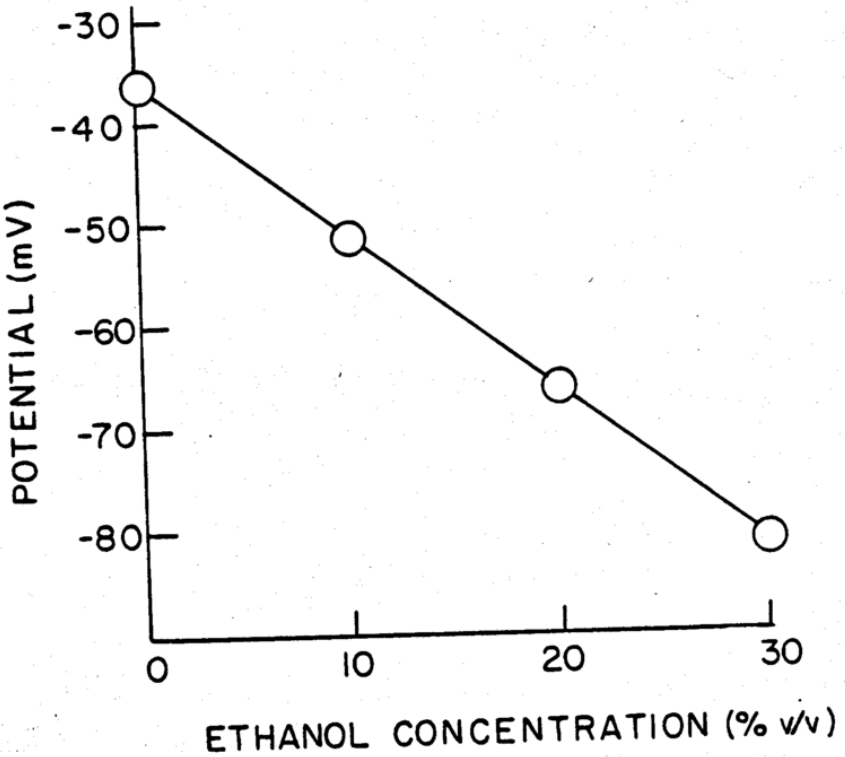
-30
-40
-50
-60
-70
-80
POTENTIAL (mV)
0
10
20
30
ETHANOL CONCENTRATION (% v/v)

TABLE 9. LIST OF EXPERIMENTAL PARAMENTERS

SOLUTE #1: Potassium Sulfate
#2: Acetaminophen

(Recrystallization) Batch:
Potassium Sulfate A through G
Acetaminophen H and J

Mesh Cut: 20/30, 30/40, 40/60, 60/80, 80/100

(Initial Column Contents) Wt: 0.43 - 1.50 gram

% Ethanol: 30, 35, 40, 50, 60 (V/V)

Flow Rate: from 3.2 to 25.3 ml/min

Column Diameter: 8 mm or 9 mm I.D.

Pump Head: A : Analytical pump head
P : Preparative pump head

Table 10. Column Dissolution Experiments

RUN#	SOLUTE	BATCH	MESH CUT	WT(g)	% Ethanol	FLOW RATE	COLM DIAM	PUMP HEAD
1	1	A	60/80	0.43	40	5.0	9	A
2	1	A	60/80	1.00	40	5.25	9	A
3	1	A	60/80	1.12	40	5.35	9	A
4	1	A	60/80	1.25	40	5.35	9	A
5	1	A	60/80	1.50	40	5.3	9	A
6	1	A	60/80	1.00	40	9.2	9	A
7	1	A	60/80	1.00	60	9.2	9	A
8	1	A	40/60	1.00	40	5.4	9	A
9	1	B	60/80	1.00	40	5.35	9	A
10	1	B	40/60	1.00	40	5.4	9	A
11	1	B	40/60	1.00	40	5.4	9	A
12	1	B	30/40	1.00	40	5.25	9	A
13	1	B	30/40	1.00	40	5.3	9	A
14	1	B	30/40	1.00	40	9.2	9	A
15	1	C	60/80	1.00	40	5.4	9	A
16	1	C	40/60	1.00	40	5.4	9	A
17	1	D	60/80	1.00	40	5.4	9	A
18	1	E	60/80	1.00	40	5.4	9	A
19	1	E	40/60	1.00	40	5.35	9	A
20	1	G	80/100	1.00	40	5.35	9	A
21	1	G	80/100	1.00	40	5.35	9	A
22	1	G	60/80	1.00	30	5.4	9	A
23	1	G	60/80	1.00	35	5.3	9	A
24	1	G	60/80	1.00	40	5.35	9	A
25	1	G	60/80	1.00	40	5.35	9	A
26	1	G	60/80	1.00	50	5.2	9	A
27	1	G	40/60	0.50	40	5.35	9	A
28	1	G	40/60	0.75	40	5.3	9	A
29	1	G	40/60	1.00	40	5.3	9	A
30	1	G	40/60	1.00	40	5.3	9	A
31	1	G	40/60	1.25	40	5.3	9	A
32	1	G	40/60	1.25	40	5.3	9	A
33	1	G	40/60	1.50	40	5.35	9	A
34	1	G	40/60	1.00	30	5.35	9	A
35	1	G	40/60	1.00	35	5.3	9	A
36	1	G	40/60	1.00	50	5.3	9	A
37	1	G	30/40	1.00	30	5.35	9	A
38	1	G	30/40	1.00	35	5.3	9	A
39	1	G	30/40	1.00	40	5.3	9	A
40	1	G	30/40	1.00	40	5.3	9	A
41	1	G	30/40	1.00	50	5.3	9	A
42	1	G	20/30	1.00	30	5.4	9	A
43	1	G	20/30	1.00	35	5.3	9	A

Table 10. (cont.)

RUN#	SOLUTE	BATCH	MESH CUT	WT(g)	% Ethanol	FLOW RATE	COLM DIAM	PUMP HEAD
44	1	G	20/30	1.00	40	5.35	9	A
45	1	G	20/30	1.00	40	5.3	9	A
46	1	G	20/30	1.00	50	5.45	9	A
47*	1	G	40/60	1.00	40	5.35	9	A
48*	1	G	40/60	1.00	40	5.35	9	A
49*	1	G	40/60	1.00	40	5.35	9	A
50*	1	G	40/60	1.00	40	5.35	9	A
51*	1	G	40/60	1.00	40	5.35	9	A
52*	1	G	40/60	1.00	40	5.35	9	A
53	1	G	##	1.00	40	5.3	9	A
54	1	G	##	1.00	40	5.35	9	A
55**	1	G	40/60	1.00	40	5.35	9	A
56**	1	G	40/60	1.00	40	5.35	9	A
57**	1	G	40/60	1.00	40	5.35	9	A
58**	1	G	40/60	1.00	40	5.35	9	A
59**	1	G	40/60	1.00	40	5.35	9	A
60**	1	G	40/60	1.00	40	5.35	9	A
61**	1	G	40/60	1.00	40	5.35	9	A
62	1	G	##	1.00	40	5.3	9	A
63	1	G	##	1.00	40	5.4	9	A
64#	1	G	40/60	1.00	40	5.35	9	A
65	1	G	40/60	1.00	40	3.2	8	A
66	1	G	40/60	1.00	40	5.35	8	A
67	1	G	30/40	0.77	40	3.25	8	P
68	1	G	30/40	0.77	40	6.4	8	P
69	1	G	30/40	0.77	40	9.8	8	P
70	1	G	30/40	0.77	40	12.7	8	P
71	1	G	30/40	0.77	40	15.8	8	P
72	1	G	30/40	1.00	40	3.25	8	P
73	1	G	30/40	1.00	40	5.25	9	P
74	1	G	30/40	1.00	40	10.6	9	P
75	1	G	30/40	1.00	40	15.6	9	P
76	1	G	30/40	1.00	40	20.8	9	P
77	1	G	30/40	1.00	40	25.3	9	P
78	2	H	40/60	1.00	0	5.6	9	A
79	2	J	40/60	1.00	0	5.6	9	A

* Stopped after 25% dissolved.
** Stopped after 50% dissolved.
\# Stopped after 75% dissolved.
See text for description of material used.

TABLE 11. K_2SO_4 CONCENTRATION (mg/ml) FOR DISSOLUTION OF VARIOUS COLUMN LOADS OF 60/80 MESH, BATCH A

TIME (min)	RUN # #1 0.43 g	#2 1.00 g	#3 1.12 g	#4 1.25 g	#5 1.50 g
0.5	3.57	4.27	4.29	4.51	4.49
1.5	3.63	4.32	4.33	4.55	4.49
2.5	3.60	4.28	4.29	4.56	4.44
3.5	3.55	4.25	4.32	4.56	4.43
4.5	3.50	4.27	4.29	4.56	4.45
5.5	3.44	4.22	4.31	4.58	4.48
6.5	3.35	4.22	4.31	4.56	4.50
7.5	3.27	4.22	4.30	4.56	4.49
8.5	3.18	4.24	4.29	4.55	4.50
9.5	3.10	4.22	4.29	4.55	4.50
15.0	2.66	4.09	4.27	4.53	4.55
20.0	2.17	3.94	4.18	4.50	4.53
25.0	1.57	3.76	4.03	4.40	4.47
30.0	1.00	3.47	3.84	4.27	4.42
35.0	0.55	3.22	3.58	4.01	4.30
40.0	0.28	2.66	3.19	3.66	4.13
45.0	0.04	2.22	2.79	3.13	3.93
50.0	0.01	1.79	2.25	2.69	3.66
55.0	<0.01	0.80	1.56	2.14	3.39
60.0		0.12	0.14	0.43	2.93
65.0		0.03	0.01	0.10	2.14
70.0		0.01	0.01	0.03	0.30
75.0		<0.01	0.01	0.01	0.07
80.0			0.01	<0.01	0.03
85.0			<0.01		0.03
90.0					0.02

TABLE 12. K_2SO_4 CONCENTRATION (mg/ml) FOR DISSOLUTION OF 1.00 GRAM OF 60/80 MESH FROM VARIOUS BATCHES

TIME (min)	RUN # #9 B	#15 C	#17 D	#18 E
0.5	4.52	4.53	4.39	4.05
1.5	4.41	4.57	4.39	4.11
2.5	4.40	4.59	4.53	4.10
3.5	4.40	4.57	4.53	4.02
4.5	4.36	4.57	4.53	4.07
5.5	4.34	4.53	4.53	4.13
6.5	4.30	4.49	4.53	4.16
7.5	4.30	4.53	4.53	4.17
8.5	4.28	4.42	4.53	4.32
9.5	4.28	4.46	4.53	4.33
15.0	4.12	4.47	4.59	4.51
20.0	3.91	4.28	4.38	4.54
25.0	3.66	3.98	4.19	4.43
30.0	3.34	3.62	3.82	4.27
35.0	3.10	3.15	3.28	3.86
40.0	2.67	2.59	2.58	2.64
45.0	2.17	2.01	0.87	0.57
50.0	1.51	1.10	0.12	0.08
55.0	0.25	0.22	0.05	0.04
60.0	0.09	0.06	0.04	0.03
65.0	0.02	0.02	0.03	0.03
70.0	0.02	<0.01	0.02	0.02
75.0	0.01		0.01	0.02
80.0	0.01		<0.01	0.01
85.0	<0.01			0.01
90.0				0.01
95.0				0.01

TABLE 13. K_2SO_4 CONCENTRATION (mg/ml) FOR DISSOLUTION OF 1.00 GRAM OF 40/60 MESH FROM VARIOUS BATCHES

TIME (min)	RUN # #8 A	#10 B	#11 B	#16 C	#19 E
0.5	4.78	4.40	4.39	4.66	4.60
1.5	4.72	4.37	4.45	4.51	4.57
2.5	4.61	4.36	4.44	4.49	4.59
3.5	4.61	4.32	4.41	4.48	4.63
4.5	4.54	4.28	4.35	4.41	4.64
5.5	4.54	4.24	4.37	4.35	4.54
6.5	4.55	4.28	4.41	4.33	4.59
7.5	4.55	4.23	4.39	4.41	4.59
8.5	4.51	4.25	4.35	4.37	4.70
9.5	4.48	4.16	4.27	4.38	4.59
15.0	4.33	4.08	4.14	4.18	4.54
20.0	4.13	3.87	3.93	4.06	4.61
25.0	3.84	3.68	3.69	3.77	4.53
30.0	3.44	3.33	3.36	3.44	4.26
35.0	2.94	2.97	3.00	2.98	3.69
40.0	2.45	2.49	2.50	2.50	2.62
45.0	1.79	2.00	1.88	1.86	0.85
50.0	1.00	1.44	1.25	1.22	0.25
55.0	0.31	0.92	0.72	0.67	0.07
60.0	0.07	0.52	0.27	0.25	0.04
65.0	0.02	0.18	0.10	0.08	0.02
70.0	0.01	0.08	0.04	0.02	0.01
75.0	<0.01	0.03	0.02	<0.01	<0.01
80.0		0.02	0.02		
85.0		<0.01	0.01		
90.0			0.01		
95.0			<0.01		

TABLE 14. K_2SO_4 CONCENTRATION (mg/ml) FOR DISSOLUTION OF 1.00 GRAM OF VARIOUS MESH CUTS AND BATCHES AT DIFFERENT FLOW RATES

	RUN #				
TIME (min)	#6 A 60/80	#7 A 60/80	#14 B 30/40	#12 B 30/40	#13 B 30/40
	Flow Rate (ml/min): 9.2	9.2	9.2	5.25	5.3
0.5	3.89	0.61	2.97	3.24	3.96
1.5	3.91	0.61	2.98	3.34	3.95
2.5	3.89	0.61	2.96	3.34	3.61
3.5	3.88	0.62	2.95	3.20	3.98
4.5	3.88	0.60	2.90	3.00	3.96
5.5	3.85	0.63	2.87	3.12	3.93
6.5	3.79	0.63	2.80	3.16	3.83
7.5	3.71	0.64	2.80	3.19	3.72
8.5	3.69	0.64	2.74	3.28	3.82
9.5	3.65	0.64	2.70	3.26	3.80
15.0	3.29	0.66	2.47	3.05	3.58
20.0	2.93	0.65	2.21	2.91	3.38
25.0	2.49	0.63	1.98	2.80	3.14
30.0	1.95	0.64	1.71	2.63	2.89
35.0	1.06	0.59	1.47	2.44	2.63
40.0	0.12	0.58	1.19	2.31	2.35
45.0	0.03	0.53	0.98	2.08	2.09
50.0	0.01	0.43	0.73	1.87	1.77
55.0	<0.01	0.38	0.53	1.68	1.43
60.0		0.33	0.35	1.51	1.08
65.0			0.21	1.29	0.81
70.0			0.11	1.10	0.56
75.0			0.05	0.88	0.36
80.0			0.02	0.68	0.22
85.0				0.50	0.12
90.0				0.34	0.05
95.0				0.19	0.01
100.0				0.13	<0.01
105.0				0.09	
110.0				0.03	
115.0				0.02	

TABLE 15. K_2SO_4 CONCENTRATION (mg/ml) FOR DISSOLUTION OF BATCH G, 40/60 MESH AND VARIOUS COLUMN LOADS

	RUN #						
	#27	#28	#29	#30	#31	#32	#33
TIME (min)	0.50g	0.75g	1.00g	1.00g	1.25g	1.25g	1.50g
0.5	3.53	4.15	4.33	4.19	4.03	3.96	4.31
1.5	3.57	4.07	4.23	4.22	4.04	3.97	4.32
2.5	3.54	4.01	4.24	4.19	4.04	3.95	4.31
3.5	3.48	4.00	4.22	4.13	4.08	3.89	4.29
4.5	3.48	4.00	4.22	4.25	4.05	3.95	4.26
5.5	3.41	4.01	4.17	4.16	4.08	3.96	4.33
6.5	3.36	3.99	4.19	4.16	4.09	3.89	4.32
7.5	3.29	3.87	4.16	4.18	3.94	3.91	4.34
8.5	3.24	3.90	4.14	4.18	3.89	3.90	4.30
9.5	3.14	3.90	4.11	4.13	4.01	3.85	4.29
15.0	2.64	3.60	4.00	4.13	3.97	3.96	4.19
20.0	2.35	3.37	3.91	3.95	3.94	3.86	4.14
25.0	1.90	3.04	3.67	3.75	3.93	3.75	4.03
30.0	1.40	2.58	3.41	3.45	3.82	3.70	4.04
35.0	0.89	2.05	3.12	3.08	3.69	3.55	3.99
40.0	0.50	1.41	2.67	2.63	3.39	3.41	3.96
45.0	0.27	0.82	2.14	1.93	3.17	3.14	3.73
50.0	0.13	0.44	1.51	1.39	2.82	2.85	3.55
55.0	0.05	0.20	0.85	0.79	2.31	2.46	3.27
60.0	0.02	0.08	0.36	0.37	1.76	2.03	2.88
65.0	<0.01	0.02	0.12	0.12	1.11	1.49	2.40
70.0		<0.01	0.03	0.03	NA	0.90	1.77
75.0			0.01	0.01	NA	0.36	1.01
80.0			<0.01	<0.01	0.05	0.08	0.19
85.0					0.01	0.04	0.05
90.0					<0.01	0.01	0.02
95.0						0.01	0.01
100.0						<0.01	<0.01

TABLE 16. K_2SO_4 CONCENTRATION (mg/ml) FOR DISSOLUTION OF VARIOUS MESH CUTS OF BATCH G

	RUN #			
TIME (MIN)	#44 20/30	#45 20/30	#39 30/40	#40 30/40
0.5	3.28	3.27	4.12	4.34
1.5	3.15	3.19	4.08	4.14
2.5	3.10	3.11	4.03	4.07
3.5	3.11	3.12	4.00	4.04
4.5	3.12	3.08	3.98	3.99
5.5	3.13	3.09	3.98	3.90
6.5	3.18	3.05	3.94	3.90
7.5	3.13	3.07	3.94	3.90
8.5	3.09	3.04	3.95	3.90
9.5	3.09	3.03	3.90	3.82
15.0	2.91	2.86	3.71	3.66
20.0	2.76	2.73	3.49	3.46
25.0	2.65	2.59	3.31	3.25
30.0	2.48	2.47	3.02	3.00
35.0	2.26	2.30	2.70	2.73
40.0	2.14	2.09	2.37	2.43
45.0	1.96	1.96	2.02	2.09
50.0	1.74	1.77	1.63	1.57
55.0	1.57	1.60	1.26	1.32
60.0	1.40	1.44	0.88	0.94
65.0	1.26	1.29	0.56	0.63
70.0	1.09	1.14	0.32	0.39
75.0	0.96	1.00	0.17	0.21
80.0	0.81	0.87	0.08	0.11
85.0	0.67	0.75	0.02	0.04
90.0	0.49	0.60	<0.01	0.01
95.0	0.43	0.47		<0.01
100.0	0.31	0.37		
105.0	0.21	0.28		
110.0	0.14	0.21		
115.0	NA	0.15		
120.0		0.09		
125.0		0.05		

TABLE 17. K_2SO_4 CONCENTRATION (mg/ml) FOR DISSOLUTION OF VARIOUS MESH CUTS OF BATCH G

	RUN #			
	#24	#25	#20	#21
TIME (min)	60/80	60/80	80/100	80/100
0.5	4.24	4.19	4.19	3.82
1.5	4.13	4.16	4.14	3.73
2.5	4.14	4.15	4.10	3.76
3.5	4.13	4.12	4.10	3.72
4.5	4.18	4.07	4.16	3.67
5.5	4.12	4.11	4.16	3.68
6.5	4.13	4.12	4.16	3.84
7.5	4.18	4.11	4.16	3.87
8.5	4.13	4.08	NA	3.98
9.5	4.13	4.22	4.18	3.96
15.0	4.10	3.91	4.10	3.90
20.0	4.06	3.84	4.02	3.87
25.0	3.89	3.76	4.08	3.84
30.0	3.69	3.49	3.74	3.63
35.0	3.37	3.22	3.40	3.30
40.0	2.95	2.88	2.98	2.94
45.0	2.37	2.39	2.51	2.49
50.0	1.37	1.53	0.40	0.47
55.0	0.12	0.26	0.08	0.18
60.0	0.06	0.07	0.03	0.03
65.0	0.03	0.04	0.01	0.01
70.0	0.02	0.02	0.01	<0.01
75.0	0.01	0.02	0.01	
80.0	0.01	0.01	<0.01	
85.0	<0.01	<0.01		

TABLE 18. K_2SO_4 CONCENTRATION (mg/ml) FOR DISSOLUTION OF VARIOUS MESH CUTS OF BATCH G IN 30% ETHANOL

	RUN #			
	#42	#37	#34	#22
TIME (min)	20/30	30/40	40/60	60/80
0.5	6.55	9.03	9.90	9.76
1.5	6.42	8.74	9.67	9.70
2.5	6.34	8.66	9.44	9.67
3.5	6.27	8.63	9.33	9.64
4.5	6.19	8.55	9.30	9.55
5.5	6.17	8.40	9.19	9.41
6.5	6.12	8.23	9.14	9.30
7.5	6.06	8.14	9.00	9.27
8.5	6.01	7.82	8.84	9.11
9.5	5.94	7.84	8.74	8.95
15.0	5.45	6.47	7.35	7.47
20.0	4.57	4.90	4.76	5.06
25.0	3.70	3.12	1.06	0.23
30.0	2.83	1.31	0.11	0.20
35.0	2.10	0.35	0.04	0.04
40.0	1.37	0.08	0.03	0.01
45.0	0.79	0.04	0.02	0.02
50.0	0.36	0.04	0.01	0.01
55.0	0.11	0.03	0.01	0.01
60.0	0.04	0.02	<0.01	<0.01
65.0	0.03	0.01		
70.0	0.02	<0.01		
75.0	0.01			
80.0	<0.01			

TABLE 19. K_2SO_4 CONCENTRATION (mg/ml) FOR DISSOLUTION OF VARIOUS MESH CUTS OF BATCH G IN 35% ETHANOL

	RUN #			
	#43	#38	#35	#23
TIME (min)	20/30	30/40	40/60	60/80
0.5	4.55	5.67	6.20	6.25
1.5	4.57	5.56	6.16	6.17
2.5	4.54	5.61	5.98	6.05
3.5	4.55	5.49	5.96	6.06
4.5	4.50	5.45	5.93	5.98
5.5	4.46	5.40	5.98	5.98
6.5	4.47	5.41	5.91	5.85
7.5	4.45	5.32	5.88	5.90
8.5	4.42	5.26	5.86	5.96
9.5	4.42	5.29	5.88	5.98
15.0	4.13	4.97	5.51	5.62
20.0	3.93	4.37	5.09	5.21
25.0	3.50	3.83	4.49	4.45
30.0	3.09	3.22	3.35	3.48
35.0	2.69	2.49	2.01	2.06
40.0	2.20	1.75	0.90	0.43
45.0	1.77	1.04	0.32	0.11
50.0	1.41	0.54	0.11	0.05
55.0	1.05	0.27	0.06	0.03
60.0	0.75	0.12	0.04	0.04
65.0	0.49	0.05	0.03	0.01
70.0	0.29	0.03	0.02	0.01
75.0	0.15	0.02	0.01	0.01
80.0	0.06	0.01	0.01	<0.01
85.0	0.03	0.01	<0.01	
90.0	0.02	<0.01		
95.0	0.01			
100.0	<0.01			

TABLE 20. K_2SO_4 CONCENTRATION (mg/ml) FOR DISSOLUTION OF VARIOUS MESH CUTS OF BATCH G IN 50% ETHANOL

	RUN #			
	#46	#41	#36	#26
TIME (min)	20/30	30/40	40/60	60/80
0.5	1.28	1.66	1.72	1.84
1.5	1.29	1.65	1.68	1.85
2.5	1.26	1.64	1.70	1.84
3.5	1.25	1.62	1.69	1.84
4.5	1.24	1.61	1.70	1.83
5.5	1.24	1.61	1.75	1.83
6.5	1.24	1.61	1.69	1.83
7.5	1.24	1.48	1.66	1.82
8.5	1.24	1.47	1.66	1.83
9.5	1.24	1.47	1.68	1.81
15.0	1.24	1.58	1.66	1.81
20.0	1.24	1.59	1.67	1.80
25.0	NA	NA	1.66	1.80
30.0	1.22	1.56	1.65	1.81
35.0	NA	NA	1.66	1.81
40.0	1.18	1.48	1.63	1.79
45.0	NA	NA	1.60	1.79
50.0	1.18	1.40	1.58	1.76
55.0	NA	NA	1.56	1.74
60.0	1.13	1.34	1.52	1.70
65.0	NA	NA	1.49	1.65
70.0	NA	1.28	1.45	1.59
75.0	1.06	NA	1.42	1.55
80.0	1.03	1.26	1.41	1.46
85.0	NA	NA	1.36	1.38
90.0	0.90	1.15	1.27	1.29
95.0	NA	NA	1.24	1.19
100.0	0.87	1.04	1.14	1.07
105.0	NA	NA	1.04	0.93
110.0	0.81	0.98	0.95	0.80
115.0	NA	0.86	0.84	0.60
120.0	0.75	0.80	0.73	0.37
125.0	0.71	0.73	0.60	0.13

TABLE 20. (CONT.)

TIME (min)	RUN # #46 20/30	#41 30/40	#36 40/60	#26 60/80
130.0	0.67	0.67	0.49	0.06
135.0	NA	0.60	0.39	0.05
140.0	0.61	0.53	0.30	0.03
145.0	NA	0.47	0.22	0.02
150.0	0.55	0.41	0.16	0.02
155.0	NA	0.36	0.11	0.01
160.0	0.49	0.30	0.07	0.01
165.0	NA	0.24	0.05	<0.01
170.0	0.43	0.20	0.04	
175.0	NA	0.16	0.03	
180.0	0.37	0.13	0.02	
185.0	NA	0.10	0.02	
190.0	0.32	0.08	0.01	
195.0	NA	0.06	0.01	
200.0	0.26	0.05	<0.01	
205.0	0.24	0.04		
210.0	0.22	0.03		
215.0	0.20	0.02		
220.0	0.18	0.01		
225.0	0.16	<0.01		
230.0	0.14			
235.0	0.12			
240.0	0.11			
245.0	0.09			
250.0	0.08			
255.0	0.06			
260.0	0.05			
265.0	0.04			
270.0	0.04			
275.0	0.02			

TABLE 21. K_2SO_4 CONCENTRATION (mg/ml) FOR DISSOLUTION INTERRUPTED AFTER 25% DISSOLVED

	RUN #					
	#47	#48	#49	#50	#51	#52
TIME (min)	1.00g	1.00g	1.00g	1.00g	1.00g	1.00g
0.5	4.27	4.43	4.68	3.88	4.36	4.08
1.5	4.27	4.42	4.57	3.93	4.27	4.10
2.5	4.25	4.31	4.48	3.89	4.15	4.08
3.5	4.26	4.35	4.38	3.79	4.13	4.01
4.5	4.24	4.24	4.37	3.79	4.07	4.01
5.5	4.27	4.25	4.33	3.75	4.07	4.01
6.5	4.22	4.29	4.30	3.77	4.06	3.96
7.5	4.24	4.24	4.29	3.75	4.01	3.96
8.5	4.22	4.26	4.25	3.71	4.00	3.95
9.5	4.18	4.28	4.24	3.62	3.96	3.95
Mass Remaining (gram)	0.75	0.74	0.73	0.77	0.76	0.77

TABLE 22. K_2SO_4 CONCENTRATION (mg/ml) FOR DISSOLUTION INTERRUPTED AFTER 50% DISSOLVED

TIME (min)	RUN # #55 1.00g	#56 1.00g	#57 1.00g	#58 1.00g	#59 1.00g	#60 1.00g	#61 1.00g
0.5	4.38	4.17	4.06	4.12	4.10	4.01	4.12
1.5	4.44	4.16	4.14	4.18	4.02	4.01	4.19
2.5	4.42	4.20	4.28	4.13	4.08	4.02	4.20
3.5	4.34	4.20	4.05	4.11	4.05	4.08	4.16
4.5	4.35	4.20	4.05	4.03	3.99	4.05	4.13
5.5	4.31	4.16	4.05	4.06	4.03	4.04	4.11
6.5	4.31	4.16	4.11	4.01	4.01	4.05	4.13
7.5	4.33	4.14	4.01	3.99	3.99	4.05	4.13
8.5	4.28	4.13	3.99	4.01	3.99	3.99	4.11
9.5	4.28	4.11	3.99	3.98	4.00	4.01	4.18
15.0	4.16	3.98	3.94	3.89	3.85	3.81	3.96
20.0	4.03	3.92	3.84	3.83	3.78	3.68	3.82
25.0	3.98	3.87	N/A	3.76	3.74	3.82	3.75
MASS REMAINING (gram)	0.44	0.46	0.52	0.50	0.41	0.51	0.53

TABLE 23. K_2SO_4 CONCENTRATION (mg/ml) FOR DISSOLUTION INTERRUPTED AT VARIOUS TIMES

	RUN #				
	#64	#53	#54	#62	#63
TIME (min)	1.00g	1.00g	1.00g	1.00g	1.00g
0.5	3.96	3.85	3.96	4.29	3.96
1.5	3.98	3.85	3.91	4.33	3.96
2.5	4.02	3.85	3.93	4.29	3.99
3.5	3.99	3.86	3.90	4.30	3.95
4.5	3.96	3.87	3.95	4.30	3.97
5.5	3.96	3.87	3.91	4.32	3.98
6.5	3.94	3.85	3.95	4.29	3.98
7.5	3.92	3.84	3.94	4.29	3.97
8.5	3.86	3.82	3.93	4.28	3.99
9.5	3.89	3.81	3.93	4.25	3.98
15.0	3.91	3.70	3.81	4.13	3.93
20.0	3.77	3.61	3.75	4.00	3.82
25.0	3.61	3.50	3.71	3.79	
30.0	3.41	3.34		3.63	
35.0	3.14	3.09		3.25	
40.0		2.83		2.74	
45.0		2.42		2.22	
50.0		1.92		1.49	
55.0		1.39		0.64	
60.0		0.81		0.14	
65.0		0.34		0.04	
70.0		0.13		0.04	
75.0		0.08		0.03	
80.0		0.06		0.01	
85.0		0.05		0.01	
90.0		0.04		<0.01	
95.0		0.02			
100.0		0.02			
110.0		0.01			
120.0		<0.01			
MASS REMAINING (gram)	0.24		0.47		0.54

TABLE 24. K_2SO_4 CONCENTRATION (mg/ml) FOR DISSOLUTION OF 1.00 GRAM IN AN 8 mm I.D. COLUMN

TIME (min)	RUN # #65 40/60 Flow Rate: 3.2 (ml/min)	#66 40/60 5.35 (ml/min)	#72 30/40 3.25 (ml/min)
0.5	4.25	3.91	4.19
1.5	4.21	3.93	4.23
2.5	4.24	3.90	4.02
3.5	4.21	3.96	4.02
4.5	4.19	3.89	4.04
5.5	4.26	3.94	4.02
6.5	4.21	3.98	4.02
7.5	4.22	3.91	3.97
8.5	4.20	3.83	4.02
9.5	4.21	3.84	3.93
15.0	4.13	3.69	3.89
20.0	4.07	3.57	3.84
25.0	4.08	3.46	3.81
30.0	4.06	3.26	3.72
35.0	4.07	2.93	3.64
40.0	3.94	2.60	3.51
45.0	3.67	2.26	3.39
50.0	3.57	1.91	3.23
55.0	3.27	1.50	3.04
60.0	3.07	0.97	2.83
65.0	2.75	0.18	2.59
70.0	2.46	0.04	2.33
75.0	1.89	0.04	2.11
80.0	1.44	0.02	1.85
85.0	1.02	0.01	1.55
90.0	0.56		1.22
95.0	0.17		0.90
100.0	0.07		0.62
105.0	0.03		0.40
110.0			0.24
115.0			0.13
120.0			0.08
125.0			0.03
130.0			0.03

TABLE 25. K_2SO_4 CONCENTRATION (mg/ml) FOR DISSOLUTION OF 0.77 GRAM IN AN 8 mm I.D. COLUMN AT FAST FLOW RATES

TIME (min)	RUN # #67 3.25 (ml/min)	#68 6.4 (ml/min)	#69 9.8 (ml/min)	#70 12.7 (ml/min)	#71 15.8 (ml/min)
0.5	4.19	3.65	2.85	2.49	1.92
1.5	4.01	3.60	2.72	2.44	1.98
2.5	3.97	3.55	2.78	2.39	1.89
3.5	3.92	3.50	2.74	2.31	1.83
4.5	3.90	3.42	2.70	2.23	1.76
5.5	3.91	3.37	2.62	2.19	1.71
6.5	3.85	3.30	2.50	2.16	1.64
7.5	3.88	3.25	2.47	2.05	1.59
8.5	3.88	3.21	2.42	2.03	1.55
9.5	3.82	3.18	2.36	1.94	1.47
15.0	3.76	2.87	1.96	1.59	1.20
20.0	3.66	2.58	1.68	1.32	1.01
25.0	3.56	2.25	1.42	1.06	0.85
30.0	3.36	1.92	1.17	0.85	0.69
35.0	3.17	1.61	0.92	0.65	0.56
40.0	2.99	1.33	0.69	0.48	0.43
45.0	2.73	0.97	0.45	0.31	0.32
50.0	2.47	0.66	0.24	0.15	0.20
55.0	2.13	0.38	0.08	0.06	0.11
60.0	1.90	0.18	0.03	0.02	0.05
65.0	1.59	0.07			0.01
70.0	1.29	0.02			
75.0	0.98				
80.0	0.71				
85.0	0.45				
90.0	0.30				
95.0	0.18				
100.0	0.10				
105.0	0.05				
110.0	0.02				

TABLE 26. K_2SO_4 CONCENTRATION (mg/ml) FOR DISSOLUTION OF 1.00 GRAM IN A 9 mm I.D. COLUMN AT FAST FLOW RATES

	RUN #				
	#73	#74	#75	#76	#77
TIME (min)	5.25 (ml/min)	10.6 (ml/min)	15.6 (ml/min)	20.8 (ml/min)	25.3 (ml/min)
0.5	3.80	2.96	2.73	2.29	2.22
1.5	3.72	2.87	2.68	2.33	2.17
2.5	3.69	2.85	2.58	2.33	2.12
3.5	3.70	2.82	2.50	2.21	2.03
4.5	3.67	2.80	2.42	2.15	1.98
5.5	3.67	2.82	2.35	2.06	1.87
6.5	3.64	2.81	2.36	1.98	1.79
7.5	3.65	2.77	2.27	1.93	1.69
8.5	3.63	2.77	2.21	1.89	1.60
9.5	3.65	2.68	2.14	1.79	1.53
15.0	3.45	2.37	1.77	1.40	1.11
20.0	3.32	2.09	1.47	1.09	0.82
25.0	3.10	1.79	1.17	0.81	0.59
30.0	2.92	1.49	0.89	0.58	0.39
35.0	2.68	1.19	0.64	0.37	0.24
40.0	2.43	0.92	0.41	0.20	0.12
45.0	2.16	0.64	0.23	0.10	0.06
50.0	1.88	0.41	0.12	0.04	0.02
55.0	1.60	0.24	0.06	0.02	0.01
60.0	1.30	0.13	0.03	0.01	
65.0	1.02	0.07	0.01		
70.0	0.77	0.03			
75.0	0.54	0.01			
80.0	0.35	0.01			
85.0	0.22	0.01			
90.0	0.12	0.01			
95.0	0.07				
100.0	0.03				
105.0	0.01				

TABLE 27. ACETAMINOPHEN CONCENTRATION (mg/ml) FOR DISSOLUTION OF 1.00 GRAM OF 40/60 MESH FROM TWO BATCHES

TIME (min)	RUN #78 Batch H	RUN #79 Batch J
0.5	14.3	14.8
1.5	14.3	14.7
2.5	14.3	14.7
3.5	14.1	13.9
4.5	14.2	14.1
5.5	14.1	14.1
6.5	14.1	13.9
7.5	13.8	13.5
8.5	13.6	12.8
9.5	13.0	11.3
15.0	1.23	1.69
20.0	0.586	0.651
25.0	0.448	0.405
30.0	0.312	0.369
35.0	0.225	0.338
40.0	0.231	0.307
45.0	0.103	0.275
50.0	0.083	0.208
55.0	0.033	0.199
60.0	0.012	0.158
65.0	0.013	0.138
70.0	0.007	0.099
75.0		0.068
80.0		0.063
90.0		0.049
100.0		0.029
110.0		0.021
120.0		0.016
130.0		0.002

Each experiment is designated by the run number assigned in Table 10.

The K_2SO_4 concentrations in these tables were calculated in the following manner:

1) The potential of the unknown or sample was measured and recorded.

2) Potential of two standard solutions which bracketed the potential of the unknown were also measured; note that these standards contain a known potassium ion concentration and the same ethanol concentration as the unknown.

3) A linear potential gradient was assumed between any two standard solutions, and the potassium ion concentration was calculated by interpolation. These values have been reported in mg/ml.

Acetaminophen concentrations listed in Table 27 were calculated from a Beer's law plot.

DISCUSSION

A column apparatus has been used by numerous investigators to assess dissolution properties of both powders and dosage forms. Studies of the dissolution kinetics for K_2SO_4 and acetaminophen in a flow-through system are reported here. The effect of several experimental parameters on dissolution rate was monitored; these variables included particle size, column load, specific surface area, solubility, column diameter, solvent flow rate, and type of pump head. Dissolution kinetics, which occurred under nonsink conditions, have been described by a mathematical model.

A. Effect of Particle Size on Dissolution Rate

Langenbucher (31) and Tingstad *et al* (38) studied the relationship between particle diameter of benzoic acid granules and prednisone powder, respectively, and dissolution rate in a column. A Reynolds number, designated Re, was defined to include a dimensional dependence on particle dimension:

$$Re = \frac{QaDp}{\nu} \qquad (6)$$

where 'Qa' is liquid velocity (cm/min), and Qa = Q/Ac = (volumetric flow rate)/(cell cross-sectional area), 'Dp' is equivalent spherical particle diameter (cm), 'ν' is

kinematic liquid viscosity (cm^2/min), and $\nu = \mu/\rho$ or viscosity/density. Langenbucher derived the following relationship (for Re of 0.1 to 1.0):

$$T \alpha (Dp,o)^{1.5-1.8} \quad (7)$$

where 'Dp,o' was the particle diameter at zero time, and 'T' was the time for 100% of the material to dissolve, as predicted by the Hixson-Crowell or cube root equation (3); dissolution occurred under sink conditions in all experiments (31). Langenbucher did not correct flow rate and liquid velocity for the porosity of the column; such a correction would be difficult to quantitate since porosity changes with time as particles dissolve. The Reynolds number, as defined by Langenbucher, would decrease to zero during the experiment as the particles dissolved.

Equivalent spherical diameters studied were 750, 410, and 260 μm. Dissolution results followed a trend; as particle diameter decreased, specific surface area increased, and thus dissolution rate increased. Agreement with the same relationship was reported by Tingstad et al (39) for dissolution of isosorbide dinitrate tablets. However, no evidence was provided about the size of particles into which these tablets disintegrated; it was assumed by those workers that the particle size of dissolving particles was related to, if not the same as,

the starting material.

In the studies reported here, five mesh cuts of K_2SO_4 were dissolved under various experimental conditions. Each mesh cut, 20/30, 30/40, 40/60, 60/80, and 80/100, contained a range of particle sizes, which was assigned average diameters of 715, 505, 335, 213.5 and 163 μm, respectively. The average diameter of particles reported for each mesh cut is an approximation based on the arithmetic mean of the sieve openings for each pair of screens used (67).

One gram K_2SO_4 samples from five mesh cuts of the same recrystallization batch G were allowed to dissolve in 40% ethanol, which was pumped at a flow rate of 5.3 or 5.35 ml/min through the 9 mm column. Data from these five dissolution runs #20, 24, 30, 39, and 44 are shown in Figure 7, which has been included as an example of the typical way in which column dissolution data have been presented in the literature to date (31,38); generally cumulative amounts dissolved (or undissolved) versus time have been plotted. Ironically, this means of presenting dissolution data fails to take advantage of a unique aspect of column dissolution (i.e. that results are obtained in differential form). Data presented in integral form look very similar; differences between runs are difficult to detect. In Figure 7, many points are graphically indistinguishable, and have been represented by solid

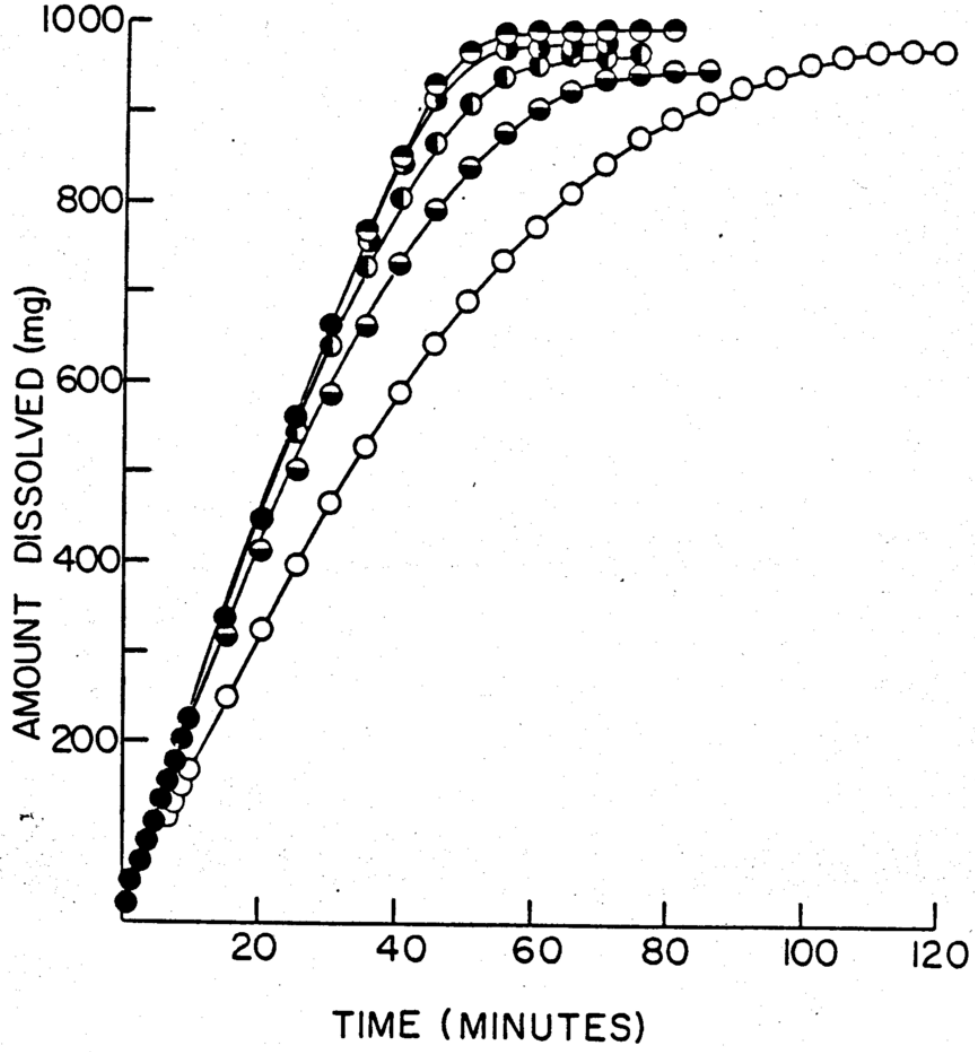
1000
800
600
400
200
AMOUNT DISSOLVED (mg)
20
40
60
80
100
120
TIME (MINUTES)

circles. All profiles appear to be linear for as long as 20 - 30 minutes, which suggests that the dissolution rate was constant for this time.

The same data have been plotted in differential form, as concentration of solute in column effluent versus time, in Figure 8. For graphical clarity, only three of the first ten data points for each profile are shown; lists of data appear in Tables 15 - 17. Solid circles represent points which are graphically indistinguishable. Comparison of Figures 7 and 8 shows some important differences between them and noteworthy features of the latter figure. While data smoothing is considered appropriate here, this differential form presents real fluctuations which are more easily discerned. Small differences in concentrations and changes in concentration among dissolution profiles are more easily distinguished. Different forms of dissolution curves (i.e. continual decline in concentration versus an apparent plateau) and the location of an inflection point, are more easily discerned from this type of plot. All subsequent dissolution results will be graphically presented here in differential form.

The five dissolution profiles in Figure 8 each had different features. Run #44 (20/30 mesh) had an initial concentration which was significantly lower than the other mesh cuts; the concentration of solute from this mesh cut

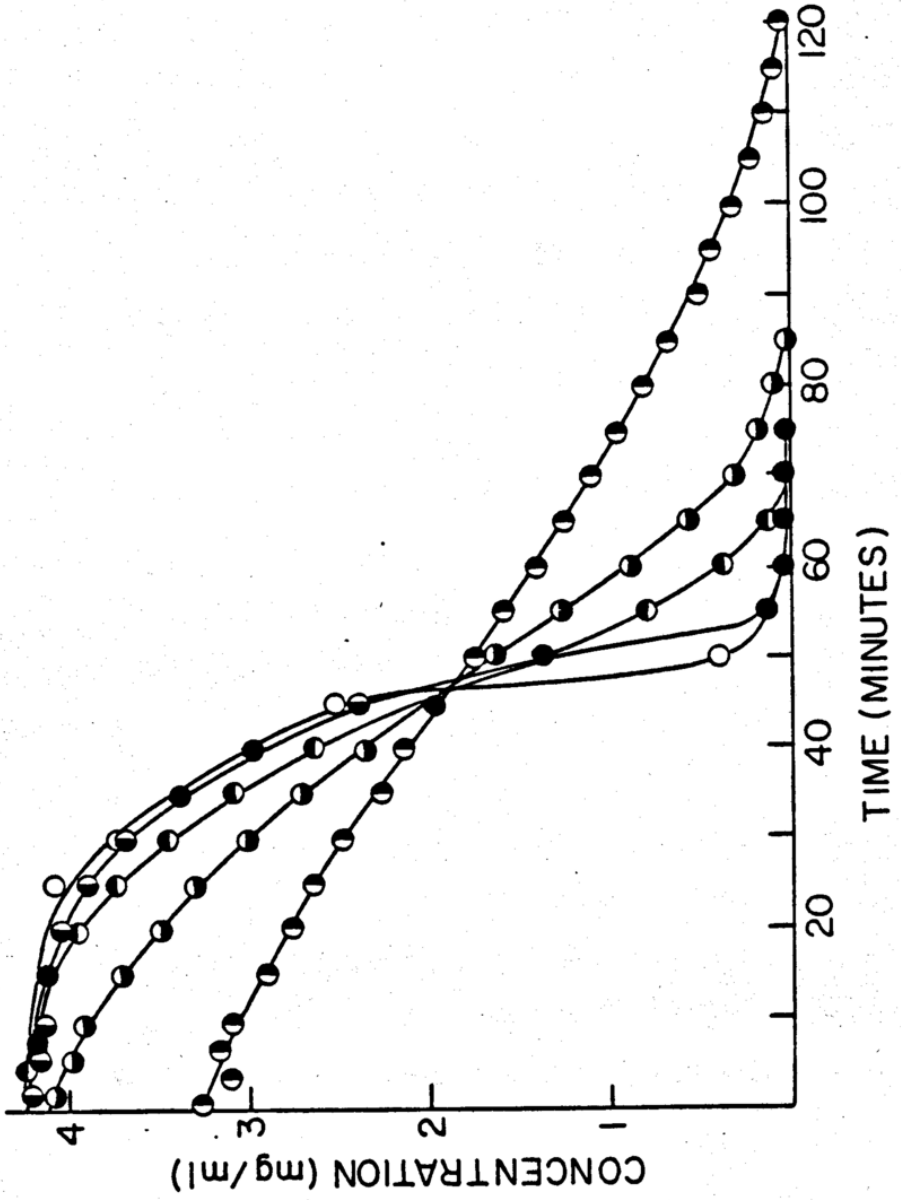
CONCENTRATION (mg/ml)
4
3
2
1
TIME (MINUTES)
20
40
60
80
100
120

decreased at (almost) constant rate after approximately 7 minutes. Since the solubility of K_2SO_4 in 40% ethanol at 25°C is 4.7 mg/ml, sink conditions occur when the concentration is less than 0.705 mg/ml. Thus, by the time the concentration of solute in the effluent had fallen to sink conditions, approximately 95% of the K_2SO_4 had already dissolved.

The 30/40 mesh sample, run #39, dissolved similarly to the 20/30 mesh. Since the specific surface area of the former mesh cut was greater (see Table 2), one would expect, as predicted by the modified Noyes-Whitney equation, that the dissolution rate would be faster; the results were consistent with that assumption. Here, less fluctuation was noted in concentrations at early times; although the concentration decreased with time, the slope was clearly not linear. An inflection point was noted at approximately 60 minutes; this also corresponded to the time when sink conditions developed.

When a 40/60 mesh cut was dissolved, an important difference was noted in the dissolution profile; run #30 is shown in Figure 8. The initial concentration was approximately the same as for the 30/40 mesh cut, but a constant concentration or plateau was recorded for approximately 10 minutes before a decline occurred. The rest of the dissolution curve had a smooth sigmoid shape;

sink conditions occurred after about 55 minutes.

The 60/80 and 80/100 mesh cuts each represented smaller particles and larger specific surface areas than the other mesh cuts (see Table 2); note that these two mesh cuts had approximately the same surface area as measured by gas adsorption. As described previously, this was related to the type of crystal clusters from which they were formed.

Upon dissolution, both runs #29 and #20 for 60/80 and 80/100 mesh, respectively, exhibited plateaus in the concentration versus time profiles, similar to that noted for the 40/60 mesh cut. The concentrations of all three plateaus were within 5%, which was within the range of reproducibility of the method (a point which will be discussed later). The length of time when a plateau occurred increased as the equivalent particle diameter decreased; the longer a plateau existed, the steeper was the subsequent decrease in concentration with time. The two smaller particle size groups (i.e. 60/80 and 80/100 mesh) did not exhibit a smooth sigmoid-shaped decline in concentration with time. Instead the "inflection point" in these profiles occurred at a very low concentration, after all particles had apparently dissolved. Further decline in concentration represented only dilution of the column contents.

Concentration and dissolution rate were clearly dependent on particle size and the related surface area; in general, as particle size decreased and surface area increased, dissolution rate increased. This dependence of dissolution rate on surface area follows directly from the modified Noyes-Whitney equation:

$$\frac{dm}{dt} = kA(S - C) \qquad (8)$$

However, as will be discussed, an apparent maximum dissolution rate was noted for some experimental conditions. An increase in surface area, beyond a given value, was not accompanied by a similar increase in dissolution rate. Also, the difference between the solubility and concentration of the solute, which served as the driving force for dissolution, appeared to approach a limiting value; the maximum concentration measured here was approximately 90% of the solubility of the compound. These conclusions will be addressed in a different fashion by the next group of experiments to be described.

B. Effect of Column Load on Dissolution Rate

In the previous section, the change in dissolution rate for 1.00 gram samples of five mesh cuts from the same recrystallization batch was described. Each mesh cut presented a different surface area to the solvent for dissolution; the surface area was a function of both the particle size and the type of crystal cluster in each mesh cut.

To minimize the effect of the dependence of surface areas on crystal cluster type, several column loads of the same mesh cut were used; samples of two K_2SO_4 mesh cuts from two different recrystallization batches were dissolved and the effluent was analyzed. The experimental results are listed in Tables 15 and 11 and shown in Figures 9 and 10, respectively.

Shown in Figure 9 are results from dissolution runs #27, 28, 30, 31, and 33, for 0.5, 0.75, 1.0, 1.25, and 1.50 grams of 40/60 mesh K_2SO_4, respectively, (batch G) in 40% ethanol at 25°C; solvent flow rate was 5.3 - 5.35 ml/min. (This is the same recrystallization batch described in the previous section.) For graphical clarity in Figure 9, except for the 0.5 g sample, only 3 of the first 10 minute concentrations are shown; all data are listed in Table 15.

The shapes of the dissolution curves were similar to

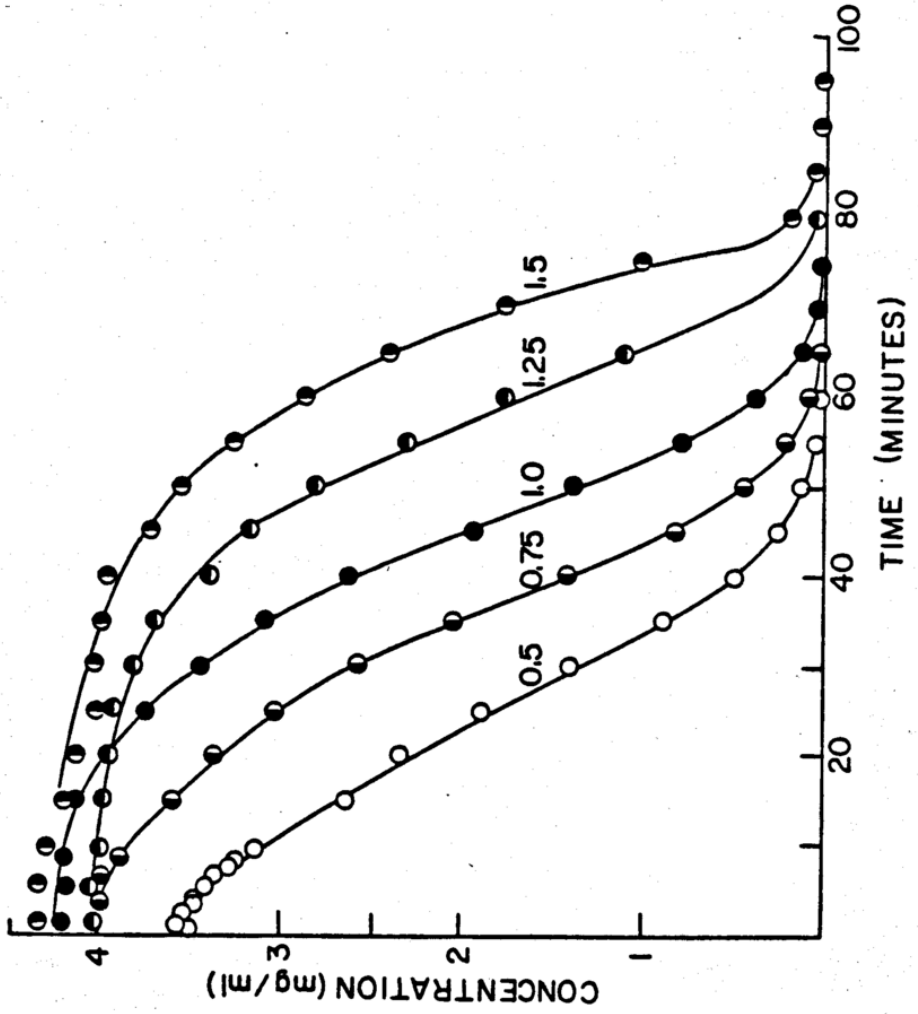
CONCENTRATION (mg/ml)
TIME (MINUTES)
1.5
1.25
1.0
0.75
0.5
1
2
3
4
20
40
60
80
100

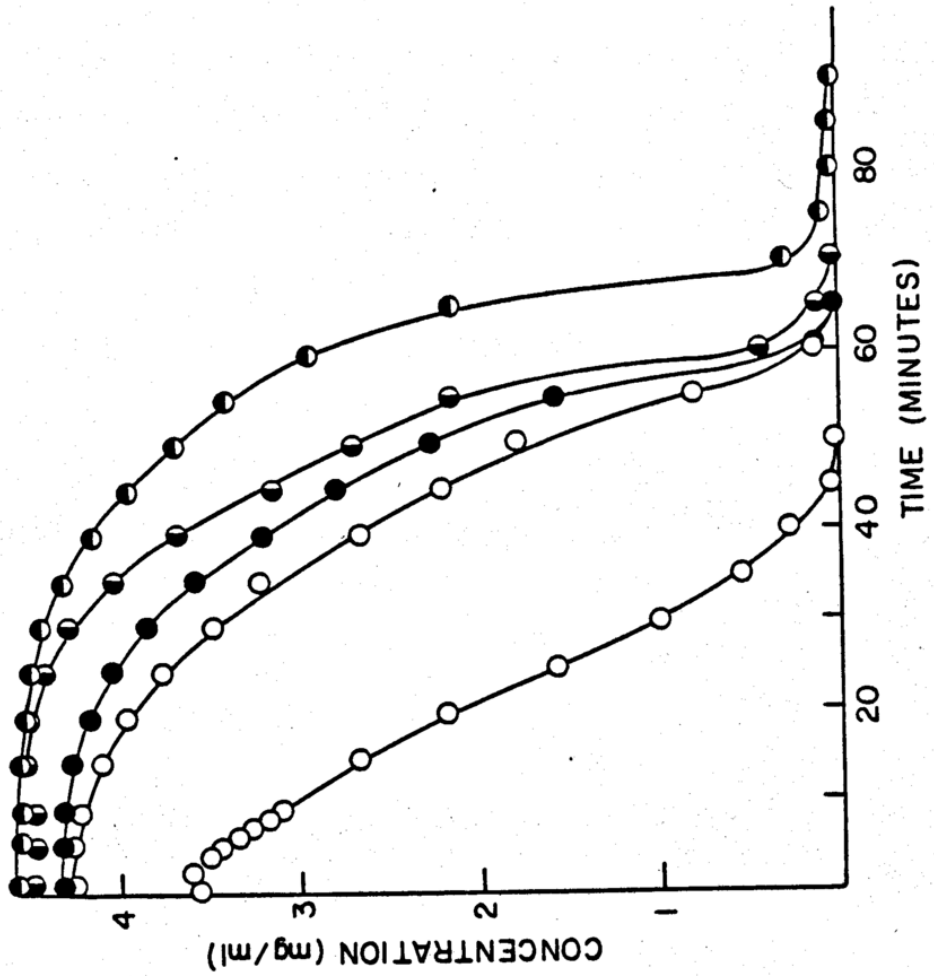
CONCENTRATION (mg/ml)
4
3
2
1
TIME (MINUTES)
20
40
60
80

those shown in Figure 8; in general, the curves were sigmoid shaped. The initial concentrations increased with increasing load, except for the 1.25 gram sample; this could only be explained on the basis of the reproducibility of the method, which will be discussed in Section E of this chapter. As the initial load of the column exceeded 0.75 grams, the initial concentrations exhibited a plateau, as was previously seen. All the concentrations followed a smooth decline; as initial load increased, a steeper decline in the concentration profile was noted.

Figure 10 shows the dissolution results for 0.43, 1.0, 1.12, 1.25, and 1.50 gram samples of 60/80 mesh K_2SO_4, (batch A) dissolved in 40% ethanol at 25°C pumped at 5.0 - 5.35 ml/min. Data for these dissolution runs #1 through 5 are listed in Table 11. The K_2SO_4 crystals were from different type crystal clusters, and the crystals had a higher specific surface area than those described above; however, these dissolution profiles followed the same trends as shown in Figure 9. Below some critical load, described in terms of mass or more appropriately in terms of surface area, the initial concentration increased as a function of load, and the later slope of the dissolution profile became steeper. Again, a plateau value was noted at a concentration of approximately 95% of the solubility of K_2SO_4, for the profiles of the three larger initial

loads.

The magnitude of this declining slope was related to the number of particles present in the column. It was assumed that all particles in the column dissolved at essentially the same rate, and thus the number of particles present throughout most of the dissolution experiment remained constant. Therefore, even after a substantial amount of material had dissolved, and the concentration had decreased below the plateau value, the amount of solid remaining was divided among many small particles. The increased surface area associated with the larger number of particles in each successive run would account for the faster dissolution rate and steeper decline in the dissolution profile.

The Noyes-Whitney equation describes the relationship between dissolution rate and the surface area of the solid; the only limiting factor comes from the concentration, which obviously cannot exceed the solubility of the compound. In a closed system, such as the sealed ampuls used for determination of the solubility of K_2SO_4, the same volume of solvent is in contact with a given amount and surface area of material. Even in a static system, a finite period of time, often several days, is required for the contents to reach an equilibrium concentration equal to the solubility of the compound; this approach to

equilibrium is asymptotic.

In an open or flow-through system, such as the column apparatus described here, new volumes of liquid are continually coming in contact with the solid surface; it is reasonable to conclude that the solid can dissolve rapidly, but the bulk concentration of solute will always remain below the solubility of the compound. A critical or minimum surface area could be defined in terms of the amount needed to give rise to this plateau in concentration at 90 - 98 % of the solubility of the compound; within a reasonable range of initial column loads, any further increase in surface would not lead to an appreciable increase in dissolution rate. If the initial column load was increased several orders of magnitude, then the concentration might increase to a value very close to the solubility; however, this could be related to the surface area to which the liquid was exposed, and the length of time the liquid and solid were in contact. Within the range of column loads which might typically be studied, the concentration should always be somewhat lower than the solubility; as long as some minimum surface area still existed in the column, dissolution would occur at essentially the same rate (i.e. concentration exhibited a plateau).

Consistent with the trends noted in the previous

section for dissolution rate as a function of particle size, there may be some minimum or critical surface area for each material and set of experimental parameters. Below this critical surface area, an increase in mass or load and a concurrent increase in surface area will lead to an increase in initial concentration and a change in the shape of the profile's decline from almost linear to sigmoid shape. But when this critical surface area or mass is exceeded, the concentration of solute in the effluent may appear constant for some time period. When sufficient material has dissolved such that the surface area now presented to the solvent is equal to or just less than this critical surface area, the concentration will decline in some nonlinear manner. The slope of that declining curve was dependent on the number of particles which were present; as the number of particles which made up any given "surface area" or "load" increased, the slope of the later portion of the concentration versus time profile was steeper.

In all these experiments, dissolution occurred under nonsink conditions until more than 85% of the column contents were dissolved; yet previous investigators have reported that sink conditions were observed during column dissolution experiments (31,38-40,43,44). Results described here show that the initial concentration is

related to the column load. As will be discussed later, dissolution kinetics are also dependent on the solvent flow rate. Thus, fluid velocity, the initial column load and its associated bed height within the column determine if sink or nonsink conditions will prevail initially.

C. Effect of Specific Surface Area on Dissolution Rate

Potassium sulfate and acetaminophen were each recrystallized to provide a large quantity of various particle sizes (mesh cuts) for dissolution studies. It was initially assumed that various recrystallization batches would provide individual crystals of the same crystal habit, and thus the same specific surface areas for each mesh cut.

Microscopic examination showed that while the crystals were of the same habit, particles of all mesh cuts from each recrystallization batch were heterogeneous mixtures of crystal clusters and of a few individual crystals. The type (i.e. number and dimensions of crystals per cluster) of clusters also varied from one batch to the next; this difference was noted microscopically and was consistent with surface areas measured by gas adsorption.

Measurements of surface area are listed in Table 2; data are reported in m^2/g. Within any one material, the reproducibility of the technique (i.e. 10% variation) is indicated by replicate measurements. Within recrystallization batches, the trends were as expected; specific surface area (m^2/g) increased as particle size decreased. However, for some batches such as B, D, E, and G, the surface area measurement of two consecutive mesh

cuts did not indicate any significant difference between them; this was not in agreement with the assumption that the particles are spheres, but was consistent with the fact that the particles consisted of crystal clusters in most cases.

Photographs of representative crystals from each mesh cut of every recrystallization batch used in dissolution studies are shown in Figure 2. Wide variation is noted between crystals from the same mesh cut of different batches. The type of crystal clusters shown are consistent with the range in surface areas measured by gas adsorption. In Table 28, the measured surface area for five mesh cuts of batch G are compared with surface areas calculated for each mesh cut, assuming the mean of the sieve openings corresponded to the diameter of spherical particles. There is approximately a three-fold difference between the measured and calculated surface areas.

Dissolution profiles were generated for both 40/60 and 60/80 mesh cuts of various recrystallization batches of K_2SO_4. For the 60/80 mesh cut, crystals from recrystallization batches A, B, C, D, E, and G were studied; corresponding dissolution runs were #2, 9, 15, 17, 18, and 24, respectively, and data are listed in Tables 11, 12, and 17. In the order of lowest to highest surface area, the batches ranked as follows:

TABLE 28. COMPARISON OF MEASURED AND CALCULATED SURFACE AREAS FOR VARIOUS MESH CUTS OF POTASSIUM SULFATE (BATCH G)

Mesh Cut	Average Spherical Diameter (μm)	Calculated Surface Area * (m^2/g)	Measured Surface Area ** (m^2/g)
20/30	715	0.0032	0.0095
30/40	505	0.0045	0.0113
40/60	335	0.0067	0.0205
60/80	214	0.0106	0.0270
80/100	163	0.0138	0.0270

* Calculated for spherical particles, ρ = 2.66 g/cm .
** See Table 2.

$$B = C < D = G < A < E$$

where batch E had two times greater specific surface area than batch B for the same equivalent spherical particle diameter. Batch G had a surface area which was approximately mid-range between the extremes.

Comparison of some dissolution profiles is presented in Figure 11, where data for batches B, G, and E only are shown. In each case, 1.00 gram of 60/80 mesh crystals dissolved as 40% ethanol was pumped through the 9 mm column at 5.35 - 5.4 ml/min. For graphical clarity, only four of the first ten data points are shown; solid circles represent multiple points which are graphically indistinguishable.

When one gram of crystals from batch B was dissolved, the initial concentration was approximately 95% of the solubility of the compound; the concentration profile followed a smooth but rapid decline. Though not shown on Figure 11, profiles for batches A and C looked similar to the profile for batch B; concentration of batch C was a bit higher initially and dissolution rate was slightly faster at the end, while the concentration for batch A was slightly lower than batch B at the beginning and was slightly higher after the concentrations had fallen below 2.0 mg/ml.

The dissolution profile for Batch E, which had the

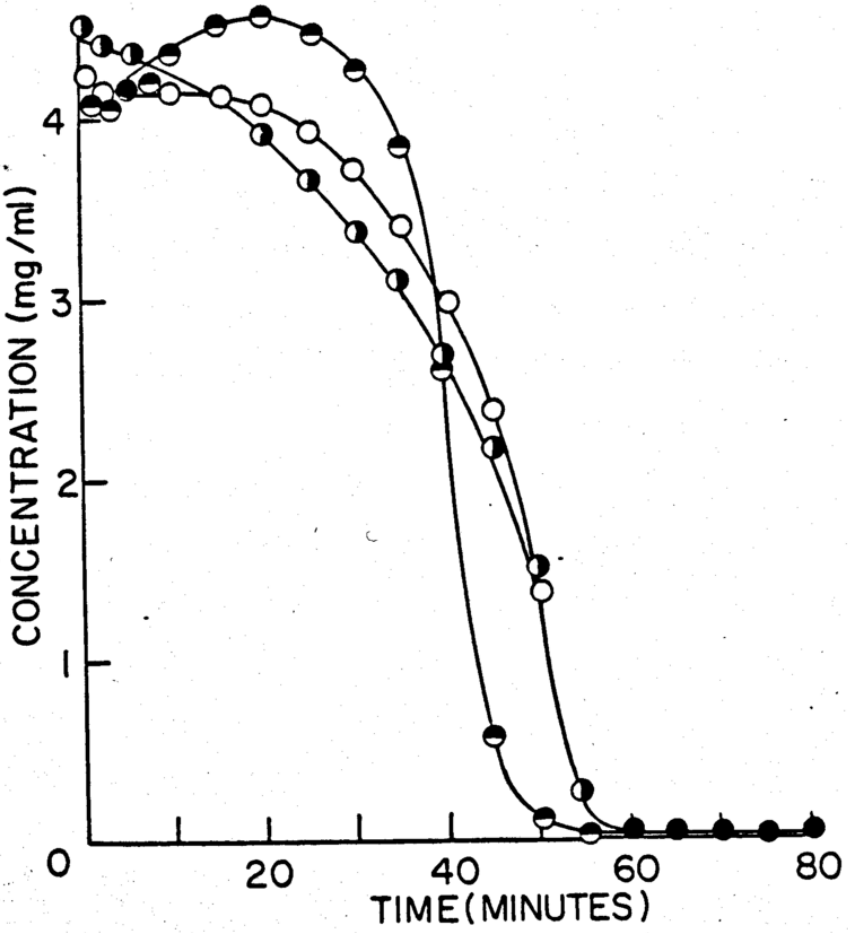
CONCENTRATION (mg/ml)
0
1
2
3
4
20
40
60
80
TIME(MINUTES)

highest specific surface area, was not typical of any reported thus far. For this run, a smooth, significant increase in concentration occurred during the first 20 minutes, followed by a very rapid decline. Such an increase could have been caused by a number of factors. If the surface of the solid was poorly wetted initially, and if wetting increased with time, then at 20 minutes, a greater surface area would have been exposed and available for dissolution. Since this type of profile was not obtained for any other batch or any other particle size and since no problem of air bubbles on the crystals was observed, this explanation was discarded.

If there was a problem in the analysis of the samples, such as fluctuations in house current giving erroneous potential readings, it is unlikely that the data would have followed such a smooth curve.

It was known from microscopic examination that these crystals represented clusters of a large number of crystals. If these clusters broke apart during dissolution, and if this resulted in an increase in surface area of K_2SO_4 as seen by the solvent, then an increase in concentration at early time could have occurred. This explanation was consistent with an observation recorded in the laboratory notebook for this experiment which described how the bed height within the column was not clearly

defined during this experiment; instead, many small particles were entrained in the solvent and moved throughout the length of the column during the entire experiment. This was not a typical observation; generally, particles of all mesh cuts remained in an expanded bed in the base of the column until particles were smaller than 100 μm.

Crystals from batch G dissolved in yet another way; this is also shown in Figure 11. A plateau was noted at a concentration approximately 88% of the solubility for about 20 minutes. Then concentration declined on a smooth, steep curve, with the concentration above but approaching the profile for batch B.

While not included in Figure 11, the profile for Batch D was very similar to that for batch G, but the plateau was higher, at about 95% of the solubility of K_2SO_4; the rest of the curve looked the same.

A similar comparison was made for 40/60 mesh cut. For five recrystallization batches, in order of lowest to highest specific surface area, the batches ranked as follows:

$$B < C < G < A < E$$

based on data from Table 2. This was the same rank order of surface areas observed for the 60/80 mesh cut. For the 40/60 mesh cuts, which represented larger particles than

the 60/80, surface area of batch E was three times greater than batch B, with batch A half-way between them.

Dissolution profiles for batches A, B, E, and G are shown in Figure 12. Results from profiles A and B were very similar in form; initial concentration for batch A was higher, and was reported to have been approximately equal to the solubility of K_2SO_4. It is unlikely that the concentration reached the solubility; if the solvent was prepared improperly so that the ethanol concentration was slightly lower than 40%, the higher solubility of K_2SO_4 could have led to a higher concentration. Unfortunately, due to the solvent preparation procedure used, it was not possible to analyze this batch of solvent, nor could the experiment be repeated due to an insufficient amount of crystals. The dissolution profile for batch C was very similar to that for batch B.

The profile for batch G looked very similar to the one shown in Figure 11; concentration values were on a plateau for approximately 15 minute, followed by a smooth sigmoid decline similar to curve B.

The dissolution profile for batch E was similar in form to that for batch G, but the initial concentration plateau was higher. This curve did not increase and then decrease as reported for 60/80 mesh; rather, the concentrations were on a plateau followed by a smooth but

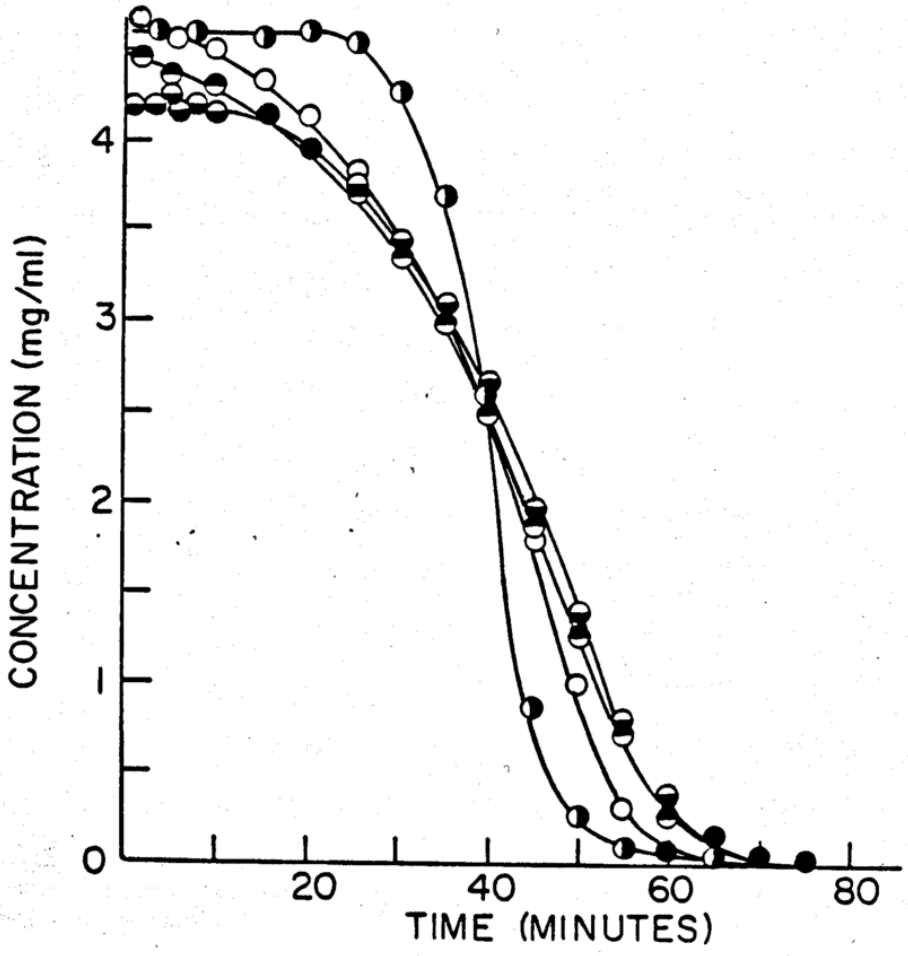
CONCENTRATION (mg/ml)
0
1
2
3
4
20
40
60
80
TIME (MINUTES)

rapid decline. During the experiment, the crystal bed remained fairly well contained in the bottom of the column; there was no dispersion of particles as was observed for 60/80 mesh.

Here, batch E, which had the largest specific surface area, had the highest concentration and fastest dissolution rate of the batches compared. However, dissolution rates for the other three batches did not fall in the same rank order as their surface areas.

Other investigators have described relationships between surface area and dissolution rates. Quay _et al_ found a rank order correlation between _in vitro_ characteristics (i.e. specific surface area measured by gas adsorption and a mass transfer coefficient from dissolution in a modified USP rotating basket) and bioavailability results (i.e.area under the blood level versus time curve) for cinoxacin capsules (68). Moller suggested that the surface area which is effective in dissolution is more accurately described by gas permeability measurements than by gas adsorption or estimates from a hemocytometer (69,70). Nimmerfall and Rosenthaler reported a correlation between mean spherically equivalent particle size, dissolution time measured with a flow-through column, and AUC(i.e. area under the blood level versus time curve) for three different crystal sizes of proquazone (71). Each of

these studies suggested that a different type of surface area was the appropriate measure to use in evaluating dissolution data.

The conclusions drawn from the experiments reported here are: 1) dissolution rate may not be directly proportional to specific surface area as measured by gas adsorption; 2) geometric area, or surface area based on equivalent spherical particle size, is not an appropriate parameter either since this would suggest that dissolution rate should have been the same for the different recrystallization batches. Based on the results discussed here, and the conclusions of other investigators, the appropriate measure of surface area to use in describing its effect on dissolution rate is not readily apparent; this will be addressed in Section J, in the development of a mathematical model for column dissolution kinetics.

D. Effect of Solubility on Dissolution Rate

To study the effect of solubility of the compound on the dissolution rate, four different ethanol-water mixtures were used as solvents. Potassium sulfate crystals from the same recrystallization batch (batch G) were dissolved in each solvent.

According to the Noyes-Whitney equation, the difference between the solubility and concentration of a compound acts as the driving force for dissolution. This suggests that a compound with a large solubility will dissolve faster than a poorly soluble material.

Column dissolution of four mesh cuts, 20/30, 30/40, 40/60, and 60/80, were studied in four solvents, 30, 35, 40, and 50% ethanol, at 25°C; flow rate of solvent was 5.3 - 5.4 ml/min with an average value of 5.35 ml/min. K_2SO_4 has a solubility range of 1.99 - 10.8 mg/ml in 50 - 30% ethanol, respectively; thus, the solubility changes more than five fold over the ethanol range studied. It has been shown that when a column dissolution cell is used, the compound may dissolve under nonsink conditions during most of the experiment.

The concentration versus time profiles for the four ethanol concentrations could be compared directly, but it would be difficult to discern if each described dissolution under the same general conditions.

If the dissolution process is the same in all solvents, and if the mass-transfer coefficient from the Noyes-Whitney equation is the same for all four solvent systems, graphs of the dissolution data in some reduced form should be superimposable.

The parameters chosen to convert concentration and time to dimensionless quantities were based on both material and experimental parameters. Reduced concentration, 'C*', is defined as C* = C/S, where 'S' is the solubility of K_2SO_4 in the solvent of choice. Reduced time, 't*', is defined in terms of the time which would be required for the contents of the column to dissolve if concentration equalled the solubility at the flow rate used. Thus, $t' = m_o / SW$ where 'm_o' is the initial column load in mg, and W is the solvent flow rate in ml/min; and $t^* = t/t'$.

The concentration and time values for the various experiments are listed in Tables 18 (for 30% ethanol), 19 (for 35% ethanol), 15, 16, 17, (for 40% ethanol), and 20 (for 50% ethanol). Values of reduced time and reduced concentration are listed in Tables 29 through 32 and are shown in Figures 13 through 16, respectively.

Reduced data from 30, 40, and 50% ethanol can be superimposed and exhibit very good agreement within the range of reproducibility of this method. While the reduced

TABLE 29. REDUCED TIME AND REDUCED CONCENTRATION FOR DISSOLUTION OF K_2SO_4 IN 30% ETHANOL

	Reduced Concentration			
Reduced Time	Run #42 20/30	Run #37 30/40	Run #34 40/60	Run #22 60/80
0.029	0.607	0.837	0.918	0.904
0.087	0.595	0.810	0.896	0.899
0.144	0.588	0.803	0.875	0.896
0.202	0.581	0.800	0.865	0.894
0.260	0.574	0.793	0.862	0.886
0.317	0.572	0.779	0.852	0.873
0.375	0.567	0.763	0.847	0.862
0.433	0.562	0.755	0.835	0.860
0.490	0.557	0.725	0.820	0.845
0.548	0.551	0.727	0.810	0.830
0.866	0.506	0.599	0.682	0.692
1.154	0.423	0.454	0.442	0.470
1.443	0.343	0.290	0.098	0.021
1.731	0.263	0.122	0.010	0.019
2.020	0.195	0.032	0.004	0.004
2.308	0.127	0.008	0.003	0.001
2.597	0.074	0.004	0.002	0.001
2.885	0.033	0.003	0.001	0.001
3.174	0.010	0.003	0.001	0.001
3.462	0.004	0.002		
3.751	0.002	0.001		
4.039	0.002			
4.328	0.001			

TABLE 30. REDUCED TIME AND REDUCED CONCENTRATION FOR DISSOLUTION OF K_2SO_4 IN 35% ETHANOL

Reduced Time	Reduced Concentration			
	Run #43 20/30	Run #38 30/40	Run #35 40/60	Run #23 60/80
0.020	0.614	0.765	0.835	0.842
0.060	0.615	0.749	0.830	0.832
0.099	0.612	0.756	0.806	0.815
0.139	0.614	0.740	0.804	0.817
0.179	0.606	0.734	0.799	0.805
0.218	0.601	0.728	0.806	0.805
0.258	0.603	0.730	0.797	0.789
0.298	0.599	0.717	0.792	0.796
0.337	0.596	0.708	0.790	0.803
0.377	0.596	0.713	0.792	0.805
0.595	0.556	0.669	0.743	0.757
0.794	0.529	0.588	0.687	0.702
0.992	0.471	0.515	0.605	0.599
1.191	0.416	0.434	0.452	0.468
1.389	0.362	0.336	0.271	0.278
1.588	0.297	0.236	0.121	0.057
1.786	0.239	0.140	0.043	0.014
1.985	0.189	0.073	0.014	0.006
2.183	0.142	0.036	0.008	0.004
2.382	0.101	0.016	0.005	0.005
2.580	0.067	0.007	0.004	0.002
2.779	0.039	0.004	0.002	0.001
2.977	0.020	0.003	0.002	0.001
3.176	0.008	0.002	0.001	
3.374	0.004	0.001		
3.573	0.002			
3.771	0.001			

TABLE 32. REDUCED TIME AND REDUCED CONCENTRATION FOR DISSOLUTION OF K_2SO_4 IN 50% ETHANOL

Reduced Time	Reduced Concentration Run #46 20/30	Run #41 30/40	Run #36 40/60	Run #26 60/80
0.005	0.645	0.835	0.863	0.927
0.016	0.650	0.828	0.846	0.929
0.026	0.635	0.823	0.853	0.924
0.037	0.628	0.813	0.851	0.924
0.048	0.624	0.808	0.854	0.919
0.059	0.625	0.810	0.878	0.921
0.069	0.624	0.808	0.851	0.919
0.080	0.624	0.743	0.836	0.916
0.090	0.624	0.739	0.833	0.921
0.101	0.624	0.737	0.843	0.910
0.160	0.623	0.794	0.836	0.912
0.213	0.624	0.800	0.839	0.906
0.319	0.611	0.786	0.829	0.912
0.426	0.591	0.745	0.817	0.901
0.532	0.593	0.704	0.794	0.882
0.639	0.566	0.673	0.765	0.856
0.798	0.532	NA	0.713	0.779
0.852	0.520	0.631	0.707	0.734
0.958	0.453	0.577	0.639	0.650
1.065	0.438	0.520	0.574	0.539
1.171	0.405	0.493	0.475	0.399
1.224	NA	0.431	0.424	0.303
1.278	0.377	0.402	0.364	0.185
1.331	0.358	0.368	0.302	0.063
1.384	0.335	0.335	0.248	0.032
1.437	NA	0.301	0.196	0.024
1.490	0.306	0.267	0.149	0.016
1.597	0.276	0.179	0.080	0.008
1.650	NA	0.179	0.055	0.006
1.703	0.245	0.148	0.035	0.006
1.810	0.216	0.102	0.019	
1.916	0.187	0.066	0.010	
2.023	0.159	0.040	0.006	
2.129	0.133	0.024		
2.182	0.120	0.019		
2.236	0.110	0.015		
2.289	0.098	0.010		
2.342	0.088	0.007		
2.502	0.062			
2.608	0.046			

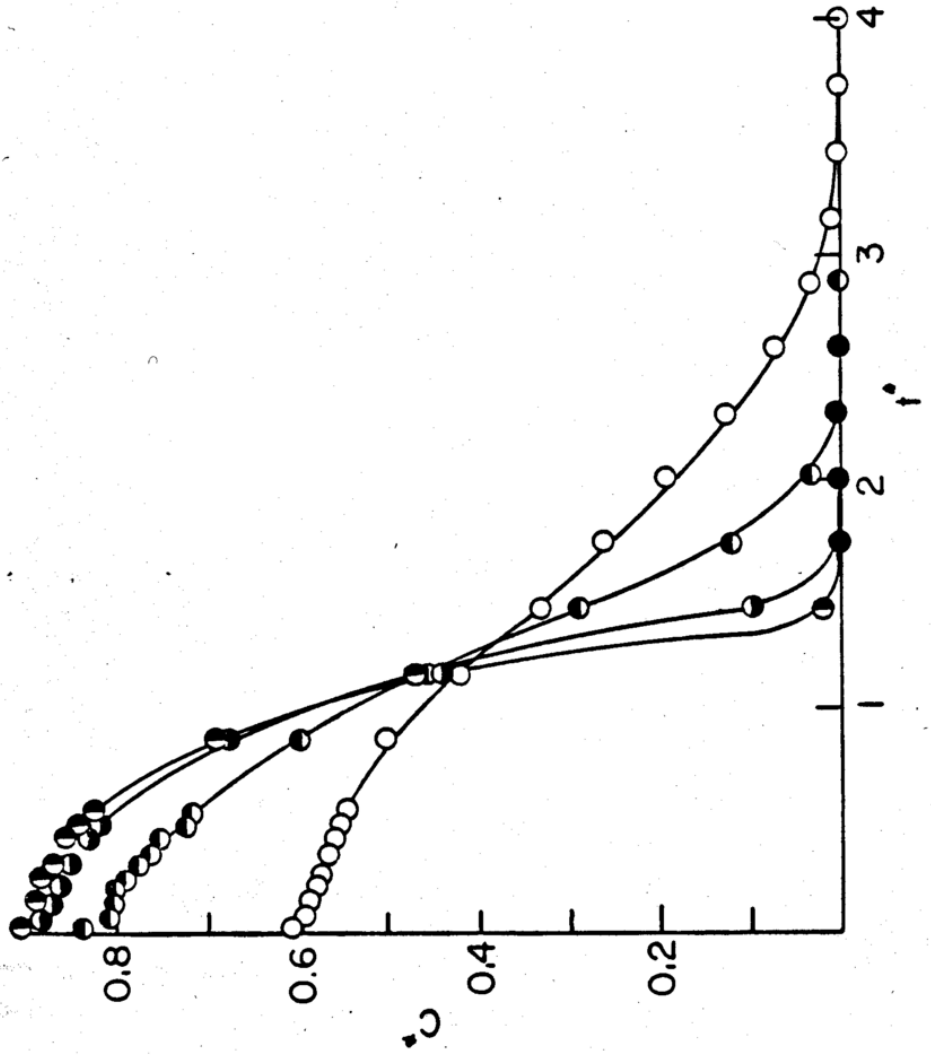
0.8
0.6
0.4
0.2
C*
1
2
3
4
t*

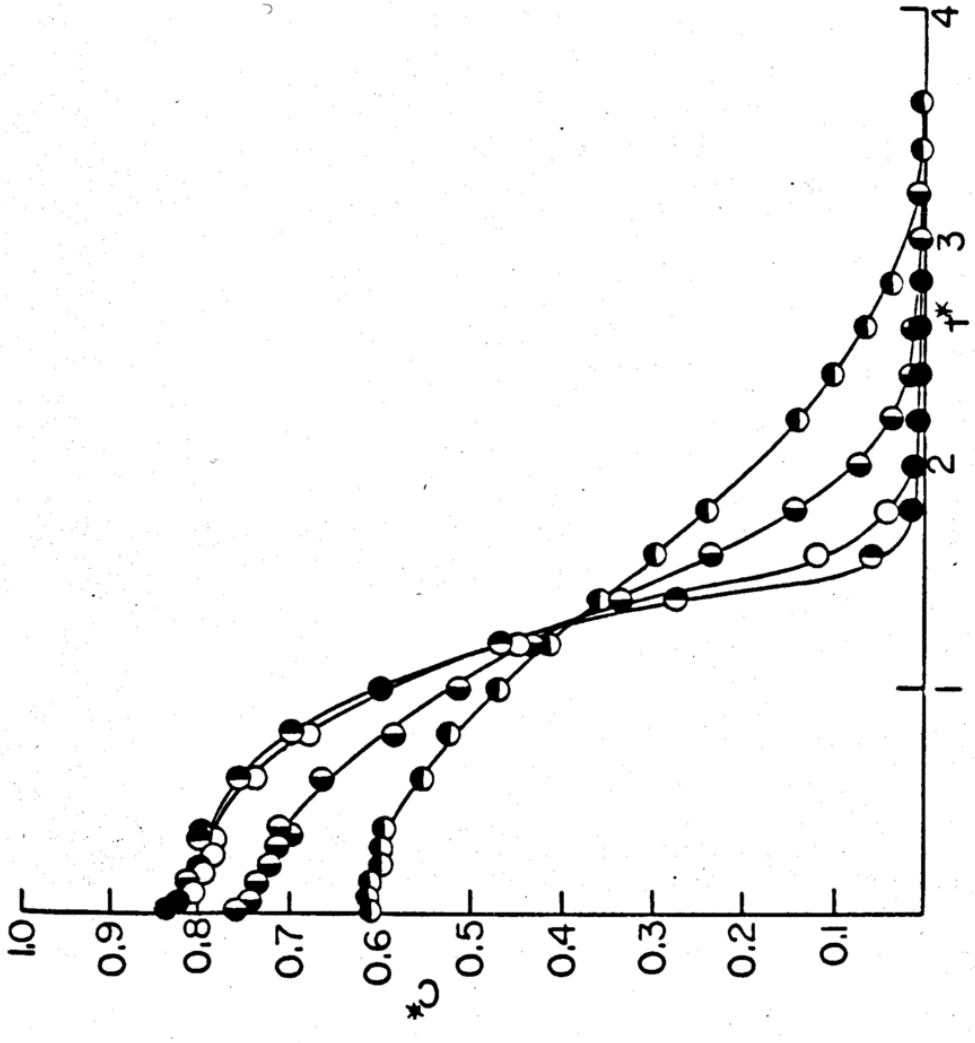
1.0
0.9
0.8
0.7
0.6
0.5
0.4
0.3
0.2
0.1
C*
1
2
3
4
t*

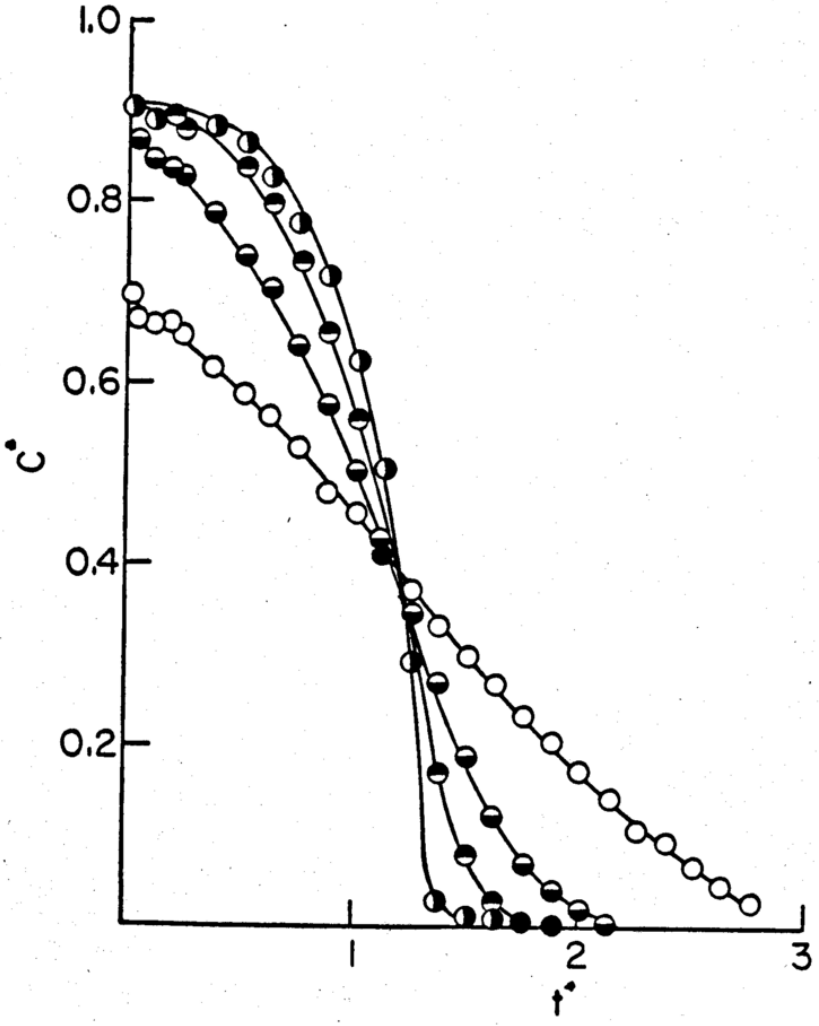
1.0
0.8
0.6
0.4
0.2
C*
1
2
3
t*

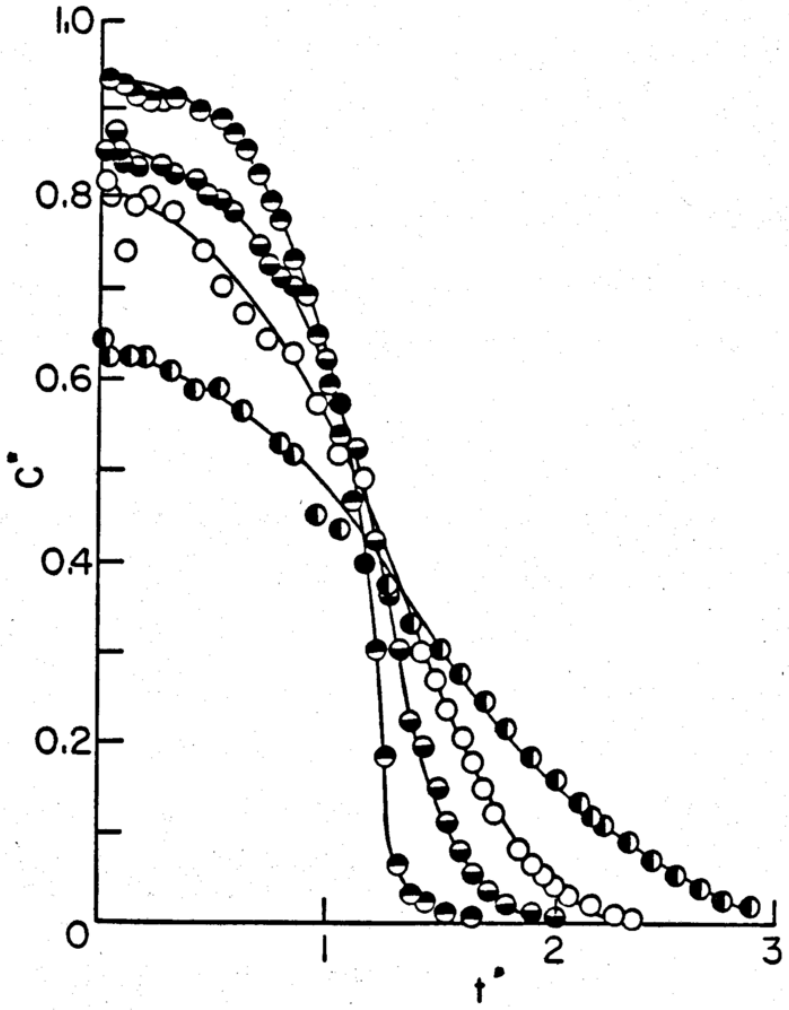
1.0
0.8
0.6
0.4
0.2
0
C*
1
2
3
t*

profile for 20/30 mesh dissolved in 35% ethanol is superimposable on the profiles for the same mesh cut dissolved in the other three solvents, the profiles for the other three mesh cuts dissolved in 35% ethanol are significantly lower than analogous profiles for the other solvents.

If the reduced profiles for different experiments are superimposable, then the mass-transfer coefficient should be the sme for these dissolution runs. Since the results for dissolution of K_2SO_4 in 35% ethanol compared to other solvents appear to be different, a change in the mass-transfer coefficient should be considered.

The mass-transfer coefficient, 'k' in the Noyes-Whitney equation, has been described as a combination of numerous parameters; some of these parameters are more easily measured or estimated than others. It is not necessary to invoke any particular theory or model for mass transfer, such as film theory, surface renewal, or boundary-layer theories in this discussion (72). The dependence of mass transfer on the diffusivity is defined by Fick's first law, which states that diffusive mobility equals the flux of a material divided by its concentration gradient. The equation of continuity (or mass balance) is a sum of terms which are dependent on the density of the system and also on the flux of the solute. Thus, when the

mass balance for a system is written, dependence on density and diffusivity, or the mass-transfer coefficient, follows directly.

For solids dissolved in liquids, the diffusivity of the solute is proportional to the flux; it is known that the diffusivity of solute 'a' in solvent 'b', or 'Dab', can be described as follows (72):

$$D_{ab} \alpha \left[\frac{(M_s)^{\gamma} T}{\mu}\right] \qquad (9)$$

where 'Ms' is molecular weight of the solvent, 'μ' is viscosity of the solution, and 'γ' is a constant. Over a wide range of concentrations, the diffusivity would be expected to change, since it is inversely proportional to viscosity. As values for various K_2SO_4 solutions in ethanol listed in Table 5 illustrate, an inorganic salt has little effect on the viscosity of its solution. Note also that the density of the liquid varies little over the same concentration range, which is as high as 90% of the solubility. Thus it has been assumed here that for each solvent, the diffusivity and mass-transfer coefficient are constant over the range of concentrations of each experiment.

The trend in the viscosity and density values reported in Table 5 is consistent with reported values (73). The lack of agreement for the reduced dissolution profiles of

K_2SO_4 in 35% ethanol cannot be explained on the basis of inconsistencies in density or viscosity; measurement of the solubility of the compound in 35% ethanol was repeated, and results were within 0.5% of the previously reported value.

Since Figures 13, 15, and 16 can be superimposed, it was concluded that the mass-transfer coefficients for K_2SO_4 dissolved in 30, 40, and 50% ethanol are the same. Lack of agreement of the data in 35% ethanol remains unexplained. The use of reduced concentration versus reduced time profiles suggests that compounds of very different solubilities can be compared; differences between profiles may be related to the mass-transfer coefficient for the solute in the system.

E. Effect of Dissolution on Surface Area

The Noyes-Whitney equation states that the dissolution rate at any time is proportional to the surface area of the material present at that time. In discussions of dissolution under sink conditions, it is generally assumed that the particles dissolve isometrically and the ratio of surface to volume of particles remains constant, independent of particle size; this assumption may be acceptable if the surface area change is small, but may not be suitable when one describes nonsink dissolution of a large number of particles which clearly deviate from spheres. Therefore, it would be of interest to know how the surface area of nonspherical particles changes during dissolution.

One advantage of the column dissolution method is that a dissolution experiment can be easily interrupted at any time, and the undissolved contents of the column can be removed and retained for further experiments. Study of dissolution profiles allows one to calculate the time when, for example, approximately 25, 50, and 75% of the column contents have dissolved. This time can then be used to establish when other dissolution experiments should be stopped.

Numerous dissolution experiments were done in which

1.00 gram of 40/60 mesh (batch G) K_2SO_4 was placed in the 9 mm I.D. column; 40% ethanol was pumped through the system at 5.35 ml/min. The surface area of the initial column load was 0.0205 m^2 (from Table 2). These experiments were then interrupted at various times.

Six dissolution runs, #47 through #52, were done in which the experiment was stopped after approximately 25% of the initial material had dissolved; the concentrations for these runs are listed in Table 21. In each case, the experiment was stopped after 10 minutes, the crystals remaining in the column were filtered, dried, and retained. Each quantity of undissolved crystals was weighed; this ranged from 0.73 to 0.77 gram, with an average of 0.75 gram.

These remaining crystals were then examined microscopically; photographs of representative crystals are shown in Figure 4. Since the particles still consisted of clusters and clearly deviated from smooth spheres, an estimate of surface area from microscopic examination would have been extremely difficult to make.

The crystals remaining from the six runs were combined and the surface area was measured by gas adsorption; thus a sample size of approximately 4.5 gram was analyzed with mixtures of krypton and helium gases. The specific surface area calculated was 0.019 m^2/g, which, within the

reproducibility of the instrument and method, is the same as the starting material. Thus for this material, a loss of 25% of the initial mass of the material represents a very small (probably no more than 10%) change in specific surface area; if the particles were assumed to be spheres, this loss in mass would suggest an 18% reduction in surface area.

An examination of the photographs of the partially dissolved crystals showed that the clusters did not break apart; the ends of some rods and the corners of larger crystals appeared to have become slightly rounded. The crystals looked quite similar to the starting material.

Then 1.00 gram of this combination of partially dissolved materials was dissolved under the same experimental conditions; the material was completely dissolved, and from its dissolution profile (i.e. run #53), the time was estimated for 50% of the material to dissolve. The dissolution data run #53 is listed in Table 23, as well as for run #54, which was interrupted when approximately 50% had dissolved.

The crystals remaining from the latter experiment were collected, dried and examined microscopically. A photograph of representative crystals is shown in Figure 4.

The starting material in these two experiments is different from any other material used in dissolution

experiments; since 25% of the mass has been previously dissolved from the surface, the remaining surface has different characteristics. While few clusters still existed, the rod-shaped particles have retained their general shape; larger single crystlas have become prolate ellipsoid in shape.

Although the surface area measurement showed no distinguishable difference, within the limits of the method, a comparison of the dissolution profile for run #53 to that for run #30 (i.e. the starting material) shows that crystals from the "25% dissolved" experiments dissolved differently than the starting material; dissolution profiles are shown in Figure 17. Despite the fact that the material in run #53 probably had a slightly higher specific surface area than the starting material, the dissolution rate was slower.

A possible explanation is based on the surface properties and, in particular, the surface energies of the two solids. There is no means of measuring this property, but it has been reported that crystals preferentially dissolve from high energy areas, such as edges, dislocations, defects, and asperities (74,75). If many of these high energy portions were dissolved in the first 25%, the remaining surface would have lower energy; and subsequent dissolution from these lower energy surfaces

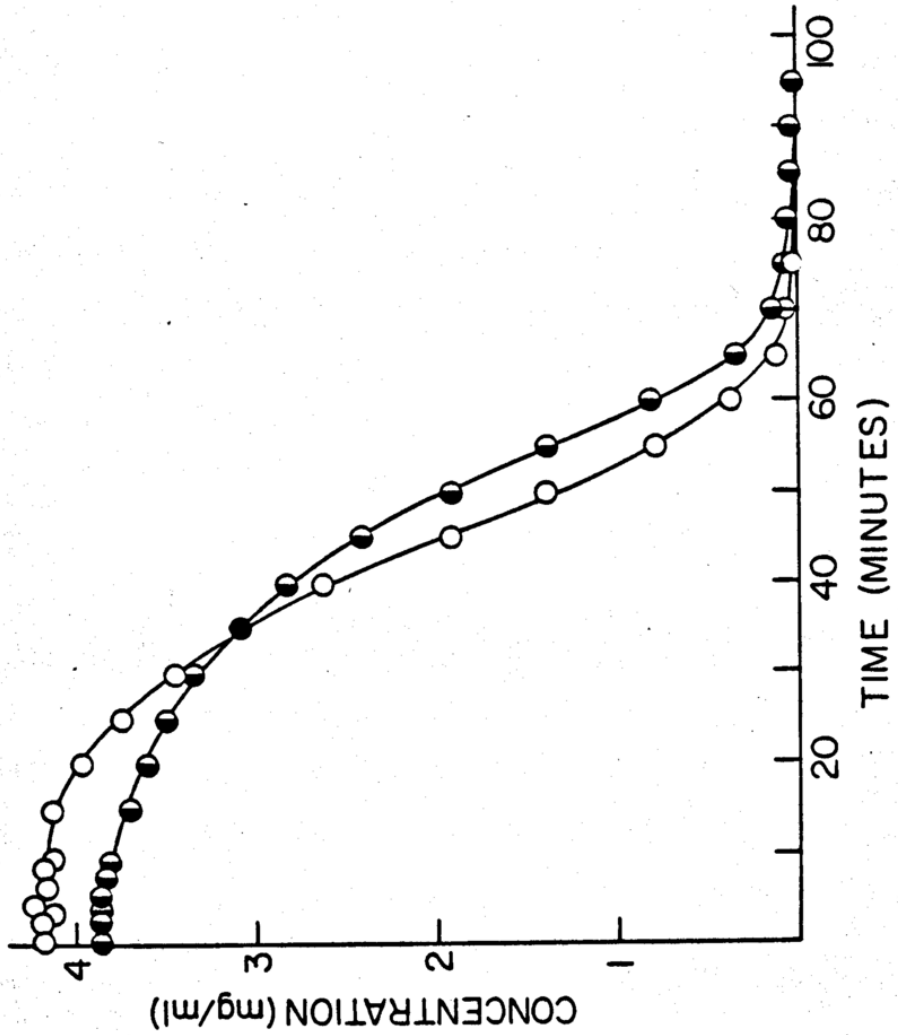
CONCENTRATION (mg/ml)
4
3
2
1
20
40
60
80
100
TIME (MINUTES)

would be slower. This explanation is consistent with the profiles shown in Figure 17.

Next, seven dissolution runs, #55 through #61, which are listed in Table 22, were done in which the experiments were stopped after approximately 50% of the initial column load had dissolved. Again the material was filtered, dried, weighed and photographed; representative crystals are shown in Figure 4.

The yield of crystals from run #59 was low due to problems in transfer of the undissolved column contents at the end of the experiment, and not due to a more rapid dissolution rate.

All crystals were combined and a specific surface area of 0.027 m^2/g was calculated from gas adsorption data. The specific surface area was more than 30% greater than that of the starting material. Thus, for each 1.00 gram sample in the column, a 50% loss in mass corresponded to

$$((0.0205\ m^2) - (0.5\ g)(0.027\ m^2/g))$$

or a loss of 0.007 m' in surface area, which is approximately a 35% decrease; if the particles were spheres of equivalent diameter, a 50% weight decrease would correspond to a 37% decrease in surface area. Note that the specific surface area here is comparable to that measured for the 60/80 mesh cut of the same batch G.

Photographs of some representative crystals, in Figure

4, show that the ends, edges, and corners became rounded. The crystal clusters remained intact; some edges receded more in the center than near the corners of the crystal faces.

Two 1.00 gram samples of the material remaining from the "50% dissolved" experiments were used in runs #62 and #63. In the former run, all the material was dissolved, so that the time for 50% of this material to dissolve could be determined and used in the latter run. Dissolution data for these are listed in Table 23.

The starting material here was notably different than the 40/60 mesh particles which were used as the original column loads. The former crystals had a surface area which was more than 30% greater than the latter. However, if the conclusion proposed in a previous discussion is correct, these "partially dissolved" crystals had lower surface energy than the original material.

A comparison of the dissolution profiles for runs #62 and #30 (the original material) is shown in Figure 18. Despite the differences between the materials, the dissolution profiles are nearly identical. From the Noyes-Whitney equation and from the previous discussion (Section C, Effect of Specific Surface Area on Dissolution Rate), it is known that dissolution rate is dependent upon the surface area presented to the solvent. As was

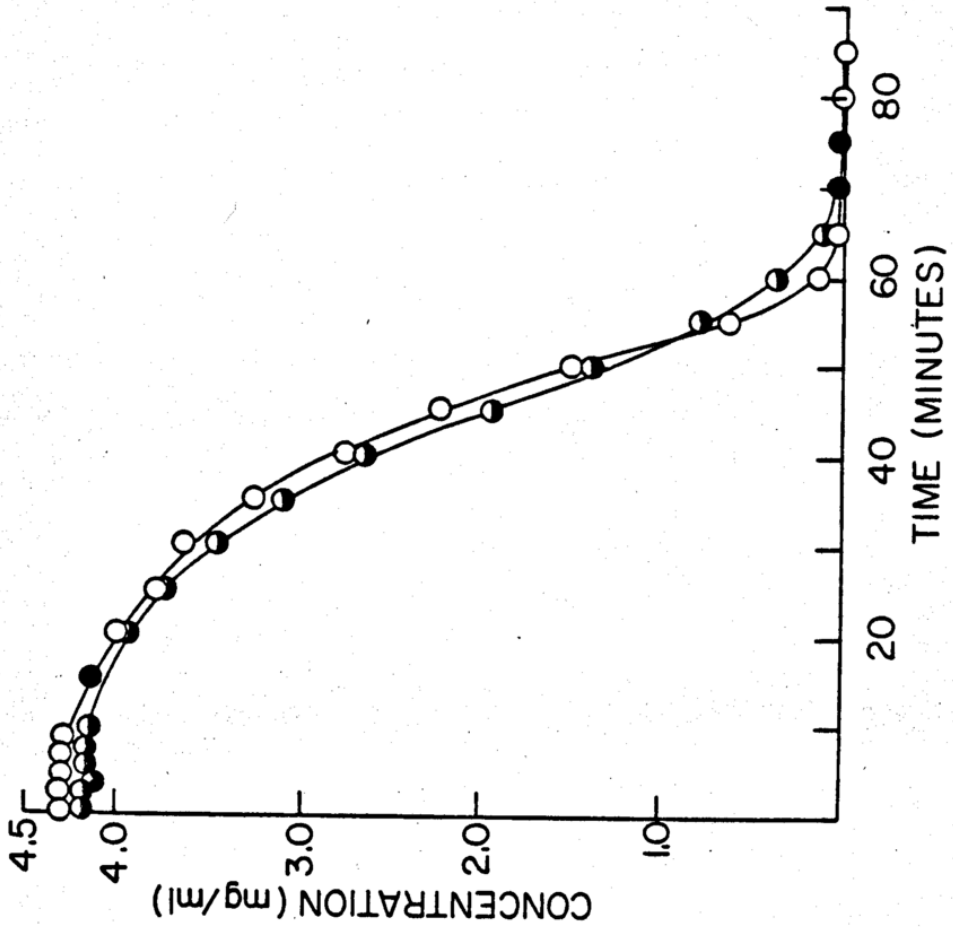
CONCENTRATION (mg/ml)
4.5
4.0
3.0
2.0
1.0
20
40
60
80
TIME (MINUTES)

concluded in the earlier discussion, the surface energy of the solid can also affect the dissolution rate. The profiles in Figure 18 suggest that these factors have opposite effects, such that they essentially counterbalance each other in their influence on dissolution rate.

A single dissolution experiment, run #64, was done in which the run was stopped when approximately 75% of the column contents had dissolved. The procedure to recover and retain crystals was the same as previously described. The yield was 0.244 gram K_2SO_4 which remained undissolved. This amount of solid was insufficient for surface area determination by gas adsorption. However, the crystals were examined microscipically; a photograph of representative crystals is shown in Figure 4. The shapes of the remaining material are very irregular; some particles have become very rounded while the rods have narrowed to sharp points.

After 75% of the material had dissolved, the remaining crystals looked quite different than the starting material. While clusters remained intact, some corners became very rounded, and others very pointed; a hole dissolved in the center of one crystal. The diameter of rod-shaped crystals decreased more in the center than at each end. In general, the crystals did not dissolve isometrically.

The large number of dissolution runs done with the same starting material, solvent and flow rate provided an indication of the reproducibility of column dissolution. When the concentrations for the first 10 minutes of these runs were compared, a range of $\pm$ 7% was noted, with most results within 5%. This compares favorably with the reproducibilities reported by other investigators for column dissolution experiments; Langenbucher: $\pm$ 9% std. dev., (31); Bathe: 15 - 20% (43); and Cakiryildiz: 1 -10% RSD (46).

F. Effect of Column Diameter on Dissolution Rate

Both Langenbucher and Tingstad *et al* studied the effect of column diameter on dissolution rate (31,38,39) Langenbucher found that dissolution time (i.e. the time to dissolve the material completely) was proportional to linear flow velocity, 'Qa', raised to a power of -0.2 to -0.5 for particle dissolution. When prednisone tablets were dissolved, Tingstad showed a linear relation between the amount dissolved in the first 15 minutes and flow rates from 10 to 54 ml/min. Both authors noted that it was important to compare experiments based on the linear velocity, 'Qa'.

Two dissolution columns, of 8 mm and 9 mm I.D. were used; the cross-sectional area of the columns differed by 14%. After 1.00 gram of 30/40 mesh K_2SO_4 crystals was poured into each column, the bed height of the crystals was measured. The height of 17 mm and 24 mm leads to a volume of 1.08 and 1.21 cm^3 for the 9 mm and 8 mm columns, respectively; these differ by 12%, which indicates that wall effects (as might be expected) are greater in the smaller diameter column; this difference in packing at the walls could have an effect on the hydrodynamics within the column.

In runs #72 and #73, 1.00 gram K_2SO_4 (batch G, 30/40

mesh) was dissolved in 40% ethanol, using the 8 mm and 9 mm columns, respectively. Dissolution results are listed in Table 24 and 26, respectively; Figure 19 shows the dissolution profile for these two runs.

Dissolution is obviously quite different in these two cases, if they are compared on the basis of concentration versus time. But since the flow rates were different, the data should be compared on the basis of mass dissolved per time; values for these two runs, reported as mg/min dissolved at various times are listed in Table 33. While the linear velocities vary by 28%, the mass dissolved in, for example, the first 10 minutes differed by as much as 47%.

These two dissolution runs represented the same total surface area, but different bed heights, of K_2SO_4 presented to the solvent. If the column load in the 8 mm column was reduced to 0.77 gram, then the bed height decreased to 17 mm, which was the bed height of 1.00 gram in the 9 mm column. Results from the dissolution of 0.77 gram in the 8 mm column, run #67, are listed in Table 25; the dissolution profile is included in Figure 19. The shape of this dissolution curve is similar to the profile for run #73 for dissolution of 1.00 gram of the same mesh cut; the concentration is higher because the linear velocity in the 8 mm column is slower than in the 9 mm (i.e. 6.46 cm/min

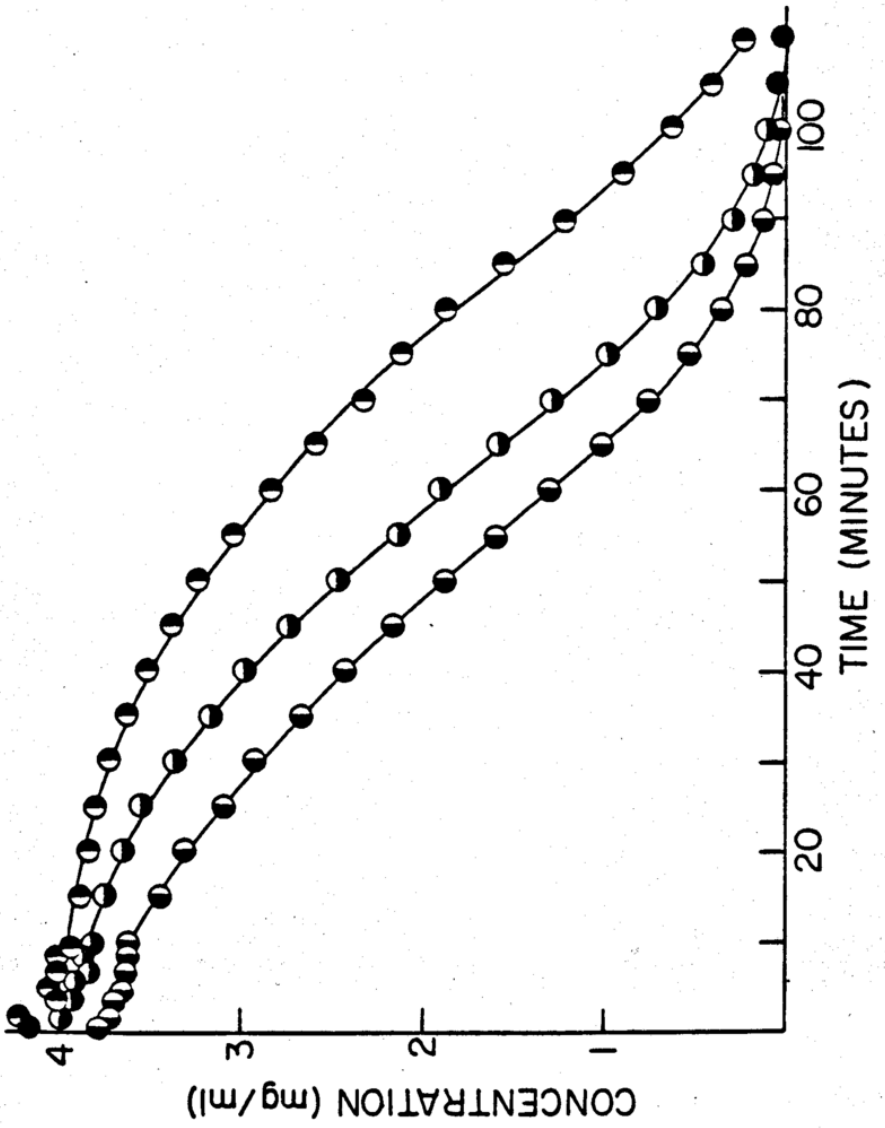
CONCENTRATION (mg/ml)
4
3
2
1
20
40
60
80
100
TIME (MINUTES)

TABLE 33. POTASSIUM SULFATE DISSOLVED PER TIME

TIME (min)	RUN #72 8mm (mg/min)	RUN #73 9mm (mg/min)
0.5	13.63	19.94
1.5	13.73	19.54
2.5	13.06	19.37
3.5	13.06	19.43
4.5	13.13	19.26
5.5	13.06	19.26
6.5	13.06	19.09
7.5	12.90	19.15
8.5	13.06	19.04
9.5	12.78	19.15
15.0	12.65	18.11
20.0	12.46	17.40
25.0	12.39	16.27
30.0	12.10	15.35
35.0	11.82	14.05
40.0	11.41	12.74
45.0	11.01	11.31
50.0	10.51	9.86
55.0	9.88	8.39
60.0	9.20	6.84
65.0	8.43	5.34
70.0	7.56	4.03
75.0	6.85	2.82
80.0	6.03	1.85
85.0	5.04	1.13
90.0	3.97	0.65
95.0	2.94	0.36
100.0	2.03	0.18
105.0	1.30	0.05
110.0	0.78	
115.0	0.42	
120.0	0.24	
125.0	0.11	
130.0	0.09	

compared to 8.25 cm/min). Thus, solvent is in contact with the material in the 8 mm column for a longer time.

G. Effect of Solvent Flow Rate on Dissolution Rate

Investigators have suggested that it is important to compare experiments in which the liquid velocity, 'Qa', is the same (31,38). They showed that if the same column load was used, then different diameter columns gave comparable dissolution results for the same linear velocity in sink conditions.

In experiments to be described here, the two columns, 8mm and 9mm , were charged with 0.77 and 1.00 gram samples of 30/40 mesh (batch G) K_2SO_4, respectively. The solvent, 40% ethanol, was pumped at five different flow rates through each column; the preparative pump head was used on the pump for all experiments.

Solvent flow rates were selected so that they were spaced at equal intervals and they utilized the maximum capacity of the pump head; the flow rates were in the approximate ratio of X:2X:3X:4X:5X. However, these were selected such that the linear velocities for the two columns were not the same, but they overlapped.

In these experiments then, the solvent flowed through powder beds of the same height; however, the mass of the solute and the linear velocity of the solvent were different between the two columns.

Data for dissolution runs #67 through #71 for the 8mm

and #73 through #77 for the 9mm are listed in Tables 25 and 26, respectively. It was difficult to compare data in this form and to reach any conclusions. But if the data were converted to a reduced form of 't*' and 'C*' as defined previously (see Section D), the differences in initial mass and flow rate would be taken into account. Then the profiles could be compared with respect to the linear velocity of the system.

Tables 34 and 35 contain the 't*' and 'C*' values for the five flow rates in each of the 8mm and 9mm columns. The linear velocities, 'Qa', are also listed for each dissolution run.

In Figure 20, only three of the reduced runs have been shown; profiles for runs #67, 69, and 77 represent the highest, lowest and an intermediate value of 'Qa' in reduced form. These are shown to illustrate how variation in 'Qa' changes the form of these reduced profiles.

If one compares the data from all ten dissolution runs in reduced form, the rank order of these profiles, based on the value of 'C*' at early 't*', should be correlated with the linear velocity of the solvent. Such a comparison of the experimental data here is excellent; all profiles fit in rank order with respect to 'Qa', with the exception of run #71, with the fastest flow rate through the 8 mm column. Table 36 lists the dissolution runs in "expected"

TABLE 34. REDUCED TIME AND REDUCED CONCENTRATION FOR POTASSIUM SULFATE DISSOLVED AT VARIOUS FLOW RATES IN 8 mm COLUMN

Run #67 W = 3.25 ml/min		Run #68 W = 6.4 ml/min		Run #69 W = 9.8 ml/min	
t*	C*	t*	C*	t*	C*
0.010	0.890	0.020	0.777	0.030	0.607
0.030	0.851	0.059	0.766	0.090	0.578
0.050	0.845	0.098	0.755	0.150	0.591
0.069	0.835	0.137	0.744	0.209	0.583
0.089	0.830	0.176	0.729	0.269	0.574
0.109	0.832	0.215	0.718	0.329	0.557
0.129	0.820	0.254	0.703	0.389	0.531
0.149	0.825	0.293	0.691	0.449	0.525
0.169	0.825	0.332	0.683	0.508	0.516
0.188	0.813	0.371	0.676	0.568	0.502
0.298	0.801	0.586	0.610	0.897	0.416
0.397	0.778	0.781	0.550	1.196	0.357
0.496	0.758	0.977	0.478	1.495	0.303
0.595	0.716	1.172	0.407	1.794	0.249
0.694	0.675	1.367	0.342	2.093	0.196
0.793	0.635	1.563	0.284	2.392	0.147
0.893	0.582	1.758	0.207	2.691	0.096
0.992	0.524	1.953	0.139	2.990	0.050
1.091	0.453	2.148	0.080	3.289	0.017
1.190	0.404	2.344	0.039	3.589	0.005
1.289	0.338	2.539	0.015		
1.389	0.275	2.734	0.004		
1.488	0.208				
1.587	0.150				
1.686	0.096				
1.785	0.063				
1.885	0.039				
1.984	0.022				
2.083	0.011				
2.182	0.005				
Qa = 6.46 cm/min		Qa = 12.72 cm/min		Qa = 19.48 cm/min	
t' = 50.41 min		t' = 25.60 min		t' = 16.72	

TABLE 34. (CONT.)

Run #70 W = 12.7 ml/min		Run #71 W = 15.8 ml/min	
t*	C*	t*	C*
0.039	0.530	0.048	0.407
0.116	0.519	0.145	0.420
0.194	0.509	0.241	0.402
0.271	0.492	0.338	0.390
0.349	0.474	0.434	0.375
0.426	0.466	0.530	0.364
0.504	0.460	0.627	0.349
0.581	0.437	0.723	0.339
0.659	0.432	0.820	0.330
0.736	0.413	0.916	0.314
1.163	0.339	1.446	0.256
1.550	0.280	1.929	0.214
1.938	0.226	2.411	0.181
2.326	0.182	2.893	0.148
2.713	0.138	3.375	0.119
3.101	0.102	3.857	0.092
3.488	0.065	4.339	0.067
3.876	0.031	4.822	0.043
4.264	0.012	5.304	0.022
4.651	0.004	5.786	0.010
		6.268	0.003
Qa = 25.25 cm/min		Qa = 31.41 cm/min	
t' = 12.90 min		t' = 10.37 min	

TABLE 35. REDUCED TIME AND REDUCED CONCENTRATION FOR POTASSIUM SULFATE DISSOLVED AT VARIOUS FLOW RATES IN 9 mm COLUMN

Run #73 W = 5.25 ml/min		Run #74 W = 10.6 ml/min		Run #75 W = 15.6 ml/min	
t*	C*	t*	C*	t*	C*
0.012	0.808	0.025	0.631	0.037	0.581
0.037	0.792	0.075	0.611	0.110	0.569
0.062	0.785	0.125	0.606	0.183	0.550
0.086	0.787	0.174	0.601	0.257	0.531
0.111	0.780	0.224	0.596	0.330	0.515
0.136	0.780	0.274	0.601	0.403	0.500
0.160	0.774	0.324	0.597	0.477	0.503
0.185	0.776	0.374	0.589	0.550	0.483
0.210	0.771	0.424	0.589	0.623	0.469
0.234	0.776	0.473	0.571	0.696	0.455
0.370	0.734	0.747	0.504	1.100	0.377
0.493	0.705	0.997	0.445	1.466	0.312
0.617	0.659	1.246	0.381	1.833	0.249
0.740	0.622	1.495	0.317	2.199	0.190
0.864	0.570	1.744	0.253	2.566	0.136
0.987	0.516	1.993	0.196	2.933	0.087
1.110	0.459	2.242	0.136	3.299	0.049
1.234	0.400	2.491	0.087	3.666	0.026
1.357	0.340	2.740	0.050	4.032	0.012
1.480	0.277	2.990	0.028	4.399	0.006
1.604	0.217	3.239	0.014	4.765	0.001
1.727	0.163	3.488	0.007		
1.850	0.114	3.737	0.003		
1.974	0.075	3.986	0.002		
2.097	0.046	4.235	0.001		
2.221	0.026	4.484	0.001		
2.344	0.015				
2.467	0.007				
2.591	0.002				
Qa = 8.25 cm/min		Qa = 16.67 cm/min		Qa = 24.53 cm/min	
t' = 40.53 min		t' = 20.07 min		t' = 13.64 min	

TABLE 35. (CONT.)

Run #76 W = 20.8 ml/min		Run #77 W = 25.3 ml/min	
t*	C*	t*	C*
0.049	0.488	0.059	0.473
0.147	0.495	0.178	0.463
0.244	0.497	0.297	0.451
0.342	0.470	0.416	0.433
0.440	0.456	0.535	0.421
0.538	0.439	0.654	0.398
0.635	0.422	0.773	0.380
0.733	0.410	0.892	0.359
0.831	0.402	1.011	0.339
0.929	0.380	1.130	0.325
1.466	0.298	1.784	0.237
1.955	0.232	2.378	0.174
2.444	0.172	2.973	0.125
2.933	0.123	3.567	0.083
3.421	0.079	4.162	0.050
3.910	0.042	4.756	0.025
4.399	0.021	5.351	0.012
4.888	0.009	5.945	0.005
5.376	0.004	6.540	0.002
5.865	0.001		
Qa = 32.70 cm/min		Qa = 39.78 cm/min	
t' = 10.23 min		t' = 8.41 min	

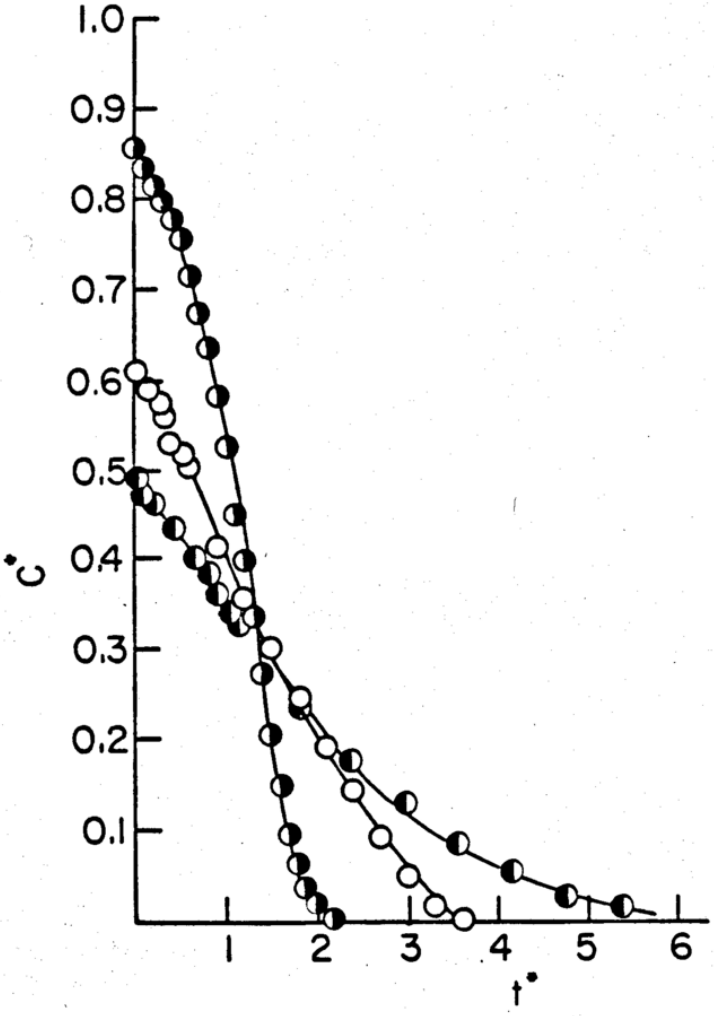
1.0
0.9
0.8
0.7
0.6
0.5
0.4
0.3
0.2
0.1
C*
1
2
3
4
5
6
t*

TABLE 36. RANK ORDER OF DISSOLUTION PROFILES

Flow Rate (ml/min)	(column)	Qa (cm/min)	Expected Order	Observed Order
3.25	(8mm)	6.46	1	1
5.25	(9mm)	8.25	2	2
6.4	(8mm)	12.72	3	3
10.6	(9mm)	16.67	4	4
9.8	(8mm)	19.48	5	5
15.6	(9mm)	24.53	6	6
12.7	(8mm)	25.25	7	7
15.8	(8mm)	31.41	8	10
20.8	(9mm)	32.70	9	8
25.3	(9mm)	39.78	10	9

and "observed" rank order. It is unclear why the profile for run #41 does not follow this trend.

From this set of dissolution runs, it can be concluded that, if compared on a reduced concentration and time basis, experiments of different initial load, flow rate and liquid velocity can be compared, and comparison is valid under nonsink conditions. A rank-order correlation is noted in reduced concentration versus time profiles between 'C*' at early 't*' and linear velocities, 'Qa'.

H. Effect of Pulsation on Dissolution Rate

Previous workers have investigated the use of various pumps for column dissolution. Lerk and Zuurman compared several pumps and found the centrifugal pump, if properly integrated with check valves and flow meters, to cause the least pulsation and therefore to be preferred for use in column dissolution (37); however, the flow rate of 120 ml/min which they used was extremely high. Tingstad et al found that pulsation from a peristaltic pump was not a (significant) problem at a flow rate of 12 - 14 ml/min (39).

Other workers have used piston, syringe, peristaltic and positive displacement pumps (31,36,39,46). At a recent conference dedicated solely to the topic of dissolution, Dr. Bernard Cabana from the U.S. Food and Drug Administration offered some comments about column dissolution and the FDA's interest in it (76). The type of pump used is presently considered to be the most critical parameter of the column dissolution method; while a positive displacement pump may meet the general pumping needs, the occurrence of pulsation and its effect on dissolution rate is a subject which requires additional investigation (77)

Here, the effect of pulsation on dissolution rate was

studied; two different pump heads were used with the same positive displacement pump. Runs #39 and #73 describe the dissolution of 1.00 gm of 30/40 mesh (batch G) K_2SO_4 in 40% ethanol pumped at 5.3 ml/min with an analytical and preparative pump head, respectively. Dissolution results are listed in Tables 16 and 26; these concentration profiles are shown in Figure 21.

The analytical pump head has pumping capacity of 9.9 ml/min, while the preparative head can pump as fast as 27.7 ml/min. Thus, to pump solvent at the same flow rate, the number of pulses per minute with each pump head would be different; the analytical head uses more pulses to pump the same volume of fluid. This increase in the number of pulses per time period would lead to more agitation of fluid in the column. From Figure 21, it can be seen that the trend of the profiles here is consistent with increased agitation in the column; increased pulsation led to a slightly faster dissolution rate. Since the column was made of glass, it was possible to observe the motion of the powder bed as fluid was pumped through the column; pulsation was clearly observed with both pump heads. This pulsation has been visually recorded by others (41).

Pulsation seemed to cause no problems with the sampling procedure used in these experiments; since the pump pulsed more than 30 times per minute, no fluctuation

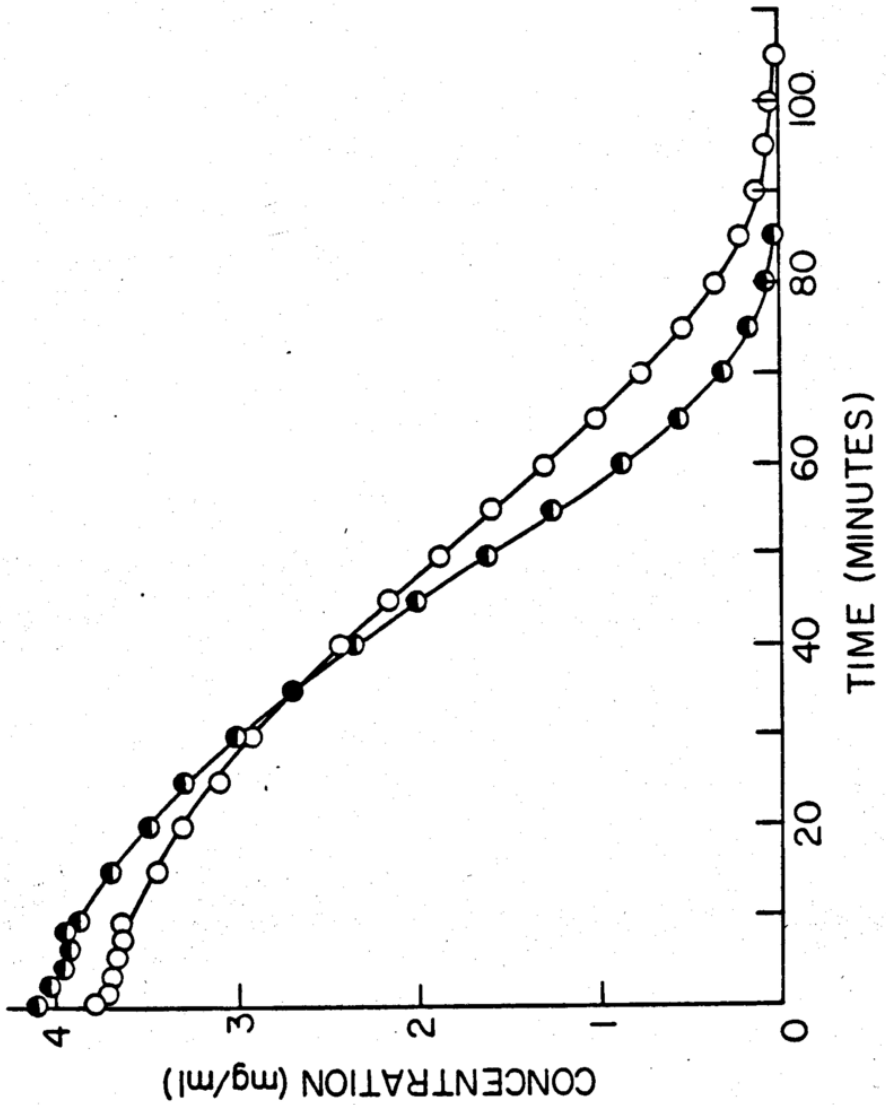
CONCENTRATION (mg/ml)
0
1
2
3
4
TIME (MINUTES)
20
40
60
80
100

was noted in sample volumes for 1 or 2 minute intervals. However, this pulsation may lead to a problem if a flow-through continuous detection method was used for analytical purposes.

Despite the fact that the positive displacement pump used was equipped with a pulse dampener, the latter apparently had little dampening effect, since no significant back pressure ever developed in the system. If back pressure were artificially established within the pumping system, then the pulse dampener might diminish pulsation during pumping.

McMichael and Hellums studied mass transfer and how it was affected by pulsation in fully developed flow of an incompressible Newtonian liquid through conduit (78); in most cases, they found that satisfactory accuracy could be obtained by ignoring the effect of pulsation. The largest effect they determined was an 8% change in flux due to pulsation; this is smaller than the inherent uncertainty in many mass-transfer coefficients.

While some pulsation is a normal characteristic of the pumping action from a positive displacement pump, its effect on dissolution rate is sufficiently small to warrant further investigation of the pump's use. The high accuracy of pumping over a moderate range of flow rates, even against a significant back pressure, is a clear advantage

of this pump, which may outweigh the pulsation problem.

I. Column Dissolution of Acetaminophen

Acetaminophen crystals were prepared for dissolution studies in two different recrystallization batches. Surface areas, measured by gas adsorption, of the 40/60 mesh cut of the two batches are reported in Table 2; these differed by less than 4%.

A 1.00 gram sample of each batch was placed in the 9 mm column and dissolved as Type II water (25°C) was pumped at a flow rate of 5.6 ml/min. Sample collection procedure was the same as previously described; all samples were diluted as necessary and analyzed spectrophotometrically. Concentrations for dissolution runs #78 and 79, for acetaminophen batches H and J, respectively, are listed in Table 27; Figure 22 shows the dissolution profiles for the two runs.

The solubility of acetaminophen in water at 25°C is approximately 15 mg/ml (79); this is much higher than the solubility of K_2SO_4 in the ethanol-water mixtures studied here. The shape of the dissolution profiles for the more soluble compound in a flow-through system is not unlike that noted for less soluble compounds (i.e. K_2SO_4). The concentration exhibited a plateau or a very shallow decline in concentration for approximately 8 minutes, followed by a steep drop in concentration when most of the material had dissolved. Most of the dissolution process occurred under

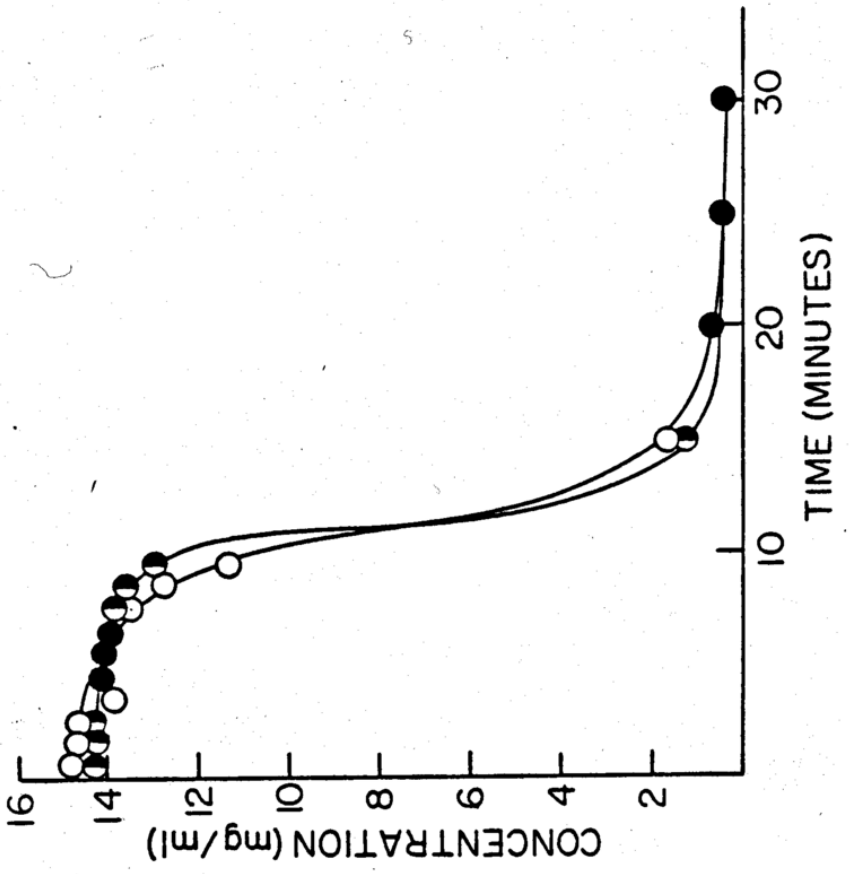
CONCENTRATION (mg/ml)
16
14
12
10
8
6
4
2
10
20
30
TIME (MINUTES)

nonsink conditions; in fact, the concentration was greater than 90% of the solubility for the first 8 minutes of each experiment. There was still some solid undissolved and visible with the column at 50 and 110 minutes in runs #78 and 79, respectively; however, as calculated from a mass balance, this represented less than 1% of the initial column load.

J. Mathematical Model for Column Dissolution

Numerous mathematical models have been proposed to describe the rate of dissolution of solids. The Noyes-Whitney equation was the first, and has served as a basis for many subsequent models (1). Nernst proposed an important modification, that dissolution rate is proportional to the surface area of the solid (2); the following equation then, often called the modified Noyes-Whitney equation, shall serve as the starting point for this discussion:

$$\frac{dm}{dt} = kA(S - C) \qquad (8)$$

As previously mentioned, most dissolution experiments reported have been done under sink conditions. Hixson and Crowell simplified the above equation to describe dissolution under these conditions (3); two assumptions were made: 1) the relationship between the surface area and volume of each particle remained constant, independent of particle size, because the particles dissolved isometrically; and 2) the concentration is small and much less than the solubility when sink conditions exist. The integrated form of Eq. (10) which resulted, commonly called the cube-root equation, describes how mass changes when particles dissolve under sink conditions.

Some investigators have found that results from column dissolution experiments were well described by the Hixson-Crowell equation (31,38); in their experiments, dissolution occurred under sink conditions. However, in the studies described here, nonsink conditions prevailed throughout most of the experiments; thus the Hixson-Crowell equation is not applicable.

Despite the numerous studies of column dissolution under sink conditions which have been reported, few models have been proposed for dissolution in this type apparatus. Langenbucher derived the relationship

$$T \alpha (Qa)^{-0.2-0.5}(Dp,o)^{1.5-1.8} \qquad (10)$$

where 'T' is the time for 100% of the material to dissolve, as predicted by the cube-root law, 'Qa' is the linear velocity of the solvent, and 'Dp,o' is the equivalent spherical particle diameter at zero time (31). This correlation applied to sink dissolution in flow-through conditions only at low Reynolds number (Re between 0.1 and 1.0); here, the dimensionless Reynolds number was defined:

$$Re = \frac{QaDp}{\nu} \qquad (11)$$

Carstensen and Dhupar wrote an equation to describe nonsink dissolution in a column apparatus; it described

dissolution kinetics in terms of the degree of saturation of the incoming and exiting streams (45). For dissolution of oxalic acid, a highly soluble compound, the model could account for change in powder bed height as a function of time and change in bed height as a function of liquid velocity. They also reported measurement of the concentration gradient over the length of the column; concentration asymptotically approached the solubility of the compound as the solvent moved (from bottom to top) through the column. This relationship can be written as:

$$C = S\left(1 - e^{-\frac{k_1 A}{V}t}\right) \qquad (12)$$

where 'k_1' is the mass transfer coefficient, 'A' is the surface area of solid in the column, 'V' is the column volume and 't' is time.

The form of the Noyes-Whitney equation has been previously discussed. A similar equation can be written for dissolution in a flow-through system; it describes dissolution rate in terms of the concentration in the exit stream from the column:

$$\frac{dm}{dt} = -WC_t \qquad (13)$$

where 'W' is the flow rate and 'C_t' is the concentration of solute in the column effluent at any time 't'. Equation

(12) can be written to describe the same 'C_t' where 'τ' is the residence time of fluid within the column:

$$C_t = S\left(1 - e^{-\frac{k_1 A}{V}\tau}\right) \tag{14}$$

Since the volume per residence time, or 'V/τ' is equal to 'W', the flow rate, then Eq. (14) becomes:

$$C_t = S\left(1 - e^{-\frac{k_1 A}{W}}\right) \tag{15}$$

If Eq. (15) is substituted into Eq. (13), then:

$$\frac{dm}{dt} = -SW\left(1 - e^{-\frac{k_1 A}{W}}\right) \tag{16}$$

This expression contains the variable 'A', the surface area of the column contents, which decreases during dissolution. Change in area as a function of time is an implicit relationship; explicitly, area changes as a function of mass. This can be written as:

$$A = A_o\left(\frac{m}{m_o}\right)^{\beta} \tag{17}$$

where 'A_o' and 'm_o' are the area and mass of the initial column load, respectively, 'm' is mass remaining undissolved in the column at any time 't' and 'β' is a constant. If the particles are assumed to be spherical, then $\beta = 2/3$; $\beta = 1/2$ for rod-shaped particles, assuming that these right cylinders dissolve from the side but not

the ends.

If mass is written in a dimensionless form, then dissolution from different initial loads are more easily compared; in reduced form, let:

$$m^* = \frac{m}{m_o} \tag{18}$$

Substituting Eqs. (17) and (18) into Eq. (16) leads to:

$$\frac{dm^*}{dt} = -\frac{SW}{m_o}\left[1 - e^{-\frac{k_1 A_o}{W}\left(m^*\right)^{\beta}}\right] \tag{19}$$

As was previously discussed, the mass transfer coefficient 'k_1' is assumed to be a constant here. When it is combined with other constants, a new variable is defined:

$$\alpha = \frac{k_1 A_o}{W} \tag{20}$$

Then Eq. (19) can be written:

$$\frac{dm^*}{dt} = -\frac{SW}{m_o}\left[1 - e^{-\alpha(m^*)^{\beta}}\right] \tag{21}$$

which in integral form is:

$$\int_1^{m^*} \frac{dm^*}{\left[1 - e^{-\alpha(m^*)^{\beta}}\right]} = -\frac{SW}{m_o}\int_0^t dt \tag{22}$$

There are two possible methods for solution of Eq. (22). It might be solved by variable substitution for

'm*', followed by a series expansion of exp(-x). In order to solve this analytically, only the first three terms of the expansion could be used (79). Such a termination of the series was unacceptable here however; neglecting the higher order terms in the series expeansion is valid only if 'x' is very large or very small. As will be discussed later, values for 'x', or '$\alpha(m^*)^{\beta}$', are not of this magnitude. Thus, an acceptable analytical solution does not exist for Eq. (22).

Numerical integration does provide a means to evaluate Eq. (22). A computer program was written in BASIC language to integrate 'm*' from 0.9999 to 0.005 in steps of -0.0001; this will evaluate the function at approximately 10,000 points. A copy of the program titled 'NAREA.BAS' is shown in Appendix B; a portion of a typical computer output is also included in that appendix.

The program contains an algorithm for calculation of the time for successive 'm*' values and the corresponding concentrations; values for reduced time, 't*' and reduced concentration, 'C*', are also calculated for both a sphere and rod models. Values are then printed for each 100th calculation. The function in Eq. (22) was evaluated for only two values of 'β', for $\beta = 2/3$ (i.e. sphere model) and for $\beta = 1/2$ (i.e. rod model); selection of 'β' need not be

limited to these two values however. The computer program could be easily modified to allow evaluation for other values of 'β'.

An upper limit of $\beta = 2/3$ follows directly from the geometric relationship between mass and surface area; a sphere represents the smallest surface to volume (or mass) ratio physically possible. Any other shape will have a larger surface to volume ratio, which corresponds to a smaller value for 'β'.

It is necessary to provide an estimate of 'α', as well as values for flow rate, initial column load, and solubility, to initiate the integration program. Equation (20) defined 'α' in terms of three experimental parameters. Equation (15) showed how these parameters were related to measurable quantities (i.e. concentration at any time 't' and solubility). It can be assumed that since 'A' changes little during the first minutes of the dissolution experiment, then 'A' is approximately equal to 'A_o'. Thus, one can obtain an estimate of 'α' from dissolution data at early times, where:

$$\alpha = -\ln\left(1 - \frac{C_t}{S}\right) \qquad (23)$$

Various 'α' values have been calculated from the dissolution experiments described here; corresponding values for 'm*' and concentrations for both shapes (rod and

sphere) have been generated accordingly. Figure 23 shows the profile for run #44, dissolution of 1.00 gram of 20/30 mesh K_2SO_4 in 40% ethanol at flow rate of 5.35 ml/min; also shown are the concentrations predicted by the model for both sphere and rod-shaped particles. Here, $\alpha = 1.20$ was calculated from the concentration of the solute measured in the first one-minute sample. Agreement between calculated and experimental concentration values is very good; the sphere model was in better agreement with experimental data than the rod model over the entire dissolution profile. The lowest concentration shown on each line in Figure 23 corresponds to the time calculated for 99% of the material to dissolve. No better agreement between experimental data and generated models occurred for the values of $\alpha = 1.10$, 1.15 or 1.25. Here, the model predicted a higher concentration for rods as compared to spheres, until approximately 85 - 90% of the material had dissolved.

A similar figure could be drawn for each dissolution run, with 'α' calculated from the concentration measured at early time points, as defined by Eq. (23). If the concentration of solute in the column effluent decreased from early time, very good agreement between experimental

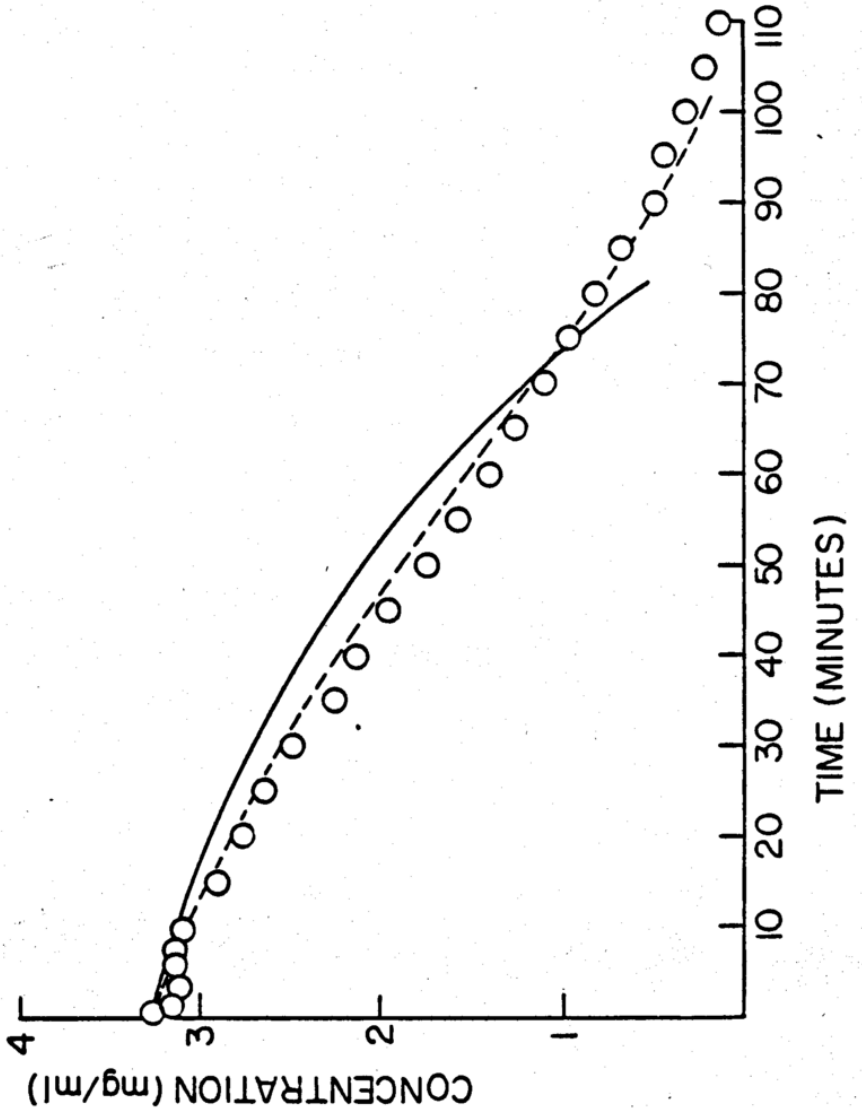
CONCENTRATION (mg/ml)
4
3
2
1
10
20
30
40
50
60
70
80
90
100
110
TIME (MINUTES)

and calculated concentrations can generally be obtained for $0.10 < m^* \leq 0.99$. However,if the concentrations exhibited a plateau value at early times, as was observed in numerous dissolution runs, the calculated concentrations deviate markedly from measured concentrations.

The model is based on the premise that during any dissolution experiment, concentration should always decline with time; if the initial mass is sufficiently large, the model predicts that the initial concentrations may exhibit an apparent plateau, but at a concentration almost indistinguishable from the solubility.

However, as was noted for numerous dissolution runs previously described, the concentration often exhibited a plateau at values of 90 to 98% solubility; the length of time when this apparent plateau existed also varied proportionally to the initial load and surface area.

The parameter 'α' was defined in terms of and calculated from actual dissolution data. However, in cases when an apparent plateau existed in the concentration profile, 'α' must be used as an adjustable parameter, if concentration profiles generated by the model are to coincide with the declining slope of the dissolution curves. A value of 'α' calculated from initial concentration values could be used as a first estimate, but

then 'α' must be adjusted (generally higher) to generate other sphere and rods profiles which might be in closer agreement with the experimental data.

Figure 24 shows the dissolution profile of run #20, for 80/100 mesh (batch G) which dissolved as 40% ethanol was pumped at 5.35 ml/min; also shown are the concentrations predicted by the model for $\alpha = 2.20$, which was calculated from concentration at early time. Neither sphere nor rod geometric model prediction is in close agreement with observed concentrations. However, Figure 25 shows how this agreement can be improved if a larger value of 'α' is used. While these values of 'α' predict higher than observed concentrations at early times, they can more closely describe the declining part of the dissolution profile, even when it is very steep as shown here. The rod model predicted concentrations which were in excellent agreement with experimental results for 20-50 minutes of the experiment. The lowest concentration shown on each line in Figure 25 corresponds to the time calculated for 99% of the material to dissolve.

This mathematical model has been compared to column dissolution data for K_2SO_4 only. No assumptions were made in the derivation which would limit its applicability to

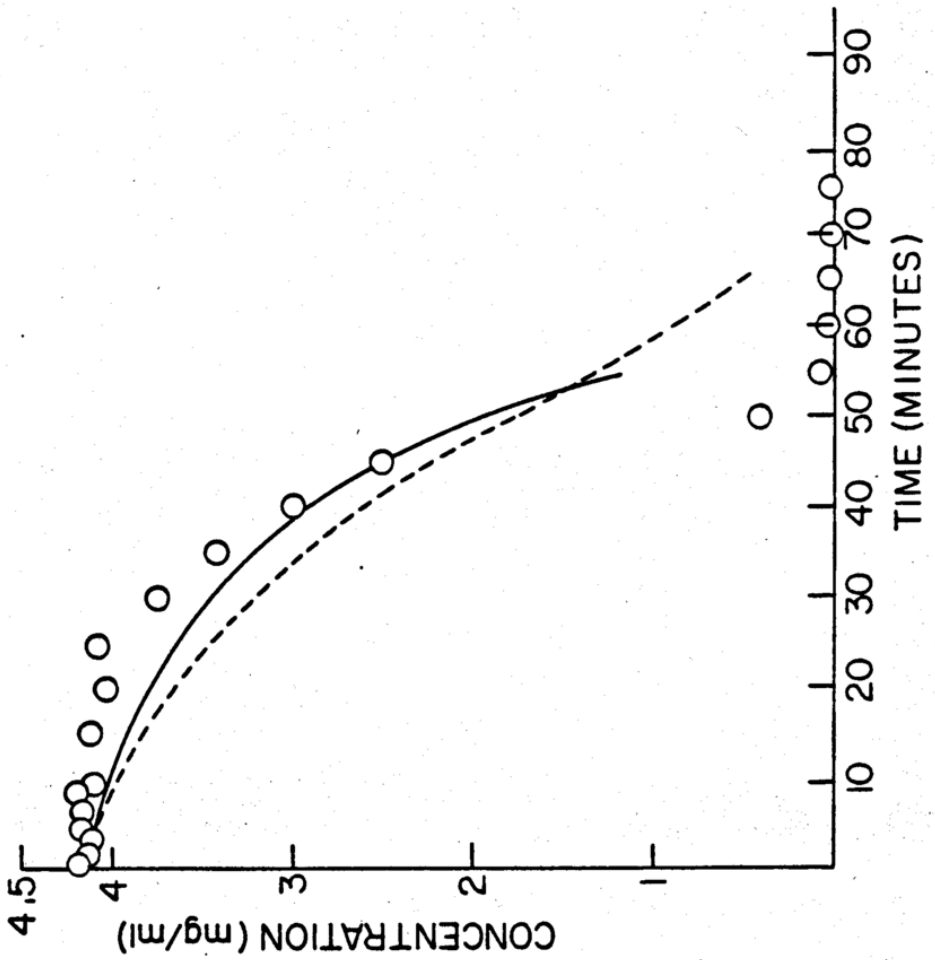
CONCENTRATION (mg/ml)
4.5
4
3
2
1
10
20
30
40
50
60
70
80
90
TIME (MINUTES)

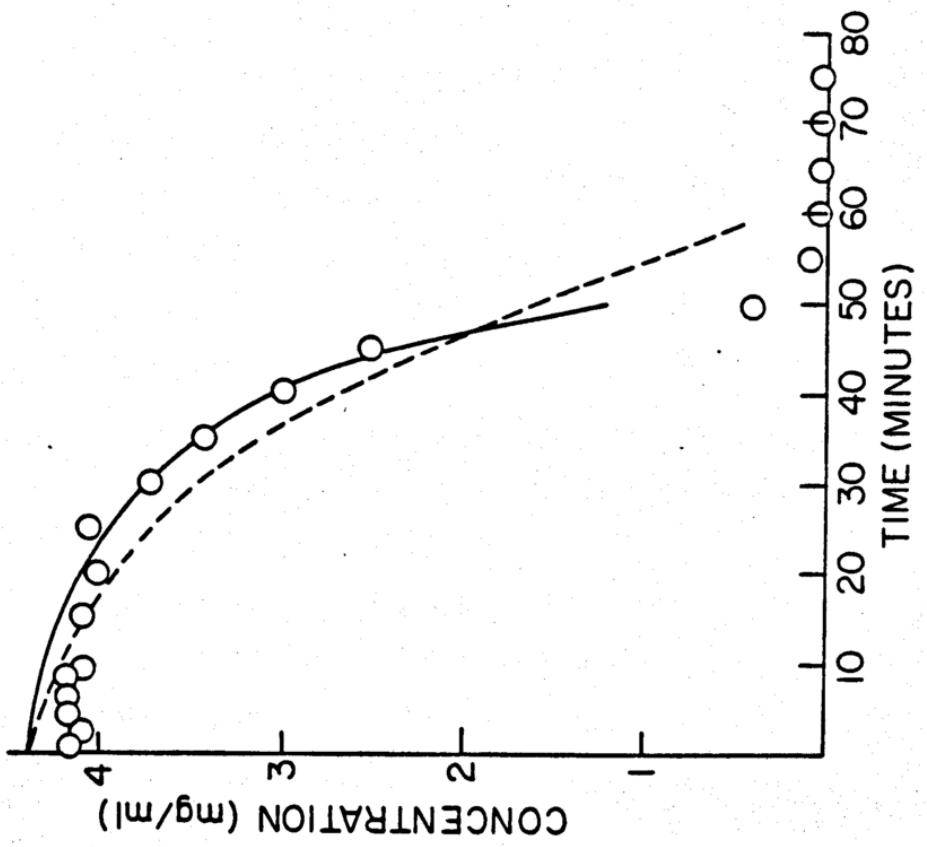
CONCENTRATION (mg/ml)
4
3
2
1
TIME (MINUTES)
10
20
30
40
50
60
70
80

poorly soluble substances. Test of the versatility of the model should include a comparison of the agreement between measured and calculated concentrations for acetaminophen, a compound of moderate solubility.

Profiles for dissolution runs #78 and 79 have been previously described and shown in Figure 22. The initial concentration noted for run #79 (i.e. C = 14.80 mg/ml) was used to calculate a value for 'α'; from Eq. (23), with S = 15.0 mg/ml, α = 4.3. Shown in Figure 26 is the experimental data from Figure 22, with the profiles generated for both a rod and sphere model, as previously described. Agreement between these models and results is very good; at 11 minutes, where the results from run #78 fall below the concentrations predicted by the model, 85% of the column contents has already dissolved. Note that the time scale is expanded here compared to that used in Figures 23, 24, and 25. Thus, the mathematical model appears to be applicable to column dissolution for more soluble materials, which also dissolve under nonsink conditions.

It would be desirable to have a means of comparing dissolution profiles from runs under different experimental conditions; this would test the capability of the model to

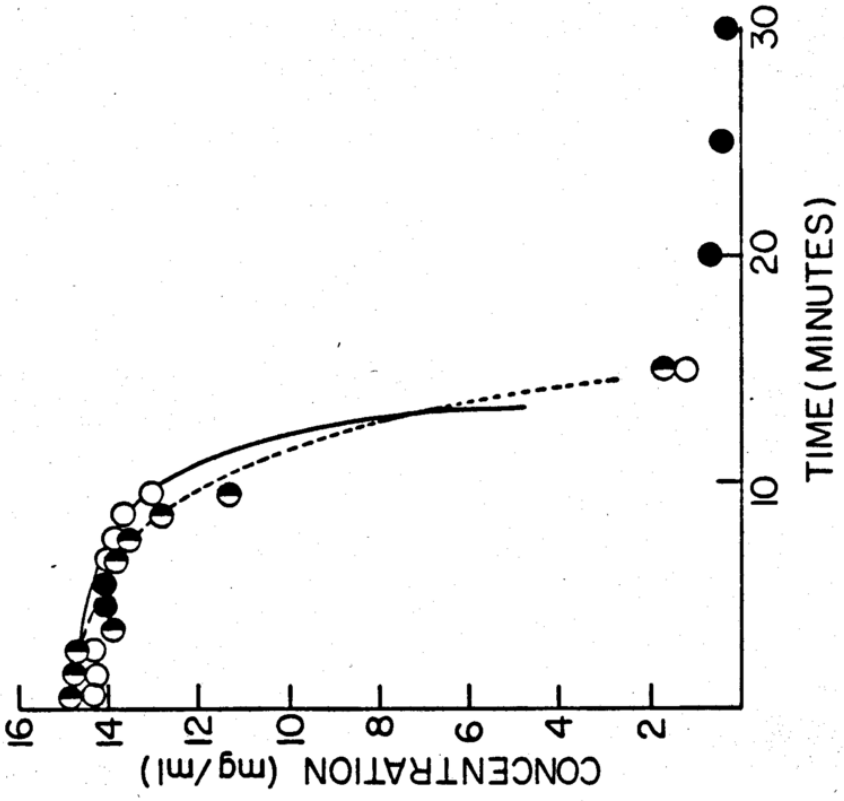
CONCENTRATION (mg/ml)
16
14
12
10
8
6
4
2
1
10
20
30
TIME (MINUTES)

describe dissolution with respect to various flow rates, surface areas, initial mass, and solubilities. As described in previous sections, concentration and time can be converted to dimensionless forms, and various dissolution runs can be compared. Again reduced concentration and reduced time, as they were previously defined

$$C^* = \frac{C}{S} \qquad t^* = \frac{t}{t'} \qquad (24)$$

where

$$t' = \frac{m_o}{SW} \qquad (25)$$

The dependence of dissolution on the mass-transfer coeffieient 'k_1' (which is assumed to be constant), initial surface area 'Ao' and flow rate 'W' has been included in 'α'. The influence of these parameters can be determined from a plot of reduced concentration versus reduced time for different values of 'α'.

In Figures 27 and 28, 'C*' versus 't*' is plotted for values of 'α' from 1.2 to 10.0 for the rod and sphere model, respectively. Although there is no maximum value of 'α', the limiting values for 'C*' and 't*' at large 'α' are each 1.0; this follows directly from the way in which each was defined. This range of values for 'α' provides dissolution profiles of virtually all the shapes noted in

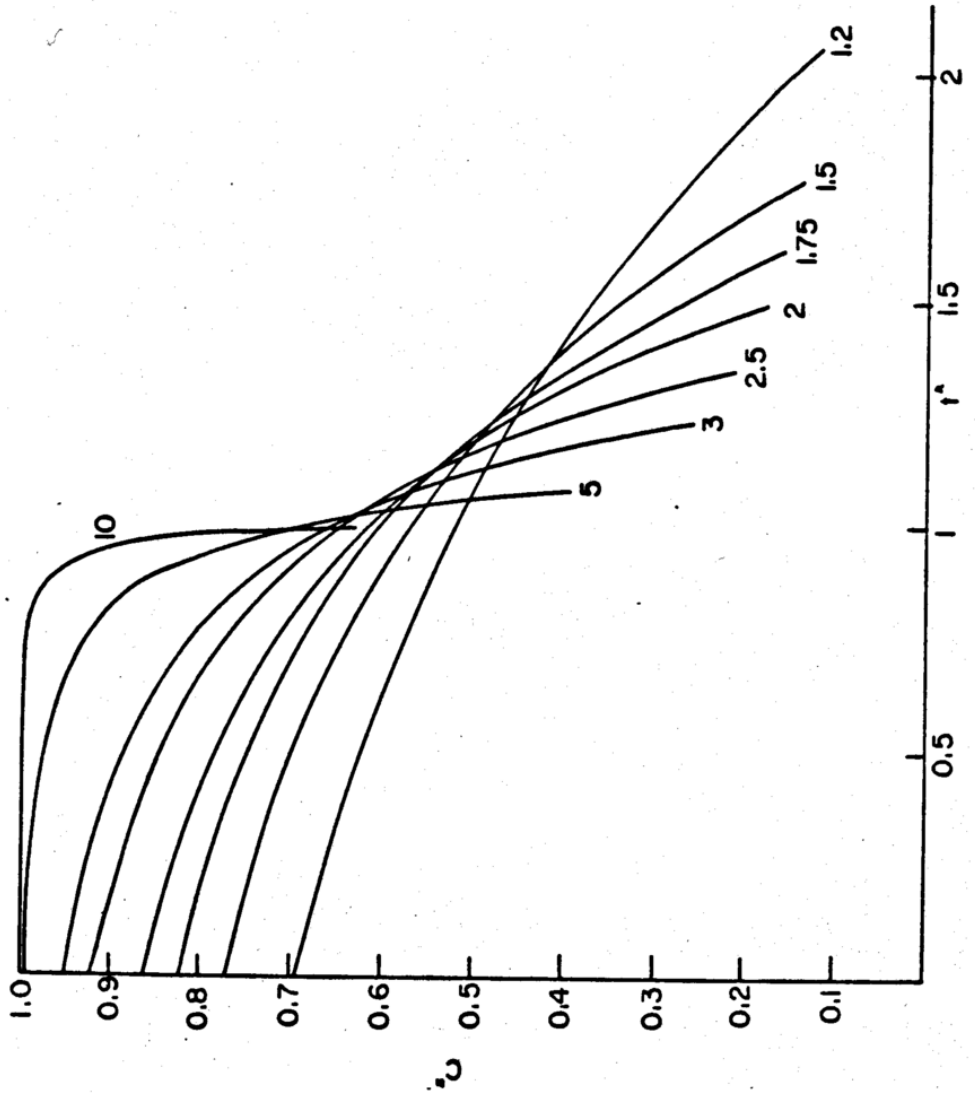
1.2
1.5
1.75
2
2.5
3
5
10
2
1.5
1
0.5
1.0
0.9
0.8
0.7
0.6
0.5
0.4
0.3
0.2
0.1

these experiments; however, it predicts that any plateau will occur at C* >0.999, not at the values of C* observed here. The lowest concentration shown on the line in Figures 27 and 28 corresponds to the time (t*) for 99.0% of the material to dissolve.

Profiles for the rod model are higher than profiles for sphere-shaped particles for all 't*' values; however, the slope of the former profiles is greater at small 'm*', and they generally cross the sphere profiles at 'm*' of 0.8 to 0.9.

A different 'β' value [illegible] if another geometric shape [illegible] appropriate for dissolution [illegible] use of any single 'β' value throughout the profile suggests that the particles [illegible] and retained the same shape during the dissolution experiment. If the observed [illegible] were in fact [illegible] with one geometric model for [illegible] but were better simulated by another [illegible]

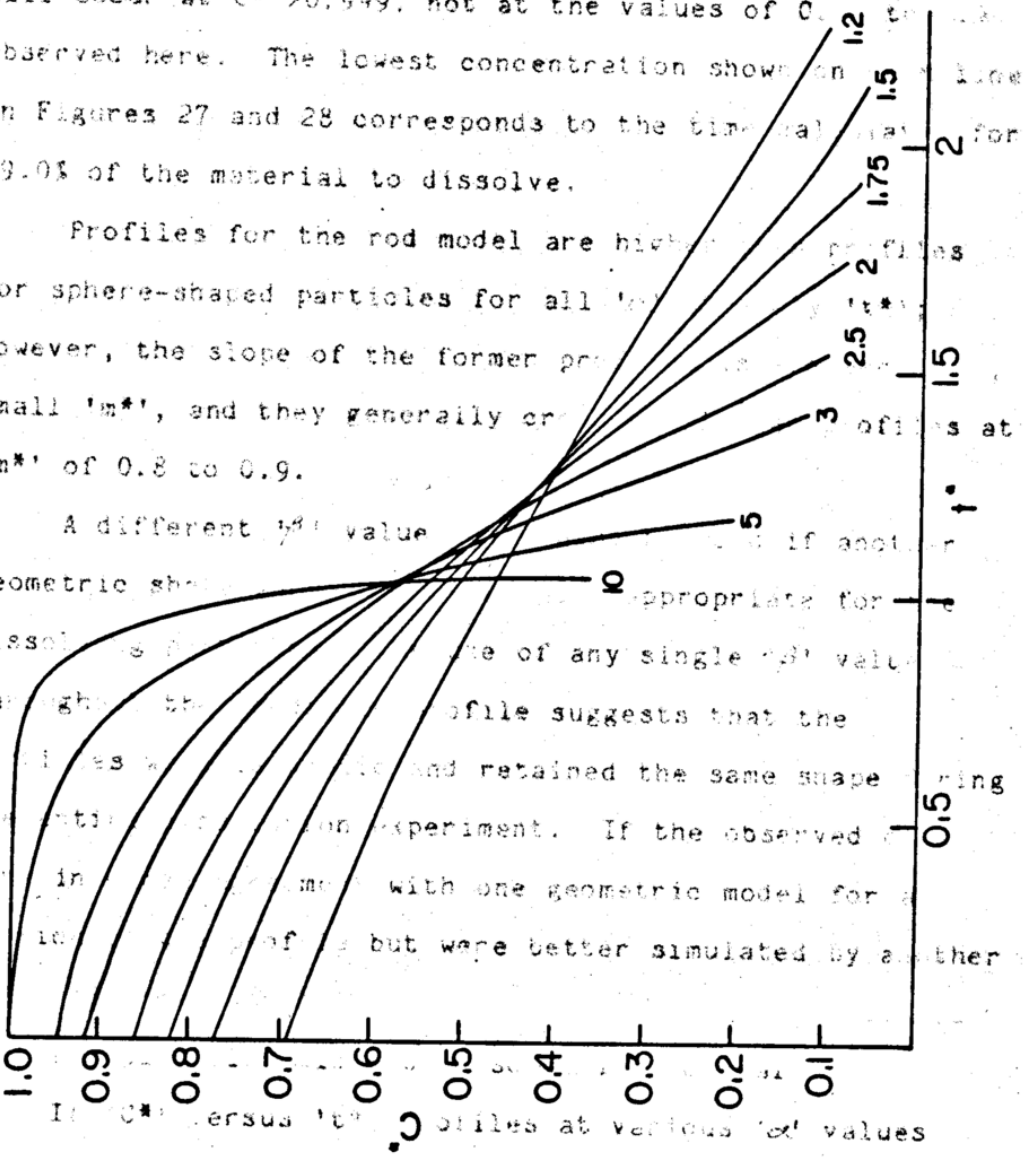

If C* versus 't*' profiles at various 'β' values were prepared for other particle shapes (i.e. other 'β' values), similar trends would be expected. Smaller 'β' values would lead to profiles with more curvature and steeper decline than those in Figure 27; however, the

these experiments; however, it predicts that any plateaus will occur at C* >0.999, not at the values of 0.90 to 0.98 observed here. The lowest concentration shown on each line in Figures 27 and 28 corresponds to the time calculated for 99.0% of the material to dissolve. Profiles for the rod model are higher than profiles for sphere-shaped particles for all 'α' at early 't*'; however, the slope of the former profiles is steeper at small 'm*', and they generally cross the latter profiles at 'm*' of 0.8 to 0.9. A different 'β' value could also be used if another geometric shape were considered more appropriate for the dissolving particles. The use of any single 'β' value throughout the predicted profile suggests that the particles were isotropic and retained the same shape during the entire dissolution experiment. If the observed data were in close agreement with one geometric model for a portion of the profile but were better simulated by another geometric shape in a later portion, it might be concluded that the particles did not dissolve isotropically.

If 'C*' versus 't*' profiles at various 'α' values were prepared for other particle shapes (i.e. other 'β' values), similar trends would be expected. Smaller 'β' values would lead to profiles with more curvature and steeper decline than those in Figure 27; however, the

limiting values of 1.0 for 'C*' and 't*' at large 'α' would still exist.

Equation (21), the differential form of the model derived here, is similar in form to the Rosin - Rammler - Sperling or Weibull distribution (80); the Weibull function has been used to describe numerous processes, including kinetic processes such as dissolution (81,82). The Weibull function, applied to dissolution rate data, expresses the cumulative fraction of material dissolved 'm#' at time 't' by

$$m^{\#} = \left[1 - e^{-(t - T_i)^{b/a}}\right] \qquad (26)$$

where 'a' is a "scale" parameter (i.e. for time 't'), 'b' is a "shape" parameter to describe the shape of the curve, and 'T_i' is a "location" parameter which accounts for lag time in the process, if necessary.

By comparison, Eq. (21) as previously presented is:

$$\frac{dm^*}{dt} = -\frac{SW}{m_o}\left[1 - e^{-\alpha(m^*)^{\beta}}\right] \qquad (21)$$

Many similarities exist between Eqs. (21) and (26). If the location parameter, 'T_i' is eliminated from the latter, then each equation contains two parameters. The terms 'α' and 'a' are each scale factors for time; as shown in Figures 27 and 28, 'α' affects the length of time for

the process of dissolution to occur. The parameter 'a' in the Weibull function is used to define the time scale of the process. While 'b' and 'β' are both described as shape factors because they characterize or determine the general shape of the curve, they lack further similarity; 'b' is not related to any specific physical characteristic of the system (81), while 'β' defined in Eq. (17) is related to a specific particle shape of rods or spheres, and how the surface area changes with change in mass.

The left hand sides of Eqs. (21) and (24) clearly differ; while the former describes the first derivative of 'm*' with respect to time, the Weibull function describes an integral form, or cumulative amount dissolved, 'm#'. For reasons described previously, column dissolution data can be presented in integral form, but it is easier to discern the influence of various experimental factors if data are presented in differential form.

CONCLUSIONS

1. The column was a simple, versatile apparatus with well defined hydrodynamics, which was used in the study of dissolution kinetics under both sink and nonsink conditions. A positive displacement pump delivered solvent to the column at a uniform rate, with minimal pulsation; either an analytical or a preparative pump head can be used, the latter provided a maximum flow rate of approximately 28 ml/min.

2. For a poorly soluble substance, column dissolution kinetics are affected by numerous variables. Dissolution rate increased as average spherical particle diameter decreased; as column load, or total surface area of solid, increased, dissolution rate increased. While dissolution rate was proportional to some measure of surface area, no correlation or rank order was seen between dissolution rate and specific surface area as measured by gas adsorption for the same mesh cut of several recrystallization batches. The plateau exhibited in concentration profiles was apparently related to some critical surface area for the column contents; while surface area was equal to or above this value, a maximum dissolution rate was noted, and

concentrations were 0.90 to 0.98 times the solubility. Nonsink conditions apparently developed due to the bed height in the column and the length of time solvent was in contact with the solid.

Dissolution profiles for experiments using different solvents or different flow rates were more easily compared if concentration and time were converted to a reduced form; the reduced dissolution profiles were similar for 3 of the 4 solvents, suggesting that the same mass-transfer coefficient existed for these systems. When experimental results for 10 runs with different flow rate and initial load were compared, rank order correlation was observed between reduced concentration at early time and the linear velocity of the solvent.

Both an analytical and preparative pump head were used on a positive displacement pump. While each pump delivered solvent at a uniform flow rate, undesirable pulsation of solvent due to stroke frequency caused some agitation of fluid within the column. The pulsation may have some (small) effect of dissolution rate.

Dissolution of a more soluble compound, acetaminophen, showed a similar profile; concentration initially was very close to the solubility, remained virtually constant for some time, and then declined very rapidly after more than 85% of the material had dissolved. Nonsink conditions

existed for most of the experiment.

3. When dissolution experiments were interrupted, it was observed that nonspherical particles dissolved in many ways; clusters remained intact, rods became rounded or very pointed, and larger single crystals became prolate ellipsoid-shaped after more than 50% had dissolved. Differences in dissolution rates between equal masses of materials with different past histories (i.e. original starting material versus pooled sample from "25% or 50% previously dissolved") were consistent with change in surface energy of a solid; higher surface energy surfaces dissolved faster than lower energy surfaces.

4. A mathematical model was derived which described the change in mass undissolved with respect to time as a function of the flow rate of solvent, the solubility and mass-transfer coefficient of the solute; excellent agreement was found between the model and dissolution profiles for compounds of poor to moderate solubility. While the model was versatile and described the relationship between the area and mass as a function of time for any geometric particle shape, two geometric shapes were chosen for this analysis; concentration profiles consistent with dissolution of rods and spheres were in

very good agreement with experimental data for both K_2SO_4 and acetaminophen. The main assumption used in the development of the model was that the concentration gradient in the column could be described by an exponential function; it was also assumed that the mass-transfer coefficient was constant throughout each dissolution experiment. Applicability of the model should not be limited to nonsink conditions; the concentration measured at early time was used to define the dependence of dissolution kinetics on initial load, solubility and solvent flow rate.

APPENDIX A: GLOSSARY OF SYMBOLS

A	surface area in Noyes-Whitney equation
a	activity of potassium ion
Ac	cross-sectional area of dissolution cell
As	specific surface area from BET equation
B	constant in BET equation
C	concentration of solute
C*	reduced concentration
C_t	concentration at any time 't'
D	constant in BET equation
Dp	equivalent spherical particle diameter
G	cross-sectional area of adsorbate molecule, in Eq.(3)
H	heat of adsorption, in Eq.(2)
H	heat of liquefaction, in Eq.(2)
k	mass-transfer coefficient
m	mass undissolved
m_o	initial column load
m*	reduced mass
M	molecular weight of krypton
N	Avogadro's number
P/Po	relative pressure of adsorbate gas
Q	volumetric flow rate
Qa	liquid velocity

R	gas constant
Re	Reynolds number
S	solubility
Sa	specific surface area(m^2/g)
T	absolute temperature
t	time
t*	reduced time
V	volume of dissolution column
Vc	volume of calibration
W	solvent flow rate
W	weight of krypton at any P/Po
Wm	weight of monolayer of krypton
Ws	weight of sample for gas adsorption
α	(adjustable) parameter in Eq.(20)
β	shape parameter for rod or sphere model, in Eq.(17)
ν	kinematic viscosity
μ	viscosity
ρ	density
Θ	angle of diffraction
τ	residence time

APPENDIX B: COMPUTER PROGRAM FOR NUMERICAL INTERGRATION OF EQUATION (22)

A computer program was written in BASIC language to provide a means to numerically integrate Eq. (22). The program, titled NAREA.BAS, is listed on a subsequent page, along with an abbreviated form of the typical output printed. The variables names within the program are consistent; however, they may not refer to the same parameters described in the previous text.

Each two lines of the output consist of results of each 100th calculation. The values represent the following quantities, as defined in the text:

t(rod) t(sph) m* cum.mass dissolved C(rod) C(sph)
t*(rod) t*(sph) m* cum.mass dissolved C*(rod) C*(sph)

The output lists some of the first and final values calculated for dissolution of 1.00 gram of 20/30 mesh potassium sulfate dissolved in 40% ethanol at 5.35 ml/min; the values are shown in Figure 23.

```
type narea.bas
10 input 'alpha';a
11 input 'flow rate';w
12 input 'mass';m0
13 input 'solubility';s
14 print  'time rod  time sph  mstar   mass    rod conc  sph conc'
15 z=s*w/m0
20 for mstar=.9999 to 0.005 step -.0001
25 mg=m0*(1-mstar)
30 roda=roda-1/2*.0001*(1/(1-exp(-a*mstar^.5))+1/(1-exp(-a*(mstar+.0001)^.5)))
32 rodc=s*(1-exp(-a*mstar^.5))
35 sa=sa-1/2*.0001*(1/(1-exp(-a*mstar^.667))+1/(1-exp(-a*(mstar+.0001)^.667)))
37 sc=s*(1-exp(-a*mstar^.667))
40 counter=counter+1
41 r=-roda/z
42 q=-sa/z
43 p=mstar
44 wt=mg
45 d=rodc
46 e=sc
47 k=-roda
48 j=-sa
49 m=rodc/s
50 n=sc/s
51 if counter=100 then goto 55 else 70
55 print using '###.###   ###.###  #.####  ###.###  ##.####   ##.####';r;q;&
   p;wt;d;e
56 print using '##.####   ##.####  #.####  ###.###  #.#####   #.#####';k;j;&
   p;m;n
57 print
60 if counter=100 then counter=0
70 next mstar
80 end
```

```
 RUN NAREA
alpha? 1.20
flow rate? 5.35
mass? 1000.0
solubility? 4.70
```

time rod	time sph	mstar	mass	rod conc	sph conc
0.570	0.570	0.9900	10.002	3.2758	3.2730
0.0143	0.0143	0.9900	10.002	0.69699	0.69638
1.141	1.142	0.9800	20.003	3.2672	3.2615
0.0287	0.0287	0.9800	20.003	0.69515	0.69393
1.714	1.716	0.9700	30.005	3.2585	3.2498
0.0431	0.0432	0.9700	30.005	0.69329	0.69145
2.288	2.293	0.9600	40.007	3.2496	3.2380
0.0575	0.0576	0.9600	40.007	0.69141	0.68894
2.864	2.871	0.9500	50.008	3.2407	3.2261
0.0720	0.0722	0.9500	50.008	0.68951	0.68640
3.442	3.451	0.9400	60.010	3.2317	3.2140
0.0865	0.0868	0.9400	60.010	0.68759	0.68383
4.021	4.034	0.9300	70.012	3.2225	3.2018
0.1011	0.1014	0.9300	70.012	0.68564	0.68123
4.602	4.619	0.9200	80.013	3.2133	3.1894
0.1157	0.1161	0.9200	80.013	0.68368	0.67860
72.942	84.062	0.0499	950.053	1.1056	0.7053
1.8341	2.1137	0.0499	950.053	0.23523	0.15006
74.715	86.896	0.0399	960.054	1.0023	0.6143
1.8787	2.1850	0.0399	960.054	0.21325	0.13071
76.699	90.215	0.0299	970.054	0.8813	0.5130
1.9286	2.2685	0.0299	970.054	0.18752	0.10916
79.013	94.333	0.0199	980.054	0.7327	0.3965
1.9868	2.3720	0.0199	980.054	0.15589	0.08437
81.967	100.124	0.0099	990.054	0.5301	0.2534
2.0611	2.5176	0.0099	990.054	0.11279	0.05391

REFERENCES

1. Noyes, A.A. and Whitney, W.R.: The rate of solution of solid substances in their own solutions. J Amer Chem Soc 19 930-934 (1897).

2. Nernst, W: Theorie der reaktionsgeschwindigkeit in heterogenen systemen. Z Physik Chem 47 52-55 (1904).

3. Hixson, A.W. and Crowell, J.H.: Dependence of reaction velocity upon surface and agitation. I. Theoretical considerations. Ind End Chem 23 923-928 (1931).

4. King, C.V. and Braverman, M.M.: The rate of solution of zinc in acids. J Amer Chem Soc 54 1744-1757 (1932).

5. King, C.V. and Schack, M.: The rate of solution of zinc in acids. J Amer Chem Soc 57 1212-1217 (1935).

6. King, C.V. and Cathcart, W.H.: The rate of dissolution of magnesium in acids. J Amer Chem Soc 59 63-67 (1937).

7. King, C.V. and Brodie, S.S.: The rate of dissolution of benzoic acid in dilute aqueous alkali. J Amer Chem Soc 59 1375-1380 (1937).

8. VanName, R.G. and Hill, D.U.: On the influence of alcohol and of cane sugar upon the rate of solution of cadmium in dissolved iodine. Am J Sci 36 543-554 (1913).

9. VanName, R.G. and Hill, D.U.: On the rates of solution

of metals in ferric salts and in chromic acid. Am J Sci 42 301-332 (1916).

10. VanName, R.G. and Edgar, G.: On the velocities of certain reactions between metals and dissolved halogens. Am J Sci 29 237-255 (1910).

11. VanName, R.G. and Bosworth, R.S.: On the rates of solution of certain metals in dissolved iodine, and their relation to the diffusion theory. Am J Sci 32 207-224 (1911).

12. Burt, H.M. and Mitchell, A.G.: Dissolution anisotropy in nickel sulfate a hexahydrate crystals. Int J Pharm 3 261-274 (1979).

13. Burt, H.M. and Mitchell, A.G.: Effect of habit modification on dissolution rate. Int J Pharm 5 239-251 (1980).

14. Nelson, E.: Comparative dissolution rates of weak acids and their sodium salts. J Amer Pharm Assoc, Sci Ed. 47 297-299 (1958).

15. Ullah, I. and Cadwallader, D.E.: Dissolution of slightly soluble powders under sink conditions. I. Development of an apparatus and dissolution studies of salicylic acid powders. J Pharm Sci 59 979-984 (1970).

16. Ullah, I. and Cadwallader, D.E.: Dissolution of slightly soluble powders under sink conditions. II.

Griseofulvin powders. J Pharm Sci 60 230-233 (1971).

17. Edwards, L.J.: The dissolution and diffusion of aspirin in aqueous media. Trans Faraday Soc 47 1191-1210 (1951).

18. Levy, G.: Effect of particle size on dissolution and gastrointestinal absorption rates of pharmaceuticals. Am J of Pharmacy 135 78-92 (1963).

19. Wurster, D.E. and Taylor, P.W.: Dissolution Rates. J Pharm Sci 54 169-175 (1965).

20. Levy, G., Leonards, J.R., and Procknal, J.A.: Interpretation of *in vitro* dissolution data relative to the gastrointestinal absorption characteristics of drugs in tablets. J Pharm Sci 56 1365-1367 (1967).

21. Wagner, J.G.: Biopharmaceutics. 20. Rate of dissolution *in vitro* and *in vivo* . V. Factors affecting rate of dissolution of drugs from tablets and capsules and interpretation of dissolution rate data from *in vitro* testing of tablets and capsules. Drug Intel 4 132-137 (1970).

22. Levy, G. and Hayes, B.A.: Physicochemical basis of the buffered acetylsalicylic acid controversy. New Eng J Med 262 1053-1058 (1960).

23. Levy, G. and Hollister, L.E.: Inter- and intrasubject variations in drug absorption kinetics. J Pharm Sci 53 1446-1452 (1964).

24. Hersey, J.A.: Methods available for the determination of *in vitro* dissolution rate. Manuf Chem & Aerosol News 40 32-35 (1969).

25. Wagner, J.G.: Biopharmaceutics and Relevant Pharmacokinetics. Drug Intelligence Publications, Hamilton, IL (1971), pp 110-114.

26. Cooper, J. and Rees, J.E.: Tableting research and technology. J Pharm Sci 61 1511-1555 (1972).

27. Pernarowski, N.: Dissolution Methodology, in Leeson, L. and Carstensen, J.T. (eds): Dissolution Technology. Academy of Pharmaceutical Sciences, Washington,D.C. (1974).

28. Dakkuri, A. and Shah, A.C.: Dissolution methodology: an overview. Pharmaceutical Technology 6 (6):28-86 (1982).

29. Hanson, W.A.: Handbook of Dissolution Testing. Pharmaceutical Technology Publications, Springfield, Oregon (1982).

30. Myers, E.L.: Experimental determination of sustained action. Drug Cosmetic Ind 87 622-624, 707-711 (1960).

31. Langenbucher, F.: *In vitro* assessment of dissolution kinetics. Description and evaluation of a column-type method. J Pharm Sci 58 1265-1272 (1969).

32. Chu, J.C., Kalil, J., and Wetteroth, W.A.: Mass

transfer in a fluidized bed. Chem Engr Prog 49 141-149 (1953).

33. Dryden, C.E., Strang, D.A., and Withrow, A.E.: Mass transfer in packed beds at low Reynolds number. Chem Engr Prog 49 191-196 (1953).

34. Evans, G.C. and Gerald, C.F.: Mass transfer from benzoic acid granules to water in fixed and fluidized beds at low Reynolds numbers. Chem Engr Prog 49 135-140 (1953).

35. Weinspach, P.M.: Dissolution processes in fluidized beds and in stirrer vessels. Chem Ing Tech 39 231-236 (1967).

36. Baun, D.C. and Walker, G.C.: Apparatus for determining the rate of drug release from solid dosage forms. J Pharm Sci 58 611-616 (1969).

37. Lerk, C.F. and Zuurman, K.: The influence of pulsation on the dissolution rate measurements in column type apparatus. J Pharm Pharmac 22 319-320 (1970).

38. Tingstad, J.E. and Riegelman, S.: Dissolution rate studies I: Design and evaluation of a continuous flow apparatus. J Pharm Sci 59 692-696 (1970).

39. Tingstad, J., Gropper, E., Lachman, L., and Shami, E.: Dissolution rates studies II: Modified column apparatus and its use in evaluating isosorbide dinitrate tablets. J Pharm Sci 61 1985-1990 (1972).

40. Tingstad, J., Gropper, E., Lachman, L., and Shami, E.: Dissolution rate studies III: Effect of type and intensity of agitation on dissolution rate. J Pharm Sci 62 293-297 (1973).

41. Tingstad, J., Dudzinski, J., Lachman, L., and Shami, E.: Dissolution rate studies IV: Solvent flow paterns in a column-type apparatus. J Pharm Sci 62 1527-1530 (1973).

42. Seth, P.: A study of the influence of formulation factors and processing techniques on the dissolution rates of hydrochlorothiazide tablets. Pharm Acta Helv 47 457-465 (1972).

43. Bathe, R.V., Hafliger, O., Langenbucher, F., and Schoenleber, D.: In vitro comparison of the beaker, the rotating-basket and the column dissolution-rate methods. Pharm Acta Helv 50 3-10 (1975).

44. Groves, M.J., Alkan, M.H., and Deer, M.A.: The evaluation of a column type dissolution apparatus. J Pharm Pharmac 27 400-407 (1975).

45. Carstensen, J.T., and Dhupar, K.: Dissolution rate equations in column-confined dissolution. J Pharm Sci 65 1634-1639 (1976).

46. Cakiryildiz, C., Mehta, P.J., Rahmen, W., and Schoenleber, D.: Dissolution studies with a multichannel continuous-flow apparatus. J Pharm Sci

64 1692-1697 (1975).

47. Koehler, H.J., Soliva, M., and Speiser, P.: Dissolving behaviour of two crystal modifications of 2-benzosulfonamido-5-(b-hydroxyathoxy-)pyrimidine. Pharm Acta Helv 50 17-24 (1975) from CA 82 144904p.

48. Shah, A.C., and Nelson, K.G.: Evaluation of a convective diffusion drug dissolution rate model. J Pharm Sci 64 1518-1520 (1975).

49. Ogata, H., Shibazaki, T., Inoue, T., and Ejima, A.: Comparative studies on eight dissolution methods using 21 commercial chloramphenicol tablets and a nondisintegrating benzoic acid tablet. J Pharm Sci 68 708-712 (1979).

50. Ogata, H., Shibazaki, T., Inoue, T., and Ejima, A.: Dissoution studies for chloramphenicol tablet bioavailability. J Pharm Sci 68 712-715 (1979).

51. Levy, G., Leonards, J.R. and Procknal, J.A.: Development of *in vitro* dissolution tests which correlate quantitatively with dissolution rate-limited drug absorption in man. J Pharm Sci 54 1719-1722 (1965).

52. Underwood, F.L. and Cadwallader, D.W.: Effects of various hydrodynamic conditions on dissolution rate determinations. J Pharm Sci 65 697-700 (1976).

53. Gibaldi, M., and Feldman, S.: Establishment of sink

conditions in dissolution rate determinations. Theoretical considerations and application to nondisintegrating dosage forms. J Pharm Sci 56 1238-1242 (1967).

54. Wurster, D.E. and Polli, G.P.: Investigation of drug release from solids. IV. Influence of absorption on the dissolution rate. J Pharm Sci 50 403-406 (1961).

55. Wagner, J.G.: Biopharmaceutics: Absorption aspects. J Pharm Sci 50 359-387 (1961).

56. Mattok, G.L., Lovering, E.G., and McGilveray, I.J.: Bioavailability and Drug Dissolution, in Bridges, J.W. and Chausseaud, L.F. (eds.): Progress in Drug Metabolism, Vol 2. John Wiley & Sons, London (1977).

57. Fairbrother, J.E.: Acetaminophen, in Flory, K. (ed.): Analytical Profiles of Drug Substances, Vol 3. Academic Press, New York (1974).

58. Lowell, S.: Introduction to Powder Surface Area. John Wiley & Sons, New York (1979).

59. Smith, J.V. (ed), X-ray Powder Data File, ASTM Special Technical Publication 48-J. American Society for Tesing Materials, Philadelphia (1960).

60. Morf, W.E.:The Principles of Ion-Selective Electrodes and of Membrane Transport. Elsevier/North-Holland, Inc., N.Y. (1981).

61. Durst, R.A. (ed.) Ion-Selective Electrodes. National

Bureau of Standards Special Publication 314, U.S. Government Printing Office, Washington, D.C. (1969).

62. Samuelson, O.: Ion Exchangers in Analytical Chemistry. John Wiley & Sons, New York (1953).

63. Connors, K.A: A Textbook of Pharmaceutical Analysis, ed 2. John Wiley & Sons, Inc., New York (1975).

64. Brunauer, S., Emmett, P.H., and Teller, E.: Adsorption of gases in multimolecular layers. J Amer Chem Soc 60 309-319 (1938).

65. Willard, H., Merritt, L., Dean, J. and Settle, M.: Instrumental Methods of Anaylsis, 6th. ed. Wadsworth Publishing Co., Belmont,Ca. (1981).

66. Van Campen, L.: An Approach to the Evaluation of Hygroscopicity for Pharmaceutical Solids. M.S. Thesis, University of Wisconsin-Madison (1979).

67. Brooke, D.: Sieve cuts as monodisperse powders in dissolution studies. J Pharm Sci 64 1409-1412 (1975).

68. Quay, J.F., Childers, R.F., Johnson, D.W., Nash, J.F. and Stucky, J.F.: Cinoxacin in female mongrel dogs: Effect of urine pH on urinary drug excretion and correlation of *in vitro* characteristics of oral dosage forms with bioavailability. J Pharm Sci 68 227-232 (1979).

69. Moller, N.: Studies on particle size problems. VI.

Fundamentals on pharmacopeial control of particle size in the subsieve range. Dansk Tidsskr Farm 44 348-357 (1970) through Int'l Pharm Abst 8 1054.

70. Moller, N.: Studies on particle size problems. VII. Specific particle number as a measure in pharmacopeial tests of particle size in the subsieve range. Dansk Tidsskr Farm 45 125-134 (1971) through Int'l Pharm Abst 9 0803.

71. Nimmerfall, F. and Rosenthaler, J.: Dependence of area under the curve on proquazone particle size and *in vitro* dissolution rate. J Pharm Sci 69 605-607 (1980).

72. Treybal, R.E. Mass-Transfer Operations, 3rd ed. McGraw-Hill Inc., New York (1980).

73. Washburn, E.W. (ed) International Critical Tables of Numerical Data, Physics, Chemistry and Technology. McGraw-Hill Inc., New York (1929).

74. Burt, H.M. and Mitchell, A.G.: Crystal defects and dissolution. Int J Pharm 9 137-152 (1981).

75. Friesen, M., Burt, H.M. and Mitchell, A.G.: Crystal dislocations and dissolution. J Pharm Pharmac 33 22P (1981).

76. Carstensen, J.T., Grady, L.T., Nelson, K.G. and Weinswig, M.H. (eds): Dissolution - State of the Art. Proceedings of the Second Wisconsin Update Conference.

Extension Services in Pharmacy, University of Wisconsin-Extension, Madison (1982).

77. Cabana, B.E.: personal communication, October 25, 1982.

78. McMichael, W.J., and Hellums, J.D.: Interphase mass and heat transfer in pulsatile flow. AIChE J 21 743-752 (1975).

79. Dwight, H.B.:Tables of Integrals and Other Mathematical Data, 4th ed.,Macmillan, New York (1961).

80. Grant, E.L.: Statistical Quality Control, 3rd ed., McGraw-Hill Inc., New York (1964).

81. Langenbucher, F.: Linearization of dissolution rate curves by the Weibull distribution. J Pharm Pharmac 24 979-981 (1972).

82. Langenbucher, F.: Parametric representation of dissolution-rate curves by the RRSBW distribution. Pharm Ind 38 472-477 (1976).

TITLE OF THESIS Nonsink Dissolution Kinetics of Poorly Soluble Substances Assessed in a Column Apparatus

MAJOR PROFESSOR Dr. Jens T. Carstensen

MAJOR DEPARTMENT Pharmacy (Pharmaceutics)

MINOR Chemical Engineering

NAME Sharon Marie Laughlin

PLACE AND DATE OF BIRTH Webster City, Iowa; August 15, 1950

COLLEGES AND UNIVERSITIES: YEARS ATTENDED AND DEGREES University of Iowa, 1968-1973 (B.S. Pharmacy); University of Wisconsin-Madison, 1977-1983 (M.S. Pharmacy, 1979; Ph.D. Pharmacy, 1983).

MEMBERSHIPS IN LEARNED OR HONORARY SOCIETIES American Pharmaceutical Association; APhA APS; Rho Chi

PUBLICATIONS SM Laughlin, L Van Campen, M Takieddin, D Duchene, G Puisieux, JT Carstensen, Int J Pharm 3,33-37 (1979); JT Carstensen and SM Laughlin, Powder Tech 23,79-84 (1979); SM Laughlin,"Flow Rates for Transfer of Granular Solids Through Moving Orifices: Modeling of Dynamic Flow Processes",M.S. thesis,University of Wisconsin-Madison,1979; SM Laughlin and JT Carstensen, J Pharm Sci 70 711-713 (1981).

DATE June 15, 1983

FORMULATION #1: THE OFFICIAL FIFTH FLOOR PHARMACEUTICS

RHUBARB CAKE

1 1/2 cup sugar
1/2 cup butter
1 tsp. vanilla
1/2 tsp. salt
1 egg

1 cup sour milk
2 cup flour
1 tsp. baking soda
2+ cup rhubarb, cut-up
(fresh or frozen)

Cream together the sugar, butter, vanilla and salt. Add the egg and beat well; mix soda with flour. Add flour mixture alternately with the sour milk to the previous mixture, adding flour first and last; mix well. Stir in rhubarb. Pour into a greased and floured 9 x 13" cake pan. Blend together topping ingredients and sprinkle evenly over batter before baking. Bake at 325°F for 1 hour. Cake can be frozen.

Topping: Granulated sugar mixed with cinnamon
Chopped nuts (optional)